https://ntrs.nasa.gov/search.jsp?R=19700002139 2020-03-12T04:50:45+00:00Z

N 70 11443
NASA CR 102292

BOLT BERANEK AND NEWMAN INC
CONSULTING · DEVELOPMENT · RESEARCH

Report No. 1731
Job No. 11320

A MODEL FOR HUMAN CONTROLLER REMNANT

Final Report

Contract No. NAS8-21136

CASE FILE COPY

William H. Levison
David L. Kleinman
Sheldon Baron

15 October 1968

Submitted to:

National Aeronautics and Space Administration
George C. Marshall Space Flight Center
Huntsville, Alabama 35812

Attention: Mr. Billy G. Davis
Technical Monitor

Report No. 1731
Job No. 11320

A MODEL FOR HUMAN CONTROLLER REMNANT

Final Report

William H. Levison
David L. Kleinman
Sheldon Baron

15 October 1968

Prepared under Contract No. NAS8-21136

by

Bolt Beranek and Newman Inc
50 Moulton Street
Cambridge, Massachusetts 02138

for

National Aeronautics and Space Administration
George C. Marshall Space Flight Center
Huntsville, Alabama 35812

FOREWARD

This report summarizes the research performed under Contract No. NAS8-21136, sponsored by the Advanced Studies Office of the Astrionics Laboratory, George C. Marshall Space Flight Center, National Aeronautics and Space Administration. The principal investigators for the contract were W. H. Levison and S. Baron of Bolt Beranek and Newman Inc. The technical monitors for the Astrionics Laboratory were B. G. Davis and J. F. Pavlick.

TABLE OF CONTENTS

TABLE OF CONTENTS (Cont.)

LIST OF ILLUSTRATIONS

LIST OF ILLUSTRATIONS (Cont.)

Report No. 1731 Bolt Beranek and Newman Inc

A MODEL FOR HUMAN CONTROLLER REMNANT

By William H. Levison, David L. Kleinman, and Sheldon Baron

SUMMARY

A model has been developed for predicting the spectral characteristics of human controller remnant in single-display control situations. Remnant is assumed to arise primarily from underlying psychophysical sources such as: (1) observation noise, (2) motor noise, and (3) time-variations in the controller's describing function. These sources are assumed to be white noise processes that are linearly independent of each other and of the signals circulating through the control system. It is shown that these processes are essentially indistinguishable in terms of their effects on controller behavior, and they are lumped into an equivalent (matrix) multiplicative observation noise source.

Although our model assumes that the sources of controller remnant are multiplicative in nature, we cannot readily compute the characteristics of a matrix multiplicative noise process from the available manual control data. We therefore analyze the multiplicative noise model to predict the spectral characteristics of an equivalent scalar additive observation noise which is more easily obtainable. The model predictions are validated by the data obtained from tracking studies involving foveal viewing of a single display. We find that the equivalent observation noise spectra obtained experimentally can be accounted for by white, multiplicative, noise processes having power density levels of about 0.01 units of normalized power per rad/sec acting on each of the observed variables. This normalized noise level is shown to be invariant with respect to input bandwidth, input amplitude, system

dynamics, and to the variable (i.e., position or rate) being estimated by the controller from his display. We are thus able to account for controller remnant in a large class of manual control situations by a model that contains only a single parameter.

We find that a simple multiplicative model of remnant is insufficient to explain the remnant data obtained when displays are viewed peripherally. Although the spectral characteristics of the observation noise remain white, the power level is highly dependent on the nature of the viewing conditions. This result suggests that a measure of equivalent observation noise may prove to be a useful metric for evaluating the quality of an instrument display.

I. INTRODUCTION

The remnant is an important component of the quasi-linear representation for the human controller. It frequently accounts for a large fraction of the controller's output, sometimes for most of it. All too often the remnant is ignored in the analysis of manual control systems. The principal reason for this, we suspect, is the lack of good models for the remnant. Development and verification of such models has been the objective of the research discussed in this report.

We adopt as our operating definition of human controller remnant the portion of the controller's response that is linearly uncorrelated with the system forcing function. This remnant, which we can measure directly via appropriate experimental and analytical techniques, is assumed to arise from one or more of a number of potential psychophysical noise processes whose characteristics can be inferred from analysis of the remnant data.

In the main body of this report we postulate a model of the noise processes responsible for controller remnant, develop a theoretical framework which allows us to predict the nature of controller remnant, and test these predictions against existing manual control data.* These data were obtained from experiments which were not necessarily designed specifically to investigate controller remnant. However, they include a sufficient variety of control conditions to provide tests of the major conclusions of our theoretical development.

A dominant theme in our model development has been to search for underlying remnant sources which themselves are processes whose characteristics are relatively independent of control system parameters, such as input spectral characteristics and plant dynamics.

*The manual control data analyzed in depth in this report were provided by a series of experimental studies by NASA-Ames Research Center under Contract NAS2-3080. The results of these studies have been reported in the literature (Ref. 1).

We have tried to avoid as much as possible the construction of a catalog of processes each of which describes remnant in a particular control situation.

The organization of the report is as follows. Background information is presented in Chapter II. First, we discuss two possible definitions of controller remnant: a general definition which is not restricted to quasi-linear models of the controller, and the more restrictive definition which we adopt as the operating definition for this report. The remainder of Chapter II is devoted to a review of the literature relating directly to studies of controller remnant and to a review of psychophysical data which illustrate the basic nature of human randomness. Certain aspects of visual information processing are also discussed.

A model for the generation of controller remnant is developed in Chapter III. A number of multiplicative white noise sources are postulated as sources of remnant, and these processes are shown to be indistinguishable for the most part in terms of the analysis that can be performed on the existing manual control data. These processes are then lumped mathematically into an equivalent vector observation noise process which serves as a basis for predicting controller remnant in a variety of control situations.

Experimental and analytical techniques are summarized in Chapter IV. Procedures are described for computing observation noise spectra from existing manual control data. These spectra, presented in Chapter V, validate the model predictions of Chapter III and provide the necessary quantification of the equivalent observation noise process to allow the prediction of controller behavior and system performance for a large class of manual control situations.

The conclusions of this report are summarized in Chapter VI. In addition, we suggest areas of further research aimed at: (1) obtaining a fuller understanding of the sources of remnant, (2) determining the characteristics of the equivalent observation noise process in a variety of control situations, and (3) developing techniques of applying models of observation noise in complex control situations.

This report contains three appendices. Appendix A presents a theoretical investigation of the linear correlation between system error and the multiplicative noise process assumed to operate on that signal. A set of controller remnant spectra presented in an earlier report is reanalyzed in greater detail in Appendix B. Appendix C contains a detailed description of our experimental and analytical procedures.

II. BACKGROUND DISCUSSION

Definition of Controller Remnant

Two definitions of human controller remnant are discussed in this section. We present first a general definition of remnant - one which does not restrict the form of the deterministic portion of the controller's behavior. We then discuss a more conventional definition - one tied to a quasi-linear description of controller behavior - which we are essentially forced to adopt because of the limitations of our data base.

A general definition. --One dictionary definition of remnant is "residue; remainder." Remainder from what? With respect to human response theory, "remnant" has generally been the term used to describe the portion of the controller's behavior not accounted for by some model (usually linear, time-invariant) of the controller. The difficulty with this definition is that it does not uniquely relate to a specific component of the controller's response, but it includes modelling inadequacies on the part of the experimenter as well. A truly unique definition of controller remnant is desired for philosophical reasons, even if such a definition cannot be put to immediate practical use. Taylor (Ref.31) has suggested a method for extracting the stochastic component of the controller's output. Our general definition of remnant is an extension of this idea.

We propose that human controller remnant be defined as that component of the controller's output that is not deterministically related to system inputs. No constraints on the nature of the deterministic portion of the controller's strategy are implied; it may contain nonlinearities and time-variations that are related in a consistent manner to the system input. The remnant

so defined will account for the stochastic component of the controller's output: i.e., the component that cannot be predicted except in a statistical sense. The remnant is thus the "remainder" of the controller's output in that it fails to be accounted for by the best possible deterministic model for the controller.

The remnant, when defined in this way, differs basically from the non-remnant (or deterministic) component of the controller's output in two important respects. First of all, the time history of the deterministic component can in theory be predicted exactly, whereas the time history of the remnant is a random process. Secondly, only the deterministic component of the controller's output is useful in controlling the plant; the remnant serves only to disturb the system.

This general definition of remnant, unfortunately, does not lend itself readily to practical application. The primary difficulty is that a very large data base is required to permit the measurement of remnant. Note that the remnant component cannot be extracted from a single tracking run when no a priori constraints are placed on the deterministic model of the controller. Only by obtaining the ensemble average of response waveforms elicited by a particular input waveform can the deterministic and remnant components be separated. Such a technique has been used by Taylor (Ref.31) to distinguish nonlinear (or time-varying) components of the pilot's output from the stochastic component. Because of the limitations of our data base, however, which contains only two or three runs per subject per experimental condition, we have had to forego average response techniques and instead adopt a more conventional definition of controller remnant which allows the estimation of remnant statistics from a single experimental trial.

A quasi-linear definition. - In most manual control studies the human controller has been represented by a linear time-invariant model, a describing function, and the remnant has been taken to be the portion of the controller's output not accounted for by this model (Refs. 1-4). The rationale behind this approach is that the describing function accounts for all but an insignificant portion of the deterministic component of control behavior. The remnant then represents essentially the stochastic component of the controller's output.

Because of the limitations of our data base, we shall adopt this quasi-linear definition of remnant for the remainder of this report. However, we feel that the remnant measurements analyzed in this work are close approximations to the controller remnant as defined in the more general sense, since the experimental conditions that yielded this body of data were designed to minimize non-linearities and consistent time-variations in the controller's strategy (Ref. 1).

There are two ways in which to view the remnant in the quasilinear context. One approach is to consider the remnant as the portion of the controller's response that is not related to the perceived system error by the controller's describing function. This concept of remnant is often referred to as the "open-loop remnant," since it is derived from a model of the controller alone. This concept is particularly useful for building theoretical models of controller remnant, but the distinction between remnant and input-related signal components is often difficult when there is a relatively large amount of remnant-induced power circulating around the control loop. Some investigators (Ref.1,4)have found that better estimates can be obtained of the "closed-loop remnant," which is defined as the portion of the controller's response not related to the system

forcing function. Since the deterministic component of the controller's strategy is considered to be linear and time-invariant, the open-loop and closed-loop remnant spectra are related by the linear transformation

$$\Phi_{uu_r}(\omega) = \left|\frac{1}{1+H(\omega)V(\omega)}\right|^2 \Phi_{rr_u}(\omega) \qquad (1)$$

where $\Phi_{rr_u}(\omega)$ represents the open-loop remnant spectrum, $\Phi_{uu_r}(\omega)$ the closed-loop spectrum, $H(\omega)$ the controller's describing function, and $V(\omega)$ the vehicle dynamics. Both concepts of remnant are used in this paper.

Current Knowledge of Human Controller Remnant

The remnant often constitutes a significant portion of the human controller's response and understanding remnant is, therefore, of considerable importance in providing an adequate description of controller behavior. Nevertheless, there is far less remnant data than describing function data extant in the literature. Moreover, much of the remnant data that does exist is of questionable accuracy. The most extensive, and probably most reliable, remnant data have been presented by Elkind (2), McRuer and Krendel (3), and McRuer, et al (4). Levison and Elkind (1) have also collected significant remnant data, much of which are presented elsewhere in this report.

With regard to analyzing remnant data, the work of McRuer and his collegues was, by far, the most significant. In two classic reports, in 1957 and 1965, they analyzed their own remnant data, as well as those of other investigators (including Elkind) in considerable detail. Although there has been some attention given to

remnant since 1965, these two reports are still the only published in-depth studies of remnant. As such they may be considered as definitive of the state of knowledge concerning remnant prior to the work performed under this contract. Consequently, we shall devote most of this section to a discussion of the content and conclusions, concerning remnant, of these two reports.* In 1957 McRuer and Krendel analyzed the remnant data of several investigators** and attempted to explain the remnant in terms of distinct sources each resulting in equivalent operator output power. These data covered a wide range of forcing functions and a number of controlled elements of varying degrees of complexity.

McRuer and Krendel first suggested that the closed-loop remnant could result from the following sources:

(a) Operator's Response to Other Inputs.

(b) Nonlinear Transfer Behavior.

(c) Injection of Noise into the Loop.

(d) Nonsteady Behavior of the Operator.

Since careful experimental procedures make it highly unlikely that there will be extraneous inputs for the operator to respond to, they did not consider item (a) as a source of remnant in their analysis of the data. In addition, on the basis of Elkind's data, which indicated that series nonlinear effects were minor, and in the desire to preserve a basically linear description of the operator, they did not consider such nonlinearities as a source of remnant. They did, however, consider a parallel nonlinearity, based on the Goodyear nonlinear model of the human operator, as a potential source of remnant.

* The reports deal with the general subject of quasi-linear models of the human operator and not just remnant.

** In particular, they examined the data of Elkind (2), Russell (5), Tustin (6), Goodyear (7), in addition to data they obtained on the Franklin Institute F-80-A Simulator.

In analyzing the remnant data, McRuer and Krendel first assumed that the remnant was due solely to the particular source they were examining. To quote, "Since we have no way of knowing which source is dominant our only recourse is to look at each separately and assume that all of the remnant is due solely to that particular source. We are not in any way implying that such an all or none explanation necessarily prevails, but we use this approach since any theory based on a mixture of effects leads to hypotheses for which we may have no experimental check."* Once having made this assumption, McRuer and Krendel try to fit the remnant data with analytic curves which are then interpreted in terms of the particular remnant source being considered.

Before presenting the conclusions of their analyses let us examine an intermediate finding which is of some interest and relevance to our work. In examining the hypothesis that remnant was due to noise injected into the loop, McRuer and Krendel considered the operator as a single input, single output system. They then converted the closed-loop remnant spectrum, Φ_{uu_r}, to equivalent open-loop spectra Φ_{rr_x} and Φ_{rr_u} injected at the input and output terminals of the operator, respectively.** In analyzing Elkind's data and the Franklin Institute data they found that no simple spectral form fit all the data well, but the Φ_{rr_u} data (i.e., noise injected at the output), were somewhat more orderly. They did find from Elkind's data, however, that for rectangular forcing functions of 1, 1.5, 2.5 and 4 radian/sec bandwidth and K dynamics, the Φ_{rr_x} curves were best fitted by a horizontal straight line (white noise) at -18 dB – a finding which is most interesting in view of the results presented later in this report.

---

*This statement is particularly pertinent in light of our analysis (See Chapters III and IV).

**In order that the reader need not be confronted with more than one system of notation, all mathematical expressions referenced in this chapter are shown in the notation adopted throughout the remainder of this report.

After analyzing all the aforementioned data, McRuer and Krendel concluded that there was little to choose between the three studied sources of remnant in terms of the existing remnant data,but they expressed the following opinions in terms of pilot models:

> "1. The nonsteady model is best from the point of view that the curve fits upon which it is based were the most adequate ones made;
>
> 2. The noise injection model is best from the standpoint of simplicity in using the hypothetical describing function data for system stability predictions and general servo analysis;
>
> 3. The parallel sgn function, or perfect relay, model is best from the viewpoint of point-by-point prediction of the operator's output and in creating an intuitive physical view of the operator's actions.
>
> Because of the approximate equivalence of the three models, as regards their manifest effects in the data, and the points enumerated above, we feel that the eclectic view is the most practical at this stage. By accepting this viewpoint, the choice of remnant model can be left to the engineer or psychologist analyzing a particular problem. The model can then be selected on the basis of convenience for the particular job at hand. Of course, due caution and restraint should be used in not exceeding the bounds imposed by the experimental conditions for which the models were originally derived. An experimenter's ingenuity would be challenged in designing appropriate experiments to choose between the possible remnant models. The nonsteady model is most amenable to experimental study."

As noted before, the remnant data upon which the 1957 report was based were not entirely reliable. Moreover, there were gaps in the existing data which made it even more difficult to understand the nature of remnant and its dependence on various experimental parameters. In their 1965 report McRuer, et al tried to remove some

of these deficiencies. A key quantity in McRuer, et al's measurement and analysis of remnant was the "correlation coefficient," ρ, the square of which is the ratio of the linearly correlated pilot-output power to the total pilot output power. This quantity is defined by the expression

$$\rho^2 = 1 - \frac{\Phi_{uu_r}}{\Phi_{uu}} \tag{2}$$

where Φ_{uu_r} and Φ_{uu} are the power spectral densities of the closed-loop remnant and the total operator output, respectively. The linear correlation can also be found from the crosscorrelation between the forcing function and operator output since

$$\rho = \frac{\Phi_{iu}}{\sqrt{\Phi_{ii}\ \Phi_{uu}}} \tag{3}$$

where Φ_{iu} is the appropriate cross-spectrum between input and control and Φ_{ii} is the input spectrum. Thus, ρ can be measured with a spectral and cross-spectral analyzer.

McRuer, et al claim that, when random appearing sums of sinusoids are used as forcing functions, their measured values of ρ provide a basis for estimating the degree that time variations in the humans describing function contribute to the remnant. To be more precise, we quote them:

> "For our experiments ρ is found using an analyzer which mechanizes spectral and cross-spectral measurements using multiplications and very low pass filters. If the forcing function is a sum of sinusoids, Φ_{ii} will be a sum of delta functions (i.e., a series of line spectra which exist only

at the frequencies of the individual forcing function sinusoidal components). Then, in general, the output, Φ_{uu}, will be a sum of delta functions at the same frequencies as those in Φ_{ii}, plus delta functions at other discrete frequencies (if nonlinearities or constant rate sampling are present), plus a continuous power spectral density component representing random fluctuations in the output. At the frequencies for which they exist the delta function components will generally overpower the random component, and the ρ measured at forcing function frequencies will generally be 1.0 unless low frequency time variations in H result in additional power within the measurement filter bandwidth. In fact, ρ will be 1.0 even in the presence of many kinds of system nonlinearities. At other frequencies ρ will be undefined since Φ_{ii} is zero."

The use of random appearing sums of sinusoids as forcing functions was an important aspect of their experimental program. This kind of forcing function helps clarify the remnant picture considerably since any operator output power at other than forcing function frequencies must then be, by definition, remnant. Thus, the closed-loop remnant can be measured directly at other than forcing function frequencies by determining Φ_{uu}. McRuer, et al were also able to estimate approximately the remnant at forcing function frequencies by using measurements of ρ and Φ_{uu}. They found on the basis of their measurements that the remnant had an essentially continuous spectrum (i.e., significant line spectra were absent).

An extensive experimental program was conducted covering a number of forcing function amplitudes and bandwidths and a variety of controlled element dynamics. Linear correlation coefficients and remnant power spectra were obtained for the various conditions. The remnant spectra were presented as an equivalent injected noise

on the operator's input (i.e., added to the system error), normalized with respect to mean-squared input, because they found that "the highest degree of similarity among remnants for the ... [experimental conditions analyzed] ... exists if the remnant is viewed as an open-loop quantity injected at the operator's input." This important finding was contrary to the conclusion of the 1957 report which stated that the data was most orderly when referred to the operator's output.

In addition to the linear correlation and remnant spectra data, McRuer, et al analyzed amplitude distributions of the pilot's input (the system error) and output and selected power spectral densities of his output. Since the input they used had a nearly Gaussian distribution, any deviations from Gaussianess in the error or control output distributions could be taken as an indication that nonlinear behavior could account for the remnant. Examination of the output spectrum could also reveal nonlinear behavior as well as periodic sampling if either existed.

On the basis of the analyses indicated above, McRuer, et al arrived at six conclusions which represented the "status of Remnant Data" circa 1965. We present these conclusions along with our comments, as they seem appropriate, below.

> "1. Values of the remnant computed at the forcing function frequencies generally fit a smooth curve through values measured between and above forcing function frequencies. This indicates that the power spectral density of the remnant is generally continuous and that line spectra indicating periodicities are absent."

This conclusion is difficult to prove. We have shown (Appendix A) that if the remnant is generated by the multiplicative process described in Chapter III there will be a "spike" superimposed

on the remnant spectrum at forcing function frequencies. This "spike" would, of course, be indistinguishable from the input-correlated part of the operator's output spectrum and cannot be detected by existing measurement techniques. Fortunately, we expect that the spike represents a small portion of the total remnant power at input frequencies and can, consequently, be neglected. This is, indeed, the assumption we make in our remnant measurement procedure.

> "2. At very low frequencies the remnant data for a wide variety of controlled elements coalesce best when all the remnant is reflected to the pilot's input."

We shall see that this conclusion can be extended to cover the entire measurement frequency range, if the remnant is appropriately normalized and if the expression "pilot's input" is interpreted properly.

> "3. Remnant increases with controlled element gain, with forcing function bandwidth, and with control order. For extreme controlled element forms such as $Y_c = K_c/j\omega(j\omega 1.5)$ the remnant increases greatly, primarily because of the pilot's time-varying behavior induced by his attempts to retain control over this drastically unstable controlled element."

The first part of this conclusion must be somewhat tempered in light of the McRuer, et al data and their other statements in the main body of the report. Specifically, they stated: "remnant increases with controlled element gain, but the variation is not as extreme as that of the gain"; "the data examined indicate that the effect of forcing function bandwidth on the remnant can vary from minor to none"; and "it is seen that the major effect of variation in the remnant is as much intersubject as inter-controlled element." The conclusions concerning the unstable controlled

element are apparently based on small measured linear correlation coefficients and on run-to-run variability in the pilot's describing function (in particular, the phase angle) for this case. We will have more to say about small values of ρ as an indication of time variability a little later. It should be noted that the aforementioned run-to-run variability in the describing function is demonstrated for a single pilot. Moreover, since the remnant is a large portion of the output in this case, the describing function measurements, particularly at high and low frequencies, are somewhat suspect.

We agree that, in general, as the task becomes more complex, the remnant, when normalized with respect to mean-squared input, will increase. However, we shall see that a different normalization removes this trend.

> "4. Some evidence for pulsing behavior in control of second-order controlled elements is present from output amplitude distributions. These indicate a tendency for the pilot's output to be pulse areas roughly proportional to the stimulus amplitude."

It should be noted that not all pilot's seem to adopt the pulsing strategy. In addition, McRuer, et al state that "this does not appear to result in a substantial remnant relative to other sources.

> "5. Careful examination of the output power spectral density indicated no evidence for periodic sampling or significant nonlinear behavior."

In a recent review, McRuer and Jex (8), indicate that they have recently re-examined the data over shorter intervals (as short as 20 sec.) and reached the same conclusion. They also note that random or other nonperiodic sampling behavior is not ruled out as a

source of remnant. Bekey (9) has shown that random sampling would result in continuous remnant spectra.

> "6. Partly by process of elimination and partly by direct evidence, it appears that the major source of remnant is nonstationary pilot behavior, i.e., time-varying components in the effective time delay and gain. For the second-order controlled elements the pulsing nature of the pilot's output contributes an additional remnant source."

While we do not necessarily disagree with this conclusion, we do not feel that there is sufficient evidence to support it.* The claim that, for sinusoidal inputs, small values of ρ indicate time variations in the describing function rests on the assumption that random fluctuations are small compared to the correlated part of the output. This, it seems to us, amounts to assuming that time variations are the major source of remnant rather than proving such is the case. The question is whether the measurement process can distinguish between injected noise and time variations. It would appear that if the time variations were low-frequency in nature, the remnant spectrum would tend to "bunch up" around the forcing function frequencies. If, on the other hand, the time variations were wide-band the spectrum would be indistinguishable from one produced by an appropriate injected noise. In Appendix B a remnant spectrum is analyzed in great detail in an attempt to detect low frequency time variations. We hesitate to generalize on the basis of one data point, but this spectrum shows no evidence of the "bunching up" that would be indicative of low-frequency time variation in the describing function, nor does any other data we are aware of.

*Indeed, for foveal tracking with a "good" display, we are inclined to agree that this is the major source of remnant.

Although the conclusions put forth by McRuer, et al are somewhat inconsistent as to whether or not controller remnant is sensitive to various control system parameters, there is other evidence in the literature to indicate that remnant, when properly normalized, is relatively insensitive to some of these effects. Pew, et al (Ref. 10) have compared remnant spectra obtained in their own experiments with those presented by McRuer, et al. (Their subjects were provided with positional control and were required to track a disturbance consisting of a single sinusoid.) They found that the two spectra had an almost identical functional relationship with respect to measurement frequency up to about 10 rad/sec. Since the input signals used by Pew, et al and McRuer, et al (the latter being sums-of-sinusoids) were grossly different, this finding suggests that the shape of the remnant spectrum, then, seems to be nearly invariant with respect to the nature of the input. In addition, Pew, et al reported that remnant was unaffected by control gain and display gain.

Levison and Elkind (Ref. 1) have reported remnant results which suggest that mean-squared system error, rather than mean-squared input, is an appropriate normalization factor for the injected noise process Φ_{rr_x}. They measured the fractional remnant power obtained in a series of single-axis experiments in which the mean-squared input, the input bandwidth, and the vehicle dynamics were varied. A definition of "fractional remnant power" was given as the fraction of system error power not correlated with input frequencies. This measure, then, was equivalent to the integral of the closed-loop remnant power (measured at the controller's input) divided by the total error power.

Levison and Elkind found that the fractional remnant power changed less than 5% as the input bandwidth was increased from 0.5 to 2.0 rad/sec (with the mean-squared input constant), even though

the mean-squared total error increased five-fold. When the input bandwidth was held constant and the mean-squared input increased four-fold, the fractional remnant power increased by only 5 percentage points (from 0.16 to 0.21). When the vehicle dynamics were increased from first-order to second-order, however, a substantial increase (from 0.23 to 0.46) in fractional remnant power resulted. This finding correlates with the relationship between Φ_{rr_x} and control order reported in Reference 4.

If one interprets the trend of the fractional remnant measure as indicative of the behavior of the open-loop injected noise normalized with respect to mean-squared error, then it would appear that a normalization of this type will yield an injected noise process whose characteristics are relatively invariant, at least with respect to the characteristics of the forcing function. We should expect, however, on the basis of the results reported above, that the normalized injected noise spectrum will be strongly dependent on vehicle dynamics.*

The relative invariance of the fractional remnant power with respect to input power indicates that the absolute amount of remnant power scales along with the other signals circulating throughout the system. This behavior suggests that controller remnant is basically multiplicative in its origin and is not due to fixed additive noise sources generated by the controller.

The Nature of Human Variability

In the preceding section we reviewed the important literature relating to human controller remnant. Although some investigators have speculated upon the source of this remnant, it is, nevertheless,

*We show later in this report that such a dependency can be eliminated by consideration of a vector, rather than scalar, injected noise process.

extremely difficult to differentiate among several potential sources on the basis of manual control data alone. The primary reason for this is that even a simple manual control task requires the human to perform simultaneously a number of component subtasks, such as: (1) estimation of the magnitude of one or more system variables, (2) transformation of this information into an appropriate control strategy, and (3) execution of a motor response. The sources of variability associated with each of these processes appear essentially equivalent from a mathematical point-of-view in terms of their effect on controller behavior, as we show in the next chapter.

Since it appears that the sources of remnant can be differentiated only through studies designed to investigate them in near-isolation, we have undertaken a brief review of the human response literature outside the realm of manual control. In particular, we have examined the results of some psychophysical experiments designed to investigate the ability of the controller to make perceptions or execute responses of the type appropriate to the manual control context.

Ideally, we should like to uncover data which allow computation of the spectral characteristics of the variability associated with, say, estimating the position of an indicator, in addition to the time- (or sample-) domain statistics that are more readily available. Comparison of an observational noise spectrum obtained from a basic psychophysical experiment with the spectrum of Φ_{rr_x} obtained from a manual control experiment would indicate the relative importance of observation noise in the production of controller remnant. Unfortunately, we have been unable to find such data in the literature. The reason, we suspect, is that it is extremely difficult to design a meaningful experiment which requires the observer solely to estimate a stimulus variable in a continuous manner. In order for the subject to inform the experimenter of his instantaneous estimate, it is

necessary for him to produce a continuous corresponding output variable (as he does when tracking). But since stimulus estimation, output production, and input-output transformation are involved in this situation, an experiment of this type fails our objective of investigating only one of those processes.

The results reviewed in this section, then, are concerned primarily with sample-domain statistics such as: (1) the standard deviation in the estimate of a given stimulous magnitude, and (2) the minimum resolvable stimulous difference. These measures, though limited in their scope, are nevertheless useful, because they provide a means of testing models of human randomness which may be inferred from the existing remnant data.

We have seen, for example, that remnant power tends to scale with total error power. This behavior suggests that the underlying psychophysiological noise processes are basically multiplicative in nature. A simple model for this process — one that serves as the basis for the theoretical development pursued in Chapter III of this report — is

$$x'(t) = x(t) + \delta x(t) = [1+n(t)] \cdot x(t) \qquad (4)$$

where $x(t)$ is the desired response, $x'(t)$ is the true response, $\delta x(t)$ is the variation of the true response from the desired one, and $n(t)$ is the underlying multiplicative psychophysical noise process. We shall find it convenient later in the report to consider the variational component $\delta x(t)$ as a noise term that is <u>added</u> to the desired response (or stimulus) but which originates through the multiplication of the process $n(t)$ with the desired response (or stimulus) itself, as shown in Figure 1.

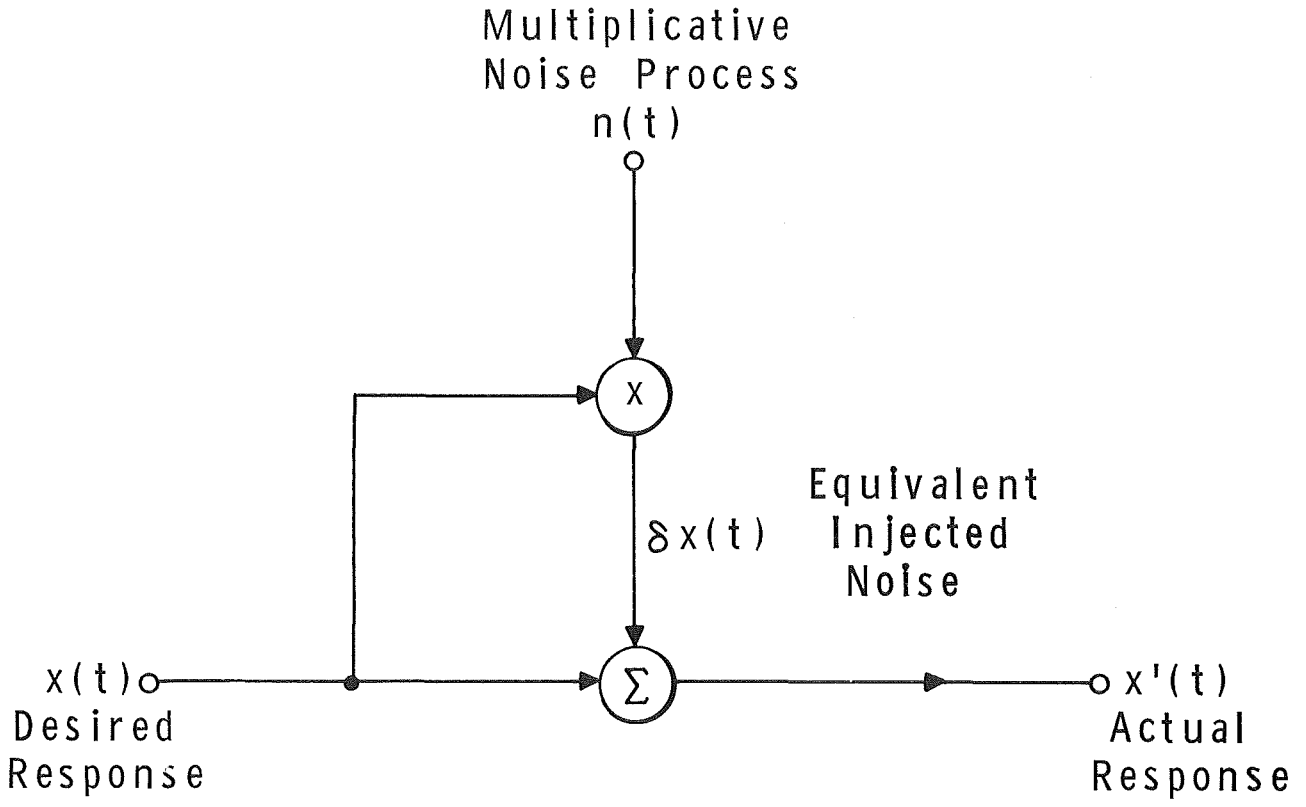

FIG. 1 A MODEL FOR THE RANDOM COMPONENT OF HUMAN RESPONSE

If n(t) and x(t) are independent variables, this model leads to the conclusion that the standard deviation of the response varies proportionally with the magnitude of the appropriate response.

An alternate model for response production (based on other than continuous tracking studies) holds that the variance, rather than the standard deviation, should scale linearly with response magnitude. The rationale behind this model is that there is a certain variance, σ_u^2, associated with responding a unit amount, r_u. If the subject is required to respond an amount $k \cdot r_u$, he effectively makes k successive, independent, responses and accumulates a total variance of $k \cdot \sigma_u^2$. The literature contains at least one experimental verification of this model (Ref. 11).

Most of the experiments reviewed show that the standard deviation varies somewhere between a linear relation and a square-root relation to the stimulus magnitude, with some residual error extrapolated to zero stimulus. Wherever the data have been tabulated, we have fitted the results with models of the form

$$\sigma = \sigma_o + k_1 X \tag{5}$$

and

$$\sigma^2 = \sigma_o^2 + k_2 X \tag{6}$$

where σ is the standard deviation of the subject's response, X is the magnitude of the stimulus or desired response, and σ_o is the standard deviation associated with a null stimulus or response.

Stimulus discrimination.--A substantial amount of work has been devoted to determining, either directly or indirectly, the ability of the observer to resolve small differences in stimulus magnitudes (Refs. 12-13). If one interprets the ability to resolve differences

as a measure of the noise level associated with estimating a stimulus variable, one would expect the minimum resolvable difference to vary with stimulus magnitude in the manner indicated in equations (5) or (6).

The ability of the observer to resolve differences along stimulus dimensions relevant to manual control can be inferred from the results of Stevens and Galanter (Ref. 13) obtained from a series of absolute-judgement experiments. As an example of their experimental technique, subjects were asked to judge the magnitude of a line length in terms of an 11-point scale. (Such a quantized scale is called a category scale.) The subjects were first shown stimuli near either end point of the scale in order to fix their range of judgements. The resulting category rating versus stimulus magnitude was strongly concave downward. Thus, the subjects included an increasingly wider range of stimulus magnitude into a single category as the stimulus magnitude was increased. This behavior was interpreted by the authors to reflect, in part, an increase in minimum resolvable difference with stimulus magnitude. A similar experiment was performed in which the subjects were asked to classify weight; the results were essentially the same as for the length-of-line experiment.

Magnitude estimation and production.--The precision with which a subject can estimate the magnitude of a stimulus or produce a desired analog response is intimately related to human controller remnant, since both these operations, plus the task of generating the appropriate transformation between the two, are required in a linear manual control task. Note that it is nearly impossible to conduct an experiment that can completely isolate a single such operation. As we have already pointed out, the subject must produce some kind of output in order to indicate his estimate of the stimulus. (Alternatively, if his task is primarily the production of an output, the subject must receive some input to inform him of

the desired output magnitude.) Even if the input or output be verbal, thereby eliminating the effects of either observation noise or motor noise, the subject must still transform between the stimulus and response spaces. Thus, at best, only one of the three operations can be eliminated from the task.

Some of the experiments reported here involved all three operations of estimation, transformation, and response. We have reviewed them, nevertheless, because they provide good examples of human variability. Since the input signal was usually removed at the onset of response, these experiments do not involve continuous tracking.

The observer's ability to estimate target velocity was estimated by Rachlin (Ref. 14). The subjects were shown a spot of light moving with constant velocity across the visual field and were required to estimate, among other variables, the magnitude of the velocity. Since the data are presented in graphical form, we cannot determine which of the two models of equations (5) and (6) is best. Nevertheless, plots of inter-quartile ranges versus velocity indicate that subject variability was roughly proportional to the magnitude of the stimulus over a 50:1 range of velocity.

The reader should be aware of the extreme sensitivity of the results of experiments of this type to the experimental conditions. This is perhaps particularly true of experiments designed to study the perception of velocity, since it is very difficult to conduct such an experiment without providing additional cues. For example, if the subject is presented with a target which moves across his visual field for a fixed length of time, he may estimate velocity indirectly by estimating the distance travelled by the stimulus. Alternatively, if the stimulus moves a given distance, then velocity may be estimated by noting the length of time the target is presented. If a string of targets is moved across the visual field, the subject

may estimate velocity by counting the rate at which the individual elements of the stimulus disappear from view. Rachlin investigated some of these experimental procedures and found that the subject's estimate of a given stimulus velocity was significantly dependent on the way in which the stimulus was presented.

Brown, et al (Ref. 15) investigated the accuracy of positioning responses. The subject was shown a stimulus pointer positioned randomly along the horizontal arc, the display was removed, and the subject was required to position a response pointer at the spot he thought was under the stimulus pointer. Weiss (Ref. 16) performed a somewhat similar experiment. The subject was provided with a control stick which controlled the position of a stimulus light. With no control being exercised by the subject, the light was displaced by the experimenter to a random position along the horizontal arc and shown briefly in that position. The light was blanked, and the subject was instructed to move the control stick the amount he thought would be necessary to center the stimulus light. The ranges of response magnitudes required in these experiments was from 0.6 to 40 cm of control movement for Brown, et al and from 1.5 to 6 degrees of angular control displacement for Weiss. Both experiments showed the variability of the response to increase monotonically with stimulus magnitude.

Against this data we tested the models of equations (5) and (6) relating either the standard deviation or the variance of the response linearly to stimulus magnitude, and we find that both models fitted both sets of data with a correlation coefficient greater than 0.90. (A slightly better fit was obtained with the model of equation (5) for Weiss's data; equation (6) fitted better the data of Brown, et al.)

The coefficients of the model of equation (5) are

$$\sigma_x = .36 + .075\ X \tag{7}$$

for the data of Weiss, and

$$\sigma_x = .56 + .050\ X \tag{8}$$

for the results of Brown, et al, where X is the desired response and σ_x is the standard deviation of the response in the same metric units. The presence of the nonzero standard deviation obtained via extrapolation of the experimental data suggests that the model of psychophysical noise presented in equation (4) should be revised to include a component of irreducible noise. A modified version of this simple model might be

$$\delta x(t) = a(t) + n(t) \cdot x(t) \tag{9}$$

where n(t) is a multiplicative noise process, as before, and a(t) is an independent additive noise process to account for the apparently irreducible component of the response variability.

In summary, we have reviewed some of the psychophysical literature in an attempt to discover the basic features of human variability. We have seen that generally (but not always) both the errors of estimating the magnitude of a stimulus and the minimum resolvable stimulus difference increase monotonically with stimulus magnitude. Much of the data can be described reasonably well by a model which assumes a linear relation between the standard deviation of the human's response and the desired response magnitude. It should be noted, however, that functional relationships other than linear provide equally good descriptions for much of the same data.

Because of the sensitivity of the experimental results to the conditions of the experiment, the psychophysical data cannot be used to predict with any degree of precision the quantity or spectral shape of controller remnant to be expected in a given manual control situation. The results reviewed here serve primarily to validate our contention that remnant sources are primarily multiplicative in nature.

Visual Processing Considerations

In this section we review a portion of the literature on visual perception which relates to the following two areas of interest to the study of manual control. First, since we shall present manual tracking results obtained during peripheral viewing of the display, we should like to predict a priori the effect on controller remnant of the location of the display in the visual field. Secondly, we would like to know whether or not the observer is able to perceive directly the velocity of a moving target, or whether velocity estimates are obtained from successive samples of position. Interpretation of the remnant data is crucially dependent on the answer to this question.

Measurement of visual thresholds.--Although it appears to be impossible to conduct an experiment in which the observer's sole task is to estimate visual position or velocity, it is quite possible to investigate thresholds related to the perception of these quantities. The results of this type of experiment are not confounded by the operations of input-output transformation and output production, since only a yes-or-no response is required. Since a threshold-like phenomenon may be interpreted as reflecting a type of perceptual noise process, one would expect a direct relationship between visual threshold and controller remnant (at least that part of the remnant that arises from an irreducible observation noise process).

The kinds of visual threshold of pertinence to the study of controller remnant are measures of visual acuity (Refs. 17-22) and motion threshold (Refs. 20-23). (Other types of threshold, such as the minimum light intensity perceivable, are not of relevance here.) It is not our intent to review this literature thoroughly, but rather to indicate trends in these thresholds that may imply trends in human controller remnant.

Visual acuity is basically a measure of the observer's ability to discriminate two closely-spaced stimuli (for example, two parallel line segments separated by a very narrow dark band). Acuity is taken as the reciprocal of the minimum angular separation at which the observer is able to distinguish between two such objects and a single object. A typical figure for this type of acuity is about 1 minute of visual arc. It should be pointed out, however, that the absolute level of acuity varies widely with experimental factors such as the type of visual object used in the acuity test (Refs. 19,20), the lighting conditions (Ref. 22), and whether the target pair is stationary or moving (Refs. 17,18). Accordingly, we can expect to obtain only qualitative predictions of controller remnant from acuity measurements reported in the literature.

The trend most relevant to our discussion is the change in visual acuity that occurs as the display is moved from the fovea into the peripheral visual field. Acuity decreases monotonically with angle-of-view for photopic levels of illumination (i.e., for light intensity sufficient to allow cone vision). For scotopic levels of illumination (rod vision), Gordon (Ref. 21) has found that the acuity reaches a maximum in the range of 5-7 degrees visual arc, then decreases monotonically with increasing visual angle. Gordon also investigated the relationship between motion threshold and form threshold (the latter being very similar to displacement threshold). He found that the two types of threshold increased with increasing peripheral angle in about the same way.

If we assume that error position and velocity are the relevant input quantities in a simple manual control situation, then we infer from the above study of visual acuity that controller remnant ought to increase as the display is moved into the peripheral region of the visual field. Whether this increase will be significant or not depends on the importance of an increase in visual threshold relative to other sources of remnant. Recent manual control results imply that such threshold effects are important. Levison and Elkind (Ref. 1) have found, for example, that fractional remnant power, along with mean-squared system error, increases with peripheral viewing angle of the display.

Another phenomenon peculiar to peripheral vision is the tendency of a peripheral image to fade after a fixation period of a few seconds. Various mechanisms for this effect have been postulated, such as retinal effects, deficiencies in the transmission of a peripherally-viewed signal, and an inability to maintain attention to peripheral stimuli (Ref. 24). Whatever the cause, we can expect this effect to degrade the subject's ability to track peripherally, since fixed elements of the display (such as a reference indicator) cannot be depended upon to provide useful information after a few seconds' time.

Perception of velocity.--Psychologists have puzzled for quite some time over whether the visual velocity of a moving object is perceived directly or is estimated from successive samples of visual position (Ref. 23). In order for us to interpret the remnant data obtained in situations that require the subject to produce an output proportional to error velocity, we must decide *a priori* whether the subject perceives rate directly or whether he really derives it from position observations.

Rashbass (Ref. 25) has obtained evidence, based on studies of occulomotor behavior, that indicates that velocity is perceived directly. He instructed his subjects to track visually a moving spot of light, and he measured the response of the subjects' fixation point to stimulus variations consisting of: (1) a step displacement, (2) a constant-velocity ramp, and (3) a step immediately followed by a ramp. Step inputs produced saccadic responses in the occulomotor system (i.e., the fixation point changed in a series of one or more sudden jumps) that were roughly proportional to the size of the input. Ramps, on the other hand, produced smooth tracking, or pursuit, movements of the eye which were linear with the input for velocities up to about 10 deg/sec. (The responses to ramps greater than about 3 deg/sec also included one or more saccades, apparently to correct for the build-up in positional error.)

When the input consisted of a step of variable size plus a ramp of fixed velocity, the response was generally the superposition of a saccade whose direction and magnitude were appropriate to the step component of the input and a pursuit movement appropriate to the ramp component of the input. Perhaps the most important experimental result was the response of the eye position to an input consisting of a step followed by a ramp directed oppositely from the direction of the step (i.e., back through the origin). Rashbass found,after a short delay,that: (1) the eye began moving in the direction of the ramp (i.e., away from the initial location of the stimulus), (2) a saccade then occurred in the direction of the initial step, and (3) the eye continued with its pursuit movement in the direction of the stimulus ramp. Rashbass concluded from this experiment that the pursuit system was responding to a direct perception of velocity; if it responded, instead, to closely-spaced samples of stimulus position, the initial motion of the eye would have been in the direction of the initial step displacement.

These results of Rashbass are confirmed by a similar set of experiments performed by Young (Ref. 26). He obtained the same results. In addition, he constructed a sampled-data model for eye-movements that incorporates direct sensing of velocity.

Perception of acceleration.--The extent to which the human can estimate the acceleration of a moving target is of direct concern to the study of manual control, particularly with respect to display requirements. We know of no experiments that have been reported which calibrate the precision with which acceleration is estimated by visual inputs alone. Some indirect evidence is available in the manual control literature, however, to indicate that perception of acceleration is not very good. Birmingham and Taylor have concluded from their studies of display quickening, for example, that high-order vehicle dynamics cannot be controlled effectively by displays of error position alone (Ref. 27). This conclusion implies that the human cannot effectively take high-order derivatives of the displayed variable.

Summary of Background Discussion

In the first section of this chapter we define controller remnant in general as that component of the controller's output that is not deterministically related to system inputs. Since no constraints are placed on the nature of the deterministic portion of the controller's response, remnant measured in a way consistent with this definition will not include the effects of modelling errors on the part of the systems analyst. Limitations of the manual control data that are available, however, require that some constraint be placed on the controller's deterministic response. A quasi-linear representation of the controller is adopted, and we adopt the working definition of controller remnant as the portion of the controller's response not related to the system inputs by the controller's describing function. The latter definition is justified on the grounds that

the experimental conditions which yielded the available manual control data were such as to minimize nonlinearities in the controller's behavior.

A review of the remnant literature indicates that the sources of remnant are basically multiplicative in nature. We find some evidence that remnant is dependent on various control system parameters. It is strongly dependent on the order of the vehicle dynamics; it is not clear whether or not there is a significant dependency with respect to input characteristics. Recent evidence indicates that a reasonably stable representation of controller remnant can be obtained by referring remnant to an equivalent noise source injected at the controller's input. Some investigators have postulated that remnant arises primarily from time-variations in the controller's gain and time delay. We do not find enough evidence in the literature, however, to support this conclusion.

A partial review of the psychophysical literature indicates that the degree of randomness in a human's response to a given stimulus varies monotonically with the magnitude of the response. In some cases we find that the standard deviation of the response varies nearly linearly with response magnitude. This phenomenon reinforces our conclusion that the sources of controller remnant are basically multiplicative in nature.

A partial review of the literature on vision reveals relationships between visual acuity, motion thresholds, and peripheral angle-of-view which imply that controller remnant ought to increase as the display is located at increasingly peripheral locations in the visual field. We also find evidence to show that the controller can estimate directly the velocity of a moving target; he apparently does not have to base such an estimation on successive samples of position. On the other hand, it appears that the controller cannot obtain derivatives higher than first-order from a signal presented visually.

III. THEORETICAL DEVELOPMENT

In this chapter we present a model of the psychophysical noise processes underlying controller remnant and develop a theoretical framework in which to predict the effects of these processes on the characteristics of the remnant.

A Model for Equivalent Multiplicative Observation Noise

Remnant may arise from a variety of sources such as: (1) errors in observing the displayed state of the vehicle, (2) errors in executing the intended control movement, (3) time-variations in the controller's strategy, and (4) structural deficiencies of the deterministic model for the human controller (e.g., deviations of the controller from a continuous, linear, control strategy). We shall not consider remnant sources of the last category. A list of possible remnant sources – those considered here as well as those not considered – is given in Table 1.

Accordingly, we shall analyze remnant obtained from manual tracking experiments in which: (1) the plant dynamics are linear, (2) the subject is required to view a single display and manipulate a single control, and (3) the task requirements are such that the subject apparently devotes continuous attention to the tracking task. The display may present one or more variables, either linearly correlated or independent, and the subject may derive additional input variables by performing linear operations on the variables that are explicitly displayed.

The human controller in such a situation can often be represented approximately by the simplified linear model diagrammed in Figure 2. The pilot's control characteristics are considered as the cascade of three linear operations: a central-processing time delay, an equalization network, and the neuromuscular dynamics.

Table 1

Listing of Potential Remnant Sources

A. Those considered in the report:

1. Observation noise
2. Motor noise
3. Random variations in the controller's gains
4. Random variations in the controller's time delay

B. Those not considered in this report:

1. Nonlinear behavior
2. Consistent time variations in the pilot's control strategy
3. Effects of discontinuous input or output behavior by the controller
4. Inadequate modelling of the controller's describing function

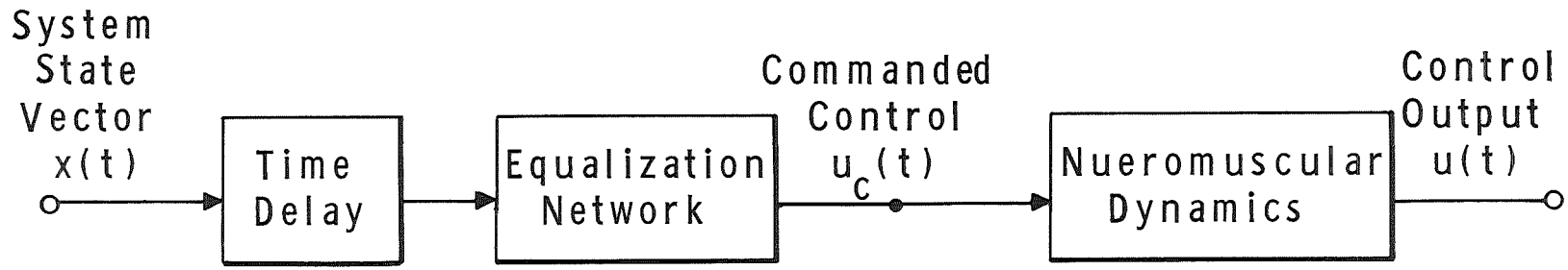

FIG.2 SIMPLIFIED MODEL OF THE HUMAN CONTROLLER IN A MULTIVARIABLE, SINGLE-CONTROL TRACKING SITUATION

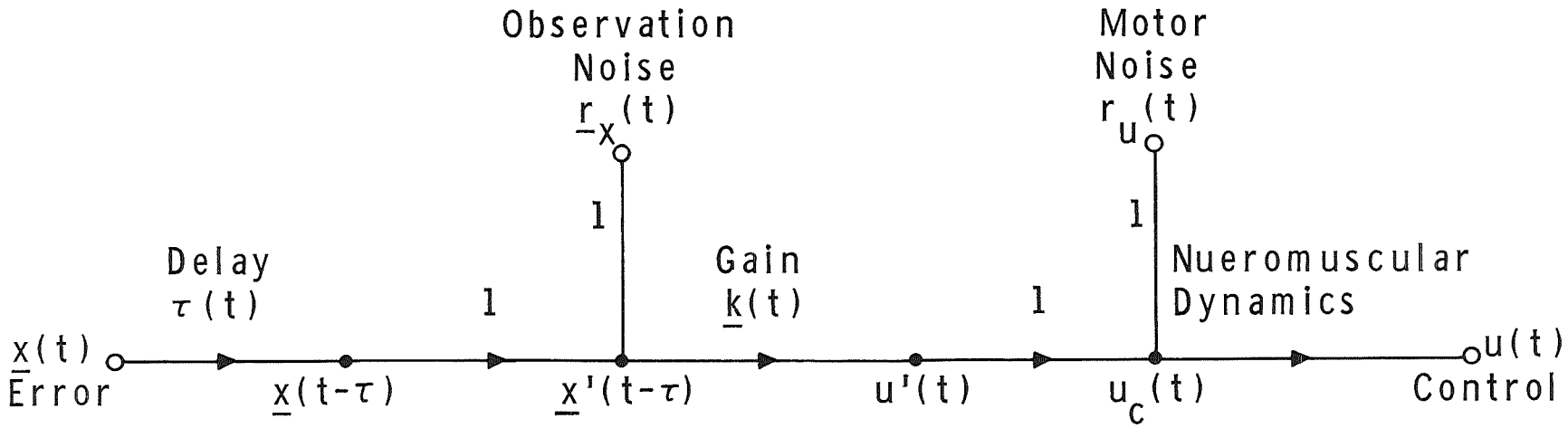

FIG.3 LINEAR FLOW DIAGRAM OF THE HUMAN CONTROLLER

The time delay is represented for mathematical convenience as occurring entirely in the visual pathways. The equalization network represents the means by which the subject attempts to optimize his control strategy to match a given control situation. The neuromuscular dynamics are assumed to be relatively invariant and not a significant source of remnant. Models for all three elements are discussed by McRuer, et al (Ref. 4). Specifically, they find that the controller's equalization can be well approximated in many control situations by a first-order lead-lag network.

In order to simplify the ensuing discussion, we shall assume that the entire state vector $\underline{x}(t)$ is displayed to the subject. This assumption is by no means crucial to the theoretical development, however; in general, the components of $\underline{x}(t)$ are those variables that are displayed explicitly, plus whatever additional variables the controller can derive from them. We also assume that the vehicle dynamics contain at least one integration so that we may neglect controller-induced lag in the following analysis.

Potential sources of remnant are shown in the linear flow diagram of Figure 3. All components of the system state vector $\underline{x}(t)$ are delayed by an amount $\tau(t)$, which is assumed to vary randomly about an average delay of τ_o. To the delayed state vector is added an observation noise vector $\underline{r}_x(t)$. The perceived error $\underline{x}'(t)$ is processed by the gain vector $\underline{K}(t)$, which varies randomly about an average gain of $\underline{K}_o$, and a motor noise component $r_u(t)$ is added to yield the "commanded" control motion $u_c(t)$.* The neuromuscular subsystem operates linearly on $u_c(t)$ to provide the control motion $u(t)$.

*One might argue that the motor noise component is more appropriately added after the neuromuscular system than before it, or that it should be distributed between input and output. Since we have adopted a linear model of the controller, however, all of these treatments of motor noise are essentially equivalent from a mathematical point of view. One source can be linearly transformed via the neuromuscular system dynamics to the other. Mathematical convenience dictated our choice of treatment here.

The controller's remnant has generally been considered to be noise added to either the controller's input or output (Refs. 1-4). While this is correct in a mathematical sense, most psychophysical data indicate that the underlying sources of remnant behavior are multiplicative, rather than additive, as discussed in Chapter II of this report. Thus, the injected noise sources and time-variations of system parameters are represented as follows:

$$\left.\begin{aligned} \underline{r}_x(t) &= \underline{N}_x(t) \cdot \underline{x}(t-\tau(t)) \\ r_u(t) &= n_u(t) \cdot u'(t) \\ \Delta\underline{K}(t) &= \underline{N}_k(t) \cdot \underline{K}_o \\ \Delta\tau(t) &= n_\tau(t) \cdot \tau_o \end{aligned}\right\} \qquad (10)$$

where $\underline{N}_x(t)$ and $\underline{N}_k(t)$ are diagonal noise matrices and $n_u(t)$ and $n_\tau(t)$ are scalar noise terms. These multiplicative noise components are dimensionless quantities. The perceived state vector, control command, and controller gain matrix, including both the steady-state and variational components, are

$$\left.\begin{aligned} \underline{x}'(t) &= [\underline{I} + \underline{N}_x(t)] \cdot \underline{x}(t-\tau(t)) \\ u_c(t) &= [1 + n_u(t)] \cdot u'(t) \\ \underline{K}(t) &= [\underline{I} + \underline{N}_k(t)] \cdot \underline{K}_o \\ \tau(t) &= [1 + n_\tau(t)] \cdot \tau_o \end{aligned}\right\} \qquad (11)$$

The following important assumptions are made concerning the noise processes and state variables:

(a) Only multiplicative noise terms are important in the production of controller remnant. Additive terms (which were found necessary to explain some of the psychophysical data reviewed in Chapter II) can be safely ignored, because the available tracking data has been obtained from experiments designed to minimize threshold effects.*

(b) The variational matrices $\underline{N}_x(t)$ and $\underline{N}_k(t)$ are diagonal. Thus, the noise associated with the estimation of one component of the state vector is independent of the behavior of the remaining components.

(c) All noise components implied by equation (11) are gaussian and linearly independent of each other, of the state vector, of the controller's output, and of the system forcing function. (Note that we do not assume linear independence of the components of the state vector.)

(d) The multiplicative noise processes are functionally independent of control system parameters in all respects. These processes, thus, are assumed to arise from basic physiological noise sources that are truly internal to the human.**

*The degree to which this assumption is valid will be evident from the experimental results reported in Chapter V.

**We shall not attempt to identify the physiological processes underlying the multiplicative noise processes postulated here. Rather, we simply offer this construct as a model which we hope will be useful in the prediction of controller remnant.

In order to simplify our treatment of the expression, we shall assume that variations of the controller's time delay are small compared to the average time delay. We may then use the first two terms of a Taylor series expansion to obtain the first-order effects of time delay variations. The general form of the first-order Taylor series expansion is

$$x(\alpha) \doteq x(\alpha_0) + (\alpha-\alpha_0)\dot{x}(\alpha_0) \tag{12}$$

Replacing α by $t-\tau(t)$ and $\alpha-\alpha_0$ by $-n_\tau(t) \cdot \tau_o$, we obtain

$$x(t-\tau(t)) \doteq x(t-\tau_o) - n_\tau(t) \cdot \tau_o \cdot \dot{x}(t-\tau_o) \tag{13}$$

By applying the relationships of equations (11) and (13) to the solution of the linear flow diagram of Figure 3, we compute the following relationship between the state vector and the commanded control motion:

$$u_c(t) = [1 + n_u(t)] \cdot \underline{K}_o' \cdot [\underline{I} + \underline{N}_k'(t)][\underline{I} + \underline{N}_x(t)] \cdot$$

$$[\underline{x}(t-\tau_o) - n_\tau(t)\tau_o\, \dot{\underline{x}}(t-\tau_o)] \tag{14}$$

where the symbol (') denotes matrix transposition. Consideration of only the first-order noise terms yields the following approximation to controller remnant:

$$u_c(t) \doteq \underline{K}_o'\, \underline{x}(t-\tau_o) + \underline{K}_o'[n_u(t)\underline{I} + \underline{N}_k'(t) + \underline{N}_x(t)] \cdot \underline{x}(t-\tau_o)$$

$$- n_\tau(t)\tau_o \underline{K}_o'\, \dot{\underline{x}}(t-\tau_o) \tag{15}$$

The first term of equation (15) represents the controller's average response characteristics (i.e., the controller's describing function exclusive of the neuromuscular dynamics). The second term indicates that motor noise, observation noise, and time-variations in controller gain contribute in a similar manner to remnant. Observation noise and gain variations are shown to be mathematically indistinguishable in the tracking context under consideration. The motor noise component differs from the observation noise only in its dimensionality (it is a scalar since we are considering single-control situations only). It is therefore conceivable that the effects of motor noise could be differentiated from those of observation noise by a series of multivariable, single-control tracking experiments, although we expect this would be extremely difficult.

Variations in controller time delay, however, appear to contribute to the controller's remnant in a somewhat different way than the other processes that we have considered. Whereas the observation noise, motor noise, and gain variation noise terms act as multipliers on the state vector, the time delay variation term operates on the first derivative of the state vector. Analysis of a series of simple manual control situations which are designed to vary the relationship between the state vector and its first derivative (as might be accomplished, for example, by varying the bandwidth of the forcing function) might therefore provide a means for determining whether time-delay variations or other noise sources are the dominant sources of remnant.

Since motor noise, observation noise, and gain variational noise terms have essentially identical effects on controller remnant, we can combine these three noise terms into a single equivalent noise term without loss of generality.* (That is, there seems

*We are not specifically considering human controller sampling effects as a source of remnant in our theoretical treatment. Nevertheless, our "equivalent" noise model may, in part, account for such behavior. We note that Bekey and Biddle (Ref. 9) have discovered the effects of random sampling on controller output to be indistinguishable from the effects of other noise processes.

to be no measurement that we can make to differentiate one noise source from another.) We have chosen to combine them into an equivalent multiplicative observation noise term which we call $\hat{\underline{N}}_x(t)$. Thus,

$$\hat{\underline{N}}_x(t) = n_u(t)\underline{I} + \underline{N}_k(t) + \underline{N}_x(t) \qquad (16)$$

We have selected observation noise, rather than some other equivalent representation, primarily for the following reasons:

1. Recent analyses of human controller remnant indicate that a model of noise injected at the controller's input provides a more consistent representation of remnant than does a model of noise injected at the controller's output. It seems most appropriate, therefore, to consider an underlying multiplicative source related to the controller's inputs.

2. We note in equation (15) above that all noise terms interact in a multiplicative way with the variables that are displayed, or with their first derivatives. Thus, the construction of the model lends itself most naturally to an observation noise treatment.

3. We feel that a model of human controller remnant based on observation noise considerations will prove to be most useful in terms of engineering applications. This is especially true in the field of display design, since one might reasonably expect the level of the controller's remnant to be related to the qualities of the displays with which he is provided.

4. Recent developments in modern control theory allow the treatment of noise added to the system state variables. An observational noise representation of controller remnant thus facilitates the application of modern control theory to the study of problems in manual control.

Since all the remnant terms in equation (15) are scaled by the controller's gain vector $\underline{K}_o$, we can write the expression for the commanded control input as

$$\underline{u}_c(t) = \underline{K}'_o[\underline{x}(t-\tau_o) + \underline{r}_x(t)] \tag{17}$$

where

$$\underline{r}_x(t) = \hat{\underline{N}}_x(t) \cdot \underline{x}(t-\tau_o) + n_\tau(t)\tau_o \dot{\underline{x}}(t-\tau_o) \tag{18}$$

Thus, although the basic remnant generating sources are considered to be multiplicative, it is still possible to refer remnant to an additive noise process, viz., $\underline{r}_x(t)$. This is important because of the limitations of our experimental procedures. Our model of observation noise is thus analogous to the model of human randomness diagrammed in Figure 1. We emphasize that the injected noise is a vector process; all variables that the controller is able to derive from the display (whether or not responded to in the particular control situation) are disturbed by linearly independent noise components.

If $\hat{\underline{N}}_x(t)$ and $n_\tau(t)$ are linearly independent of each other and of $x(t)$ and $\dot{x}(t)$, the spectrum of the equivalent injected observation noise may be obtained from convolution of the matrix noise spectrum with the vector spectrum of the state variables.* In the special case for which the multiplicative noise processes are white noise processes, the injected vector noise process is also white with a power density level of

$$\underline{R}_x = \underline{P}_x \underline{\sigma}_x^2 + \tau_o^2 P_\tau \underline{\sigma}_{\dot{x}}^2 \tag{19}$$

where $\underline{P}_x$ and P_τ are the power density levels of $\hat{\underline{N}}_x(t)$ and $n_\tau(t)$, respectively.

*The degree to which the noise processes are correlated with the state variables, and the effects of such correlations on our measurements, are discussed in detail in Appendix A of this report.

To summarize the theoretical development thus far, we have postulated that human controller remnant arises from underlying psychophysical sources that are basically multiplicative. Noise sources considered are: (1) observation noise, (2) motor noise, (3) time-variations in controller gain, and (4) time-variations in controller time delay. The first three of these processes appear to be mathematically indistinguishable and are lumped into a single equivalent multiplicative noise acting on the state variable vector. For analytical purposes, controller remnant can be considered to arise from injected (i.e., additive) observation noise components, where these signals are given as the product of the multiplicative noise components with the corresponding state variables. If we assume that the multiplicative noise sources are white noise processes, then the additive observation noise components are also white noise processes which scale with the mean-squared levels of the state variables and their first derivatives.

Predictions Based on the Observation Noise Model

We now use the model of observation noise developed in the preceding section to predict the nature of human controller remnant in simple manual control systems. We specifically analyze a set of compensatory tracking tasks in which only the system error (a scalar variable) is displayed explicitly to the controller. Note that we cannot classify this type of control situation as a "single-variable" tracking task, because we know on the basis of previous manual control studies (Refs. 1,4) and from psychophysical data (Ref. 25) that the controller can in general extract error rate information as well. We shall henceforth refer to this class of control systems as a "single-display" system to imply a single physical display with a single quantity displayed thereon.

The following assumptions are made, partly to simplify the analysis, and partly to apply necessary constraints on the controller's behavior.

1. The multiplicative noise processes responsible for controller remnant are sufficiently wideband so as to be considered white noise processes. These white noise processes are linearly independent of each other and of all other signals circulating through the system.

2. The subject perceives error rate directly; he does not estimate it by differentiation of his estimates of the error.

3. The subject is not able to obtain useful estimates of second and higher order derivatives of the displayed variable; nor can he estimate the time integral of the displayed variable with sufficient accuracy to be of use in a manual control context.

4. The subject is able to control the rate-of-change of his output (be it force or position) as well as the output variable itself.

The first assumption above was made to simplify the mathematical analysis. If we assume that the multiplicative observation noise processes are independent white noise terms, then the equivalent injected observation noise components will also be white noise processes which scale with mean-squared error and mean-squared error rate, as illustrated by equation (19). This prediction is consistent with some of the remnant data obtained by Elkind (Ref. 2), as analyzed by McRuer and Krendel (Ref. 3).

The second assumption is supported by the direct psychophysical evidence reviewed in Chapter II. There is no direct evidence to support assumptions 3 and 4. They are justified primarily on the grounds that they lead to a simple, consistent model of controller remnant.* We can take some comfort in the fact that there is indirect support for the assumption concerning the higher order derivatives in the studies of Birmingham and Taylor (Ref. 27) on systems with quickened display. In addition, there is abundant neurophysiological evidence that the human can sense his output rate (Ref. 28) thus making assumption 4 more plausible.

*As an historical aside, much of the theoretical development presented in this section benefits from the considerable hindsight gained from having first analyzed our remnant data. Nevertheless, the logical flow of the information contained in this report is considerably enhanced if our "predictions" are discussed at this stage.

We have had to make the assumptions concerning the human's perceptual and response capabilities because proper application of the observation noise model is crucially dependent upon such considerations. Before we are able to associate noise processes with each of the variables estimated by the controller, we must determine what those variables are. Consider, for example, a compensatory tracking situation in which the vehicle dynamics are a simple gain and the error position is displayed. From the describing function data reported in the literature (Refs. 1-4) we know that the controller's control strategy, to a first approximation, is to act as an integrator on the error. There are at least two ways in which he might do this: (1) he may attempt to make his control output proportional to his estimate of the integral of the displayed error, or (2) he may simply estimate the error and use this information to control his output rate. The two models of perception and response are entirely equivalent in terms of the controller's describing function, but not in terms of the remnant that we will predict. In the first case we would add a white noise term to the signal corresponding to the integral of the error, which is almost equivalent analytically to adding an integrated white noise process to the error; in the second case, we would add the white observation noise process directly to system error. The spectral characteristics of the closed-loop controller remnant will obviously differ according to which model is chosen.

According to the above assumptions, the controller's perceptual and response activities, when required to control a single-display system, are limited to: (1) estimation of system error, (2) estimation of error rate, (3) explicit control of his output variable, and (4) explicit control of the rate-of-change of his output variable. In addition, the controller generates whatever input-output transformations are appropriate. A model for controller behavior which includes all these operations is shown in Figure 4. In order to keep the analysis mathematically tractable,

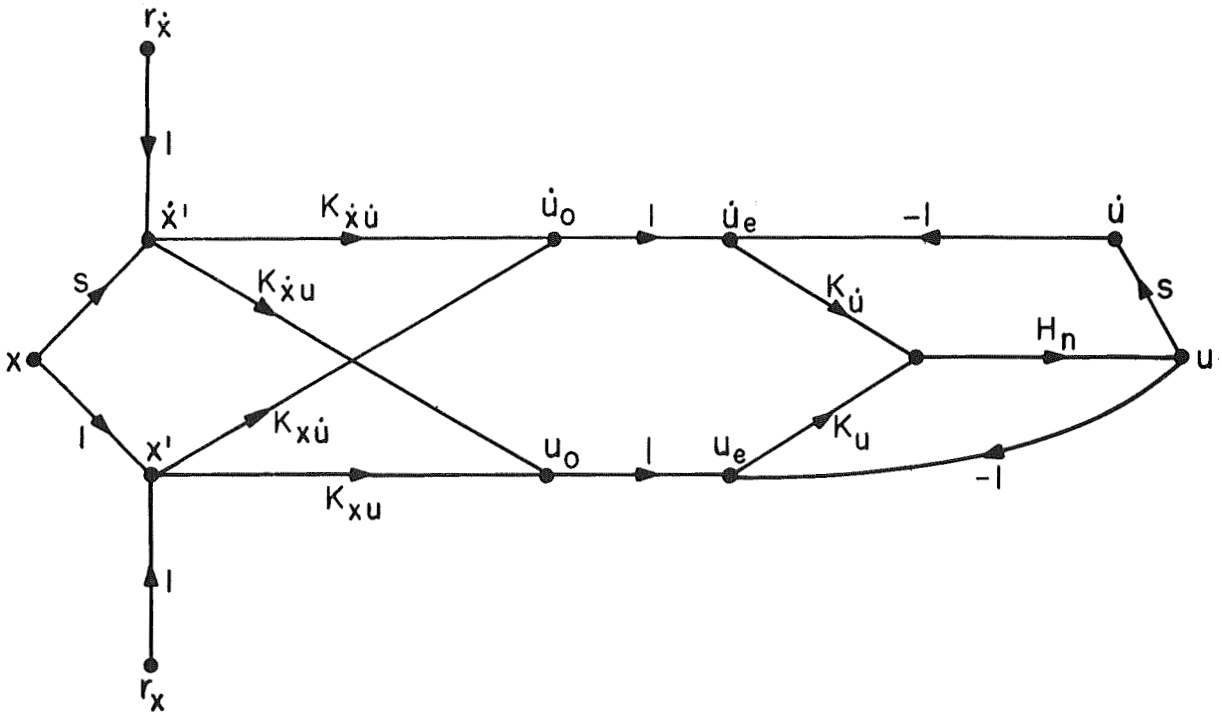

FIG.4 MODEL OF THE HUMAN CONTROLLER IN A SINGLE-DISPLAY CONTROL SITUATION

we assume that the controller generates a four-element gain network to transform his estimates of error, x, and error rate, $\dot{x}$, into a commanded control position u_o and a commanded control rate $\dot{u}_o$. Two additive observation noise processes, r_x and $r_{\dot{x}}$, are associated with the input variables x and $\dot{x}$, respectively. We assume further that the controller compares the commanded control signals with his actual control behavior u and $\dot{u}$ to yield the error signals e_u and $e_{\dot{u}}$. These signals are acted upon by the gains K_u and $K_{\dot{u}}$, the outputs of which are summed and processed by the final common pathway $H_n(s)$ into which we are lumping the controller's time delay and other aspects of the neuromuscular system dynamics.

This model is not meant to be taken literally from a neurological point of view. It is one of possibly many models that will provide the degree of freedom in the controller's response necessary to match our remnant data. The model is nevertheless physically reasonable in that it does not imply any type of signal processing that is impossible for the controller to perform.

Let us now analyze the model of Figure 4 to show that it predicts a describing function of a form that is consistent with results reported in the literature. We define the controller's describing function as the best linear relationship between the input-correlated portion of the control signal to the input-correlated portion of the system error. Since the noise terms r_x and $r_{\dot{x}}$ are, by assumption, linearly uncorrelated with the system forcing function, the controller's describing function H(s) may be derived from Figure 4 as the relationship between U(s) and X(s) with the noise terms set to zero. Thus,

$$H(s) = \frac{\{[K_{xu}\ K_u + K_{x\dot{u}}\ K_{\dot{u}}] + s[K_{\dot{x}u}\ K_u + K_{\dot{x}\dot{u}}\ K_{\dot{u}}]\}\ H_n}{1 + K_u\ H_n + s\ K_{\dot{u}}\ H_n} \qquad (20)$$

where the K's are gain components and H_n represents a dynamical system.* Note that, except for the dynamics contained in H_n, the transfer function contains a single pole and a single zero. Since only three parameters are necessary to describe such a system (the remaining parameter being an overall scale factor), the number of gain components may be reduced to three without a loss in generality.

Let

$$K_x = [K_{xu} K_u + K_{xu}^{\cdot} K_u^{\cdot}] / K_u^{\cdot}$$

$$K_x^{\cdot} = [K_{xu}^{\cdot} K_u + K_{x\cdot u}^{\cdot} K_u^{\cdot}] / K_u^{\cdot} \qquad (21)$$

$$K_u' \quad [1 + K_u] / K_u^{\cdot}$$

If we restrict our investigation to low and mid frequencies where the effects of H_n are negligible (i.e., where H_n is effectively unity), the model of equation (20) reduces to the following approximation:**

$$H(s) \triangleq \frac{K_x + s K_x^{\cdot}}{K_u' + s} \qquad (22)$$

We have now arrived at a model for the controller's describing function which is similar to the lead-lag crossover model of McRuer, et al (Ref. 4), minus the effective human controller time delay. The significant feature of our model development is that it was based on very explicit representations of the controller's perceptual and response processes. Such detail is necessary so that that we can obtain accurate predictions of controller remnant.

*For notational convenience, we shall generally omit the arguments (s) and (jω) from frequency-domain representations of system components and signals.

**Actually, this assumption is only made for convenience; the predicted observation noise spectra are unaltered if H_n is carried along in the analysis.

Before proceeding with an analysis of remnant, we should point out that the above model is capable of approximating reasonably well the low and mid frequency characteristics of the controller's describing functions obtained with simple vehicle dynamics. By appropriate adjustments of the gains K_x, $K_{\dot{x}}$, and $K_{\dot{u}}$, the controller can adjust his describing function to approximate integration (for K dynamics), differentiation (for K/s^2 dynamics), and, by locating the pole and zero at nearly identical frequencies, he can act as a simple gain (for K/s dynamics).

In order to predict the spectral characteristics of controller remnant, we must analyze a model of the entire man-vehicle system. A flow diagram of a generalized single-display tracking situation is shown in Figure 5. The observation noise sources associated with the estimation of x and $\dot{x}$ are assumed to be white with power density levels of R_x and $R_{\dot{x}}$. No restriction is placed on the vehicle dynamics, V, other than that the system be controllable when only the system error variable is displayed.

Since the noise sources $r_x(t)$ and $r_{\dot{x}}(t)$ are assumed to be linearly independent of each other and of the input i(t), the total control power spectrum Φ_{uu} can be considered as the linear combination of the power spectra produced by each of these three inputs acting alone. We find it convenient to combine the responses to r_x and $r_{\dot{x}}$ into a single remnant spectrum. We thus partition the control power spectrum into <u>two</u> components:

$$\Phi_{uu} = \Phi_{uu_i} + \Phi_{uu_r} \tag{23}$$

where Φ_{uu_i} is the input-correlated portion of the controller's response and Φ_{uu_r} is the controller remnant resulting from the joint effects of the observation noise inputs.

From the model of Figure 5 we compute that

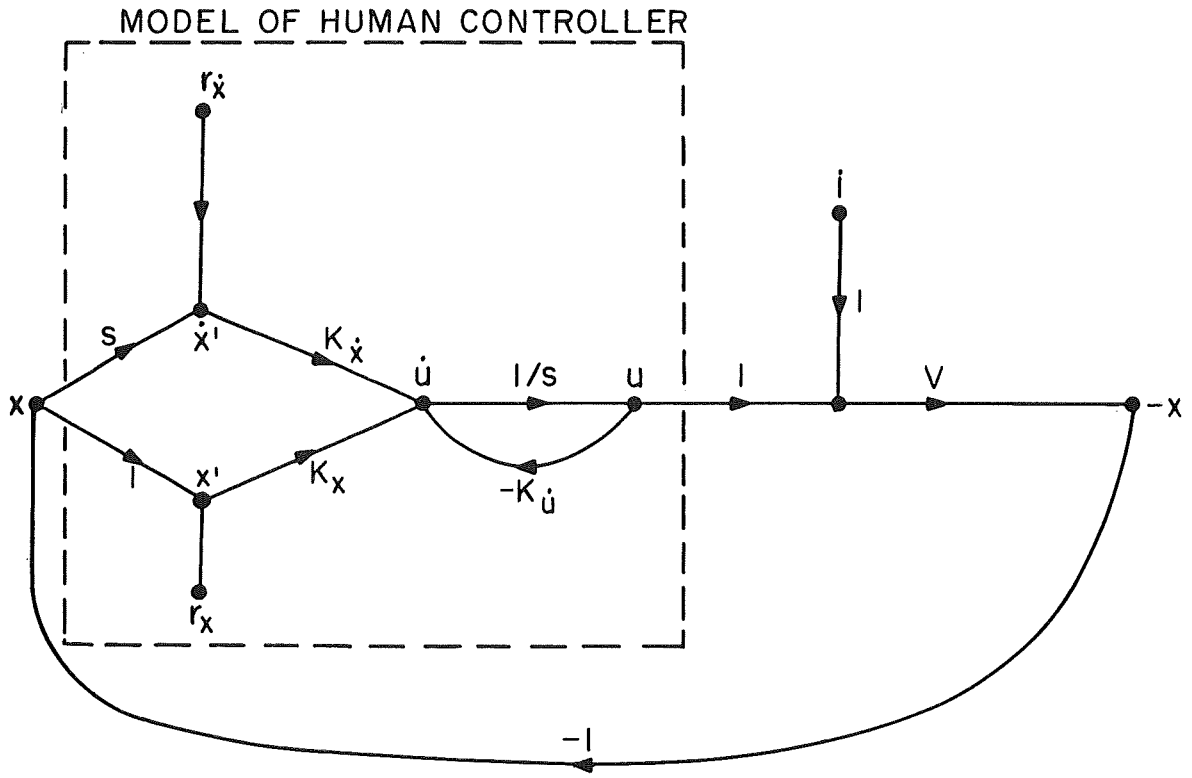

FIG.5 FLOW DIAGRAM OF THE SINGLE-DISPLAY CONTROL SITUATION

(The vehicle output is defined as-x so that we may adopt the standard practice of indicating negative feedback)

$$\left.\begin{aligned} \Phi_{uu_i} &= \frac{K_x^2 + \omega^2 K_{\dot{x}}^2}{\omega^2 + K_u'^2} \cdot \frac{|V|^2 \Phi_{ii}}{|1 + HV|^2} \\ \Phi_{uu_r} &= \frac{K_x^2 R_x + K_{\dot{x}}^2 R_{\dot{x}}}{\omega^2 + K_u'^2} \cdot \frac{1}{|1 + HV|^2} \end{aligned}\right\} \qquad (24)$$

where H is the controller's describing function as given by equation (22).

We could, at this stage, use equation (24) to predict the characteristics of the closed-loop remnant that we expect to see in various single-display situations. We have found it more fruitful, however, to reflect the closed-loop remnant spectrum Φ_{uu_r} to an equivalent scalar open-loop noise process Φ_{rr} injected at one of the controller's inputs. The choice of a particular input to which to refer the remnant is somewhat arbitrary and should not affect the model's validity; nevertheless, the choice does affect the interpretation of the data. Our rule of thumb has been to pick the "reference point" which yields the most readily interpretable results. Once we have picked the remnant injection point, we normalize the spectrum with respect to the mean-squared value of the corresponding variable.

We have chosen to examine an equivalent scalar noise injection process, because our measurement techniques do not readily permit us to reflect a single spectrum, Φ_{uu_r}, back to a vector process consisting of the two input spectra R_x and $R_{\dot{x}}$. Such a procedure would be equivalent to attempting to determine two unknowns on the basis of a single equation. Let us, then, consider an equivalent noise process injected onto the display variable, x, (i.e., the system error). With reference to the flow diagram of Figure 5, this procedure represents the addition of a noise term on the variable labelled "x" which is outside of the collection of elements included

in the "model of the human controller." (Note that this is not necessarily equivalent to setting $r_{\dot{x}}$ to zero and considering the single noise source r_x.) The question we ask then, is: What are the characteristics of a scalar noise process, injected at system error, that we can expect to compute if controller remnant is really caused by a vector noise process with white noise components injected at the variables x' and $\dot{x}$'?

As we show in Chapter IV of this report (in which we describe our computational techniques in detail), the equivalent injected noise spectrum Φ_{rr_x} can be computed from measurements of the input- and remnant-related portions of the control spectrum, plus additional known quantities. This spectrum is given as

$$\Phi_{rr_x} = \frac{\Phi_{uu_r}}{\Phi_{uu_i}} |V|^2 \Phi_{ii} \tag{25}$$

where the subscript (x) denotes the variable to which controller remnant is reflected. From equation (24) we calculate that

$$\Phi_{rr_x} = \frac{K_x^2 R_x + K_{\dot{x}}^2 R_{\dot{x}}}{K_x^2 + \omega^2 K_{\dot{x}}^2} = \frac{R_x + T^2 R_{\dot{x}}}{1 + T^2 \omega^2} \tag{26}$$

where T is a time constant equal to $K_{\dot{x}}/K_x$.

Note the functional dependence of the denominator of Φ_{rr_x} on the frequency variable ω. The numerator, on the other hand, is simply the weighted sum of two white noise processes. Thus, Φ_{rr_x} can be expected, in general, to resemble a first-order noise process.

We can take advantage of equation (19), which allows us to relate a white injected observation noise process to white multiplicative noise processes. Let

$$R_x = \sigma_x^2 \; P_x + \tau_o^2 \; \sigma_x^{\bullet 2} \; P_\tau$$
$$R_x^{\bullet} = \sigma_x^{\bullet 2} \; P_x^{\bullet} + \tau_o^2 \; \sigma_x^{\bullet\bullet 2} \; P_\tau \qquad (27)$$

where P_x and $P_x^{\bullet}$ represent the power density levels of the equivalent multiplicative processes associated with estimation of error and error rate, respectively, and P_τ is the power density level of the multiplicative white noise process associated with variations in the controller's time delay. Substituting equations (27) into equation (26), and normalizing with respect to mean-squared error, we obtain

$$\Phi'_{rr_x} = \Phi_{rr_x} / \sigma_x^2 \qquad (28)$$
$$= \frac{[P_x + \tau_o^2(\sigma_x^{\bullet 2}/\sigma_x^2)P_\tau] + T^2[(\sigma_x^{\bullet 2}/\sigma_x^2)P_x^{\bullet} + \tau_o^2(\sigma_x^{\bullet\bullet 2}/\sigma_x^2)P_\tau]}{1 + T^2 \omega^2}$$

Inspection of equation (28) allows us to predict some of the characteristics of the normalized observation noise without having to specify the vehicle dynamics. If our theoretical model of controller remnant is valid, then we should find experimentally that:

1. The basic frequency dependency of the normalized observation noise is first-order, regardless of input spectral characteristics and the vehicle dynamics.

2. Variations in vehicle dynamics will affect the break-frequency of this noise process because of the adaptive changes that occur in the controller's describing function (hence, in the ratio $K_x^{\bullet}/K_x$). Changes in dynamics may also influence the level of the observation noise through changes in the ratios $\sigma_x^{\bullet 2}/\sigma_x^2$ and $\sigma_x^{\bullet\bullet 2}/\sigma_x^2$.

3. Mean-squared value of the input affects neither the magnitude nor spectral shape of the normalized observation noise so long as the man-vehicle system operates in a linear range.

4. Changes in the shape of the input spectrum (specifically, changes in input bandwidth) will affect the magnitude of the normalized observation noise by varying the ratios $\sigma_{\dot{x}}^2/\sigma_x^2$ and $\sigma_{\ddot{x}}^2/\sigma_x^2$. Input bandwidth should not have a significant effect on the break frequency of the noise spectrum because of the relative insensitivity of the controller's describing function to input parameters, provided that the input bandwidth is sufficiently below the gain-crossover frequency (Ref. 4).

Additional predictions on the behavior of the normalized observation noise spectrum can be obtained if we specify the vehicle dynamics and draw upon our knowledge of how human controllers respond in specific control situations. Consider the situation in which the vehicle dynamics are a simple gain. We know from experimental results reported in the literature (Refs. 1-4) that the controller will attempt to generate a describing function that resembles a first-order system with a relatively low break frequency. Inspection of equation (22) indicates that the controller therefore should set his lead term, $K_{\dot{x}}$ to zero. With the time constant T thus set to zero, equation (28) then simplifies to

$$\Phi'_{rr_x} = P_x + \tau_o^2 \, (\sigma_{\dot{x}}^2/\sigma_x^2) \, P_\tau \qquad (29)$$

Thus, for simple gain dynamics, the measured normalized observation noise will be a white noise process and will be equal to the multiplicative noise process associated with the estimation of system error plus a term arising from time delay variations. We should be able to tell whether or not time delay variations are more or less important than other sources by observing the variations of the noise spectrum with respect to changes in the $\sigma_{\dot{x}}^2/\sigma_x^2$ ratio; provided, of course, that we can design an experiment which varies this ratio.

Let us now consider vehicle dynamics of pure acceleration, K/s^2. We know in this situation that the controller attempts to act as a differentiator. From equation (22) we conclude that K_x should then be very close to zero. It cannot be exactly zero, of course, because the system error would then eventually increase without limit. Nevertheless, the magnitude of this gain coefficient is so small that its effects cannot be seen in the K/s^2 describing function measurements of either McRuer, et al or Levison and Elkind (Ref. 1). Therefore, we shall assume that negligible error will be incurred in our predictions of controller remnant behavior if we assume K_x to be zero in this control situation.

We have found that the K/s^2 results are more readily interpreted when controller remnant is reflected to error rate and normalized accordingly. This transformation is accomplished by the operation

$$\Phi'_{rr_{x_\bullet}} = \omega^2 \left(\frac{\sigma_x^2}{\sigma_{x_\bullet}^2}\right) \Phi'_{rr_x} \tag{30}$$

where Φ'_{rr_x} in this case is the asymptotic solution of equation (28) as $T \to \infty$.

Thus, $$\Phi'_{rr_{x_\bullet}} = P_{x_\bullet} + \tau_o^2(\sigma_{\dot{x}}^2/\sigma_{x_\bullet}^2)P_\tau \tag{31}$$

which is equal to the equivalent multiplicative noise process that we have assumed to be associated with error rate plus the effects of time-delay variations. As in the previous example, proper experimental design should allow us to differentiate between the effects of time delay variations and other remnant sources.

We have now shown that when the vehicle dynamics are either K or K/s^2, proper mathematical treatment of the controller remnant will allow us to identify our measurements directly with the multiplicative white noise processes presumed to be associated with estimation of system error and estimation of error rate. Vehicle dynamics of K/s, however, provide a more complicated measurement situation. We know that the controller's describing function will approximately resemble a simple gain (plus an effective time delay, which we have been neglecting in the describing-function analysis). Equation (22) shows us, however, that this requirement does not constrain his strategy to the same extent as do vehicle dynamics of either K or K/s. To achieve a pure gain describing function, the controller needs only to adjust the break frequency of the numerator term to match the break frequency of the denominator term. All we can predict, then, is the relationship

$$K_x'/K_x = 1/K_u' \tag{32}$$

Since we cannot predict how the controller will choose K_u', unless we employ an optimal control scheme which is beyond the scope of this report*, we cannot predict the break frequency of the normalized observation noise process. The best we can do for this control situation is to predict that the observation noise spectrum, normalized with respect to mean-squared error, will be low-pass of the form indicated in equation (28).

Since we have available the results of tracking experiments conducted with vehicle dynamics of K, K/s, and K/s^2, we can perform the following test to determine whether or not our remnant data are self-consistent. Let $\Phi'^{(o)}_{rr_x}$ and $\Phi'^{(1)}_{rr_x}$ represent the normalized

*A brief description of an appropriate optimal control scheme is given in Chapter VI.

observation noise spectra, referred to system error, obtained with vehicle dynamics of K and K/s, respectively; let $\Phi'^{(2)}_{rr_{\dot{x}}}$ represent the normalized observation noise spectrum, referred to error rate, obtained with K/s^2 dynamics. Noting that $\Phi'^{(o)}_{rr_x}$ and $\Phi'^{(2)}_{rr_{\dot{x}}}$ are equivalent to the expressions on the right-hand sides of equations (29) and (31), respectively, we may then re-write equation (28) as

$$\Phi'^{(1)}_{rr_x} = \frac{\Phi'^{(o)}_{rr_x} + T^2(\sigma^2_{\dot{x}}/\sigma^2_x)\Phi'^{(2)}_{rr_{\dot{x}}}}{1 + T^2\omega^2} \qquad (33)$$

Since $\Phi'^{(o)}_{rr_x}$, $\Phi'^{(1)}_{rr_x}$, and $\Phi'^{(2)}_{rr_{\dot{x}}}$, are normalized observation noise spectra obtained from independent manual control experiments, equation (33) will hold only if the data are internally consistent. Specifically, this expression will allow us to determine whether the magnitude of the normalized observation noise obtained experimentally with K/s dynamics is consistent with the levels of the observation noise processes obtained with K and K/s^2 dynamics. (We do not have a consistency check on the break frequency, however, since this can be estimated only from the K/s measurements.)

Summary of Theoretical Development

Before examining the experimental data, let us review the highlights of this chapter. We begin by postulating that human controller remnant arise from underlying psychophysical sources that are basically multiplicative. Noise sources considered are: (1) observation noise, (2) motor noise, (3) time-variations in controller gain, and (4) time-variations in controller time delay. The first three of these processes appear to be mathematically indistinguishable and are lumped into a single equivalent multiplicative noise matrix acting on the state variable vector. For analytical

purposes, controller remnant can be considered to arise from injected (i.e., additive) observation noise components, where these signals are given as the product of the multiplicative noise components with the corresponding state variables. If we assume that the multiplicative noise sources are white noise processes, then the additive observation noise components are also white noise processes which scale with the mean-squared levels of the state variables and their first derivatives.

We apply this observation noise model to the analysis of a simple manual control situation in which the controller is displayed a single quantity – the system error. We assume that his control strategy consists of the following psychophysical operations: (1) estimation of system error, (2) estimation of error rate, (3) explicit control of output, (4) explicit control of output rate, plus (5) whatever linear transformations are necessary to accomplish the input-output transformations. Analysis of the resulting model of controller behavior (shown in Figure 5) indicates that controller remnant will appear as a first-order noise process when reflected to an equivalent scalar noise process injected on system error. We predict further that (a) normalization with respect to mean-squared error should lead to invariance with respect to mean-squared input; (b) variation of vehicle dynamics should affect both the level and the break frequency of the normalized observation noise; (c) input bandwidth should affect the magnitude, but not the break frequency. In addition, experiments in which the vehicle dynamics are K or K/s^2 should yield observation noise spectra which, when normalized properly, should be directly and easily identifiable with the underlying multiplicative noise processes. Manipulation of the input spectrum in these special control situations should allow us to differentiate between the effects of time-delay variations and other remnant sources.

Experimental data obtained from a variety of simple manual control situations is analyzed in the following chapter to test the predictions based on our white-noise model of equivalent observation noise.

IV. EXPERIMENTAL TECHNIQUES

Experimental Conditions

In order to provide a set of datum points against which to test models of controller remnant, the authors have computed observation noise spectra from data obtained from a variety of single-display, single-control, manual tracking experiments. These experiments were conducted under the sponsorship of the NASA-Ames Research Center during two phases of Contract No. NAS2-3080. The experimental program completed in 1966 has been described in detail in Reference 29. The program recently completed (1968) is currently being documented (Ref. 30). Both experimental programs are described briefly in this section.*

Although these experiments were not designed specifically for investigating controller remnant, we felt that they encompassed a sufficient variety of control situations to provide tests of the important model predictions. We did not analyze the remnant data of other investigators (other than what we have reported in Chapter II), because we found it necessary to have the unprocessed tracking data available in order to obtain all the relevant measures. The selected analytical results found in the literature were usually deficient with respect to one or more important measures.

Command-input system (1966 experiments).--Data from this set of experiments were obtained using the command-input control configuration diagrammed in Fig. 6a. The experimental variables relevant to the data analyzed in this report were vehicle dynamics, input cutoff frequency, mean-squared input power, and the location of the display in the visual field. The vehicle dynamics were either K, K/s, or K/s^2. The inputs were constructed by summing together up to 17 sinusoids and were designed to resemble

*A more detailed description of the experimental and analytical procedures employed in the 1968 experimental program is contained in Appendix C of this report.

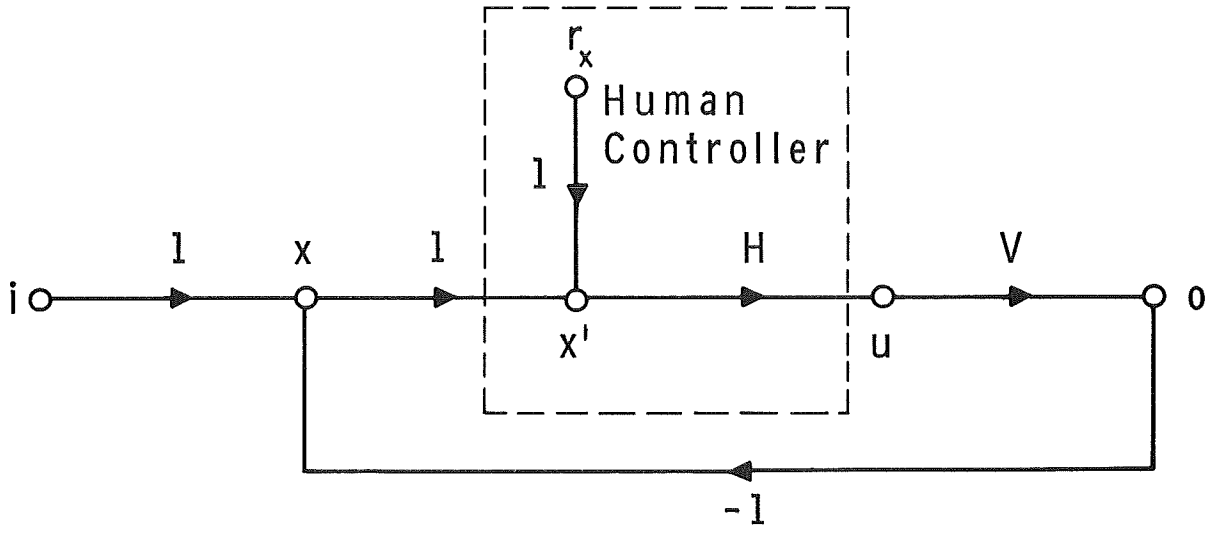

a. Command-input System

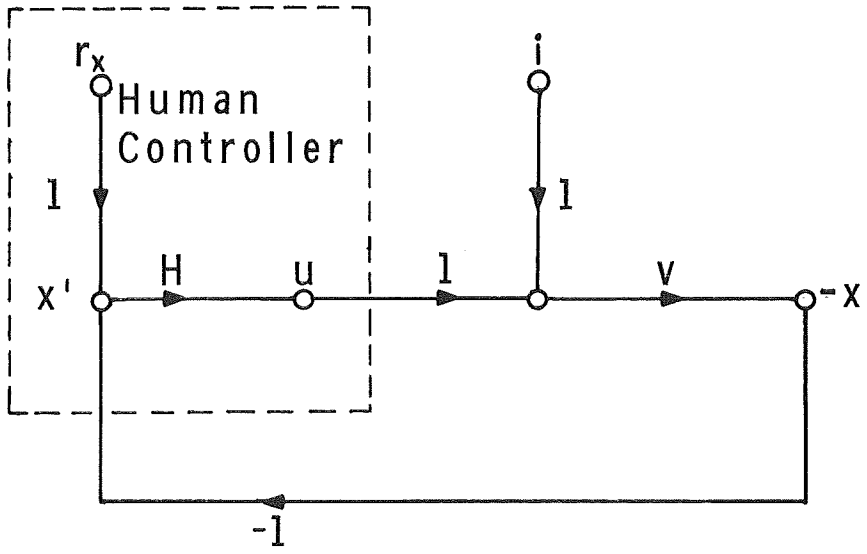

b. Vehicle-disturbance System

FIG.6 FLOW DIAGRAMS OF SINGLE-AXIS MANUAL CONTROL SYSTEMS

rectangular noise spectra augmented by a low-power, high-frequency shelf. Input cutoff frequencies investigated were 0.5, 1.0, and 2.0 rad/sec. For most experiments the mean-squared input was adjusted to yield a mean-squared error, at the display, of approximately 0.12 deg^2 deflection of visual arc. The display was viewed either foveally or was viewed peripherally at an angle of 30°.

The subjects were instructed to minimize mean-squared tracking error and were trained under each condition until an apparently stable tracking performance level was maintained. All run lengths were 4 minutes long, and performance measures were obtained during the middle three minutes of each run.

Vehicle-disturbance system (1968 experiments).--The single-axis tracking conditions investigated during this phase of the program differed from the 1966 experiments with respect to a number of experimental details, although the tracking tasks were basically similar. A vehicle-disturbance forcing function, rather than a command input, was used in the latter program. Figure 6b contains a flow diagram of this control situation. Vehicle dynamics of K/s were used consistently throughout this program, and the forcing function (again constructed as the sum of sinusoids) was designed to simulate a first-order noise process having a break frequency at 2 rad/sec.

The 1968 experimental program was designed primarily to provide manual control data against which to test models of multi-axis control and scanning behavior. The display configuration used in this program is shown in Fig. 7. In order for us to test our multi-axis model, it was necessary to obtain a full set of single-axis measures; analysis of these single-axis experiments appears in this report.

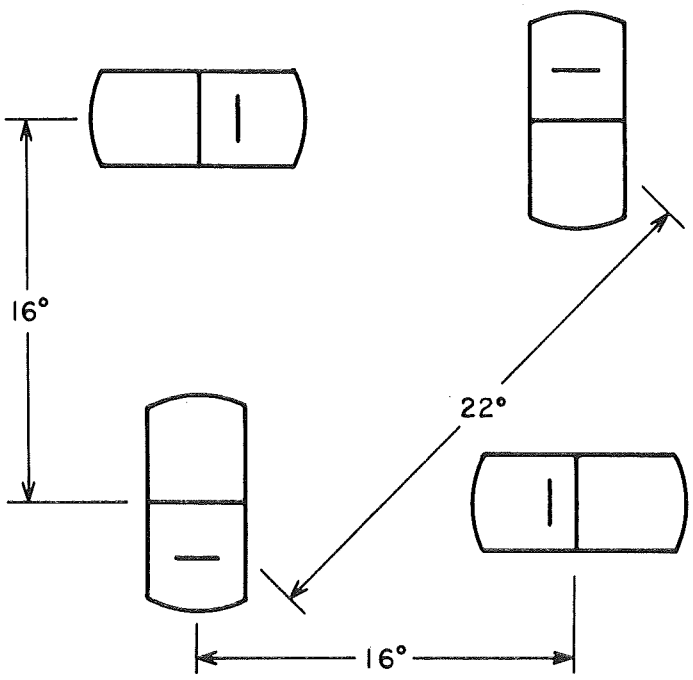

FIG. 7 DISPLAY CONFIGURATION USED IN THE MULTI-DISPLAY TRACKING EXPERIMENTS

Because we knew from previous experience (Ref. 1) that the controller could obtain useful display information peripherally, we again investigated peripheral tracking ability. Our display design had to take account of the fact that the perception of a stationary object located in the periphery would fade after a few seconds' duration (Ref. 24). In particular, all subjects remarked that the zero reference presented on the peripheral display disappeared, and we discovered that tracking performance was materially improved when the subject was able to extrapolate a zero reference line from his fixation point to the peripheral display.* Accordingly, our display arrangement provided certain viewing conditions which allowed such an extrapolation. Specifically, it provided the following four classes of viewing conditions:

(a) foveal

(b) 16° into the periphery with the potential for extrapolation of the zero reference,

(c) 16° into the periphery with no potential for reference extrapolation, and

(d) 22° into the periphery with no reference extrapolation possible.

When tracking peripherally, the subject was required to fixate a specified non-active display for the entire run length (4 minutes) and track whichever display was active in the periphery.

The importance of these data is that in varying viewing conditions, we can be fairly certain we are varying the true observation noise and can conclude that the observed changes in remnant are primarily due to changes in this remnant source.

*See Appendix C for more detail.

Computation of Observation Noise Spectra

We have postulated in Chapter III that controller remnant can be accounted for by an equivalent injected observation noise vector in which an independent noise process is associated with the estimation of each relevant display variable. This injected noise vector, in turn, is assumed to arise from underlying multiplicative noise sources. Our measurement techniques, however, essentially require us to reflect our remnant measurements to a single injection point. We shall therefore analyze most of our data with respect to computing the scalar noise spectrum Φ_{rr}. For economy of words, we shall drop the qualifying adjectives "injected," "scalar," and "equivalent," and talk simply of the measurement of "observation noise." The reader should, nevertheless, bear in mind the various ramifications associated with that expression.

As we pointed out in Chapter III, the variable on which we inject the observation noise process is not uniquely determined. Whatever the point of injection, we can, in principle, analyze the model developed in Chapter III to predict the nature of what we expect to measure. For each control situation investigated, we have chosen a noise injection site such that the computed observation noise spectrum can be most readily interpreted in terms of basic model parameters. Accordingly, we have reflected remnant to a noise on system error when the vehicle dynamics are K, and to a noise on error rate for K/s^2 dynamics, because we predict that this procedure will yield spectra that are equivalent to the spectra of the underlying noise processes. Remnant is reflected to the error signal when the dynamics are K/s, although in this situation we expect the resulting spectral measurements to be related in a more complex way to the underlying noise processes.

Use of the composite sinusoidal inputs facilitates the separation of remnant-induced signals from the linear response to the input, since signal power at other than input frequencies can arise only from controller remnant (except for small contributions due to imperfect generation of the input and to irreducible system noise). In order to compute observation noise spectra from signals that are directly measurable, we make the following assumptions:

(a) The additive observation noise r(t) is linearly uncorrelated with the input signal i(t).

(b) The remnant-induced power varies continuously with frequency in the vicinity of input frequencies.

(c) Signal power occurring at input frequencies arises almost entirely from the linear portion of the system response and only negligibly from controller remnant.

Because of the way in which we have defined remnant, we are able to compute only the component of r(t) that is linearly uncorrelated with the input. (Components of r(t) that are correlated with the input will appear at measurement frequencies and will contribute to what is interpreted as the input-correlated portion of the controller's output.) We show in Appendix A that there is some correlation between i(t) and r(t), even when the underlying multiplicative noise process is considered to be white noise. The effects of this correlation are expected to be small, however.

McRuer et al have claimed that the remnant appears otherwise to vary smoothly through the input frequencies, and some of our own results (see Appendix B of this report) bear this out. The continuity of the remnant spectrum allows us to test the validity of the third assumption in a specific measurement situation. For

example, if the control power measured at a specific input frequency is much greater than the remnant-induced power measured at neighboring frequencies, the measurement at the input frequency may be considered primarily a response to the forcing function. If the remnant-induced power is relatively large, on the other hand, measurements at input frequencies can be expected to include the effects of remnant.

Given that the above assumptions are valid at a particular frequency of interest, the closed-loop control and error spectra may be separated into the following independent input-related and remnant-related components:

$$\left.\begin{aligned} \Phi_{uu} &= \Phi_{uu_i} + \Phi_{uu_r} \\ \Phi_{xx} &= \Phi_{xx_i} + \Phi_{xx_r} \end{aligned}\right\} \qquad (34)$$

where, for the command-input system of Fig. 6a

$$\left.\begin{aligned} \Phi_{uu_i} &= \left|\frac{H}{1 + HV}\right|^2 \Phi_{ii} \\ \Phi_{uu_r} &= \left|\frac{H}{1 + HV}\right|^2 \Phi_{rr_x} \\ \Phi_{xx_i} &= \left|\frac{1}{1 + HV}\right|^2 \Phi_{ii} \\ \Phi_{xx_r} &= \left|\frac{Hv}{1 + HV}\right|^2 \Phi_{rr_x} \end{aligned}\right\} \qquad (35)$$

(The argument ω has been omitted for notational convenience.) For the vehicle-disturbance system of Fig. 6b, the input-correlated portions of both the control and error spectra contain the factor $|V|^2$. The complete set of spectra is:

$$\left.\begin{aligned}
\Phi_{uu_i} &= \left|\frac{HV}{1 + HV}\right|^2 \Phi_{ii} \\
\Phi_{uu_r} &= \left|\frac{H}{1 + HV}\right|^2 \Phi_{rr_x} \\
\Phi_{xx_i} &= \left|\frac{V}{1 + HV}\right|^2 \Phi_{ii} \\
\Phi_{xx_r} &= \left|\frac{HV}{1 + HV}\right|^2 \Phi_{rr_x}
\end{aligned}\right\} \qquad (36)$$

The reader will note that controller remnant has been reflected to a noise injected on the system error (the quantity explicitly displayed); hence, the subscript (x) on Φ_{rr_x}.

Equations 35 and 36 can be solved to yield the observation noise spectrum in terms of the closed-loop control spectra and the input spectra. For the input-command system we obtain

$$\Phi_{rr_x} = \frac{\Phi_{uu_r}}{\Phi_{uu_i}} \Phi_{ii} \qquad (37)$$

and for the vehicle-disturbance system we obtain

$$\Phi_{rr_x} = |V|^2 \frac{\Phi_{uu_r}}{\Phi_{uu_i}} \Phi_{ii} \qquad (38)$$

Although the closed-loop remnant spectrum Φ_{uu_r} could not be directly measured at input frequencies, reasonable approximations were obtained by averaging the remnant measurements obtained over a range of 1/8 octave on either side of each input frequency.

Observation noise measurements were computed according to equations (37) and (38) at frequencies greater than 1 rad/sec. At lower frequencies, this technique yielded anamolous results, apparently because of the adverse effects of irreducible system noise on low-frequency measurements of control power. Low-frequency computations of observation noise were obtained by taking advantage of the fact that the closed-loop remnant error spectrum Φ_{xx_r} is approximately equal to the observation noise spectrum at frequencies well below gain-crossover (i.e., where $|HV|>>1$). Thus, at frequencies of 1 rad/sec and lower, the observation noise was assumed equal to the error spectrum at noninput frequencies. Since the gain-crossover frequency was around 4 rad/sec for most conditions, maximum errors of about 0.25 dB were expected from this approximation.

The foregoing derivation has shown how we can reflect controller remnant to a noise injected at the system error. For some of the analyses, we shall instead wish to reflect remnant to a noise on error rate. This operation is accomplished by carrying out the computations designated in equations (37) and (38) and multiplying by ω^2, where ω is the measurement frequency in radians/second.

V. EXPERIMENTAL RESULTS

Normalized observation noise spectra obtained from the various single-display tracking experiments described in the preceding chapter are presented here and are tested against predictions based on the observation noise model of equation (19) developed in Chapter III. Experimental results obtained from peripheral and foveal viewing conditions are discussed in separate sections of this chapter because of some fundamental differences in these results.

Foveal Viewing Conditions

In this section we investigate the relationship between the normalized observation noise and (a) mean-squared input, (b) vehicle dynamics, (c) input bandwidth, and (d) the way in which the input disturbs the system.

Effect of mean-squared input.--We have predicted that the normalized observation noise will be invariant with respect to mean-squared input. This prediction is a necessary consequence of our basic assumption that (a) controller remnant arises from multiplicative noise sources and that (b) the man-vehicle system is otherwise linear.

Figure 8 shows that the observation noise spectrum, normalized with respect to mean-squared error, was essentially invariant over a 9:1 variation in input power. These normalized spectra were obtained for mean-squared input levels of 2.6 and 23 deg^2 equivalent display deflection. Vehicle dynamics were K/s, and the input cutoff frequency was 0.5 rad/sec. These measurements, coupled with the fact that mean-squared error was proportional to mean-squared input (see Ref. 1), thus validate our contentions that remnant sources are multiplicative and that the human controller is essentially linear over our range of experimental conditions.

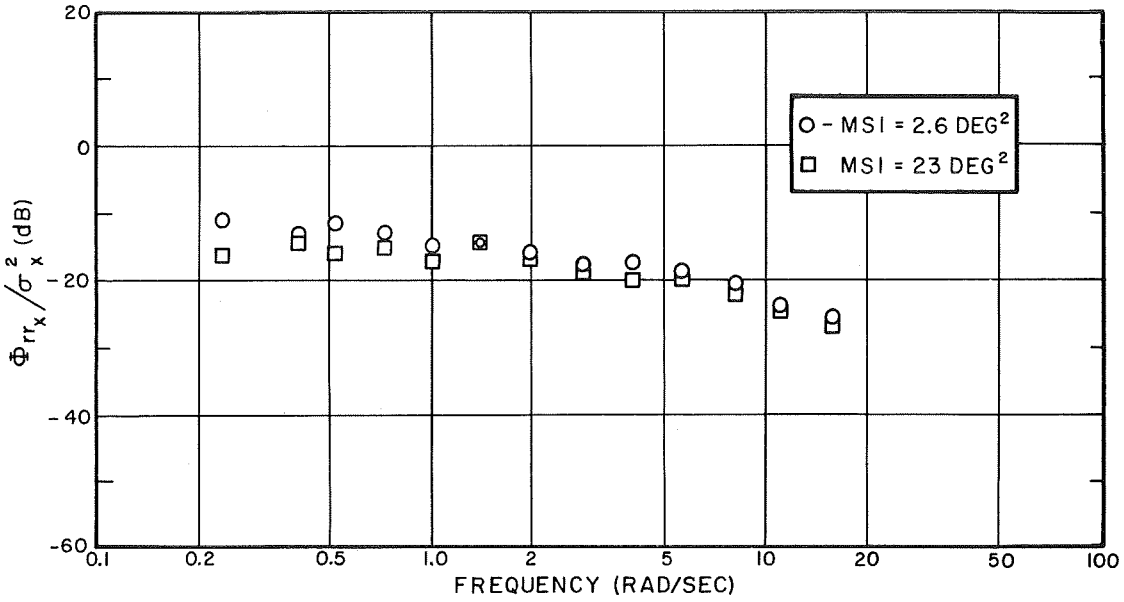

FIG. 8 EFFECT OF MEAN-SQUARED INPUT ON THE NORMALIZED OBSERVATION NOISE SPECTRUM

Vehicle Dynamics = K/s
Input Bandwidth = 0.5 Rad/Sec
Average of 3 Subjects

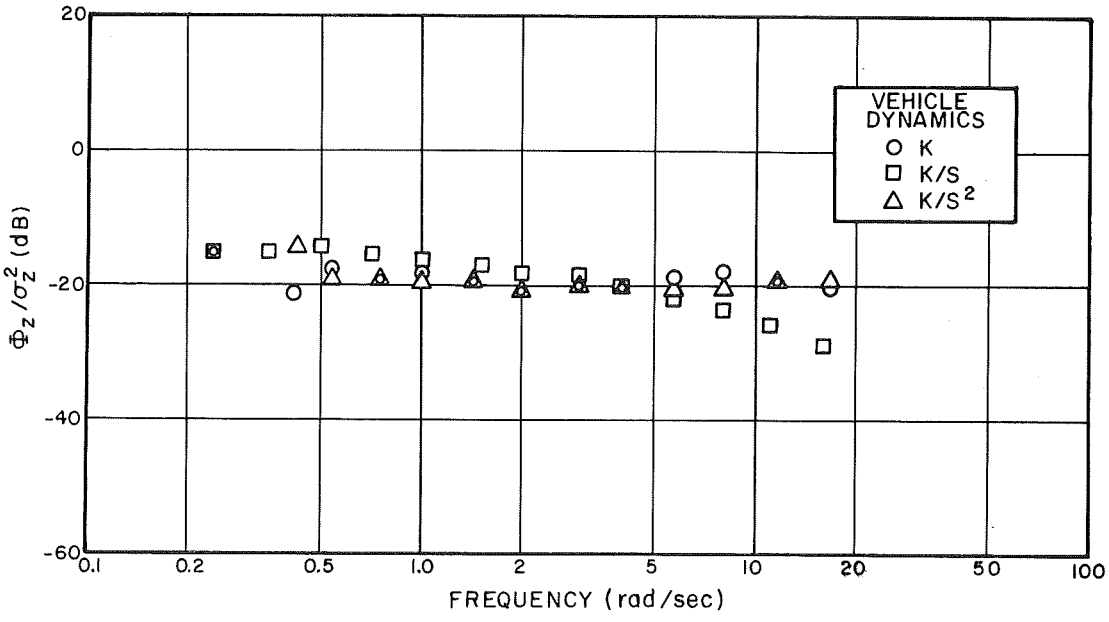

FIG. 9 EFFECT OF VEHICLE DYNAMICS ON THE NORMALIZED OBSERVATION NOISE SPECTRUM

Average of 3 Subjects (K and K/s^2)
Average of 4 Subjects (K/s)

Effect of vehicle dynamics.--Our model of controller remnant predicts that the observation noise spectrum, reflected onto system error, will in general resemble a first-order noise process when the controller is provided with a display of system error only. For the special cases in which the vehicle dynamics are K or K/s^2, however, the observation noise should appear white, so long as the noise is reflected to the signal in which the controller is primarily interested (error position when the dynamics are K, error rate for K/s^2). The situation is less constrained when the dynamics are K/s, and in this case our model cannot predict the location of the break frequency of the first-order process.*

Normalized observation noise measures were obtained from a set of tracking experiments in which the vehicle dynamics were K, K/s, and K/s^2. The data corresponding to K and K/s^2 dynamics were obtained from the command-input system of Figure 6a using the pseudo-rectangular input spectrum having a cutoff frequency at 1 rad/sec. Observation noise measures for K/s dynamics were obtained from both the command-input and the vehicle-disturbance systems, as described in the preceding section of this chapter. The vehicle-disturbance measurements are considered here, since they represent the average of a larger number of samples than do the command-input measurements and are therefore assumed to be a more reliable estimate of the true observation noise spectrum.

The normalized observation noise spectra are shown in Figure 9. The noise processes corresponding to K and K/s dynamics have been reflected to system error and normalized with respect to mean-squared error; the K/s^2 remnant data have been reflected to error rate and normalized accordingly. Figure 9 bears out our predictions concerning the frequency dependencies of the spectra: observation noise

*We are currently investigating optimal control techniques, discussed briefly in Chapter VI, to predict the detailed behavior of the observation noise spectrum as well as other measures of controller behavior.

spectra obtained from K and K/s^2 data are essentially white, and the spectrum corresponding to K/s dynamics is first-order. We also find an unexpected consistency in the results: the power density levels of the two white noise spectra are identical to within 1 dB (which is approximately our measurement error), at 0.01 units of normalized power per rad/sec.* The implications of this result are explored in the discussion presented at the end of this section.

In Chapter III we showed that if our remnant data were self-consistent with respect to our model, the three observation noise spectra would be related as

$$\Phi^{(1)}_{rr_x} = \frac{\Phi^{(0)}_{rr_x} + T^2(\sigma^2_{\dot{x}}/\sigma^2_x)\Phi^{(2)}_{rr_{\dot{x}}}}{1 + T^2\,\omega^2} \qquad (39)$$

where $\Phi^{(0)}_{rr_x}$, $\Phi^{(1)}_{rr_x}$, and $\Phi^{(2)}_{rr_{\dot{x}}}$, represent the normalized observation noise spectra obtained with vehicle dynamics of K, K/s, and K/s^2, respectively. We computed a $\sigma^2_{\dot{x}}/\sigma^2_x$ ratio of 27 from the K/s data, and a time constant T=0.29 sec was obtained by best-fitting the corresponding observation noise spectrum by a first-order noise process. These values were combined with the measured values of $\Phi^{(0)}_{rr_x}$ and $\Phi^{(2)}_{rr_{\dot{x}}}$ to yield a "theoretical" observation noise spectrum for K/s dynamics as given by equation (39). Figure 10 shows that the theoretical and measured observation noise spectra agree to within 1 dB at most measurement frequencies. The experimental measurements and the model of controller remnant presented in this report are thus seen to be internally consistent.

*All power density spectra shown in this report represent the summation of power at symmetrically-located positive and negative frequencies.

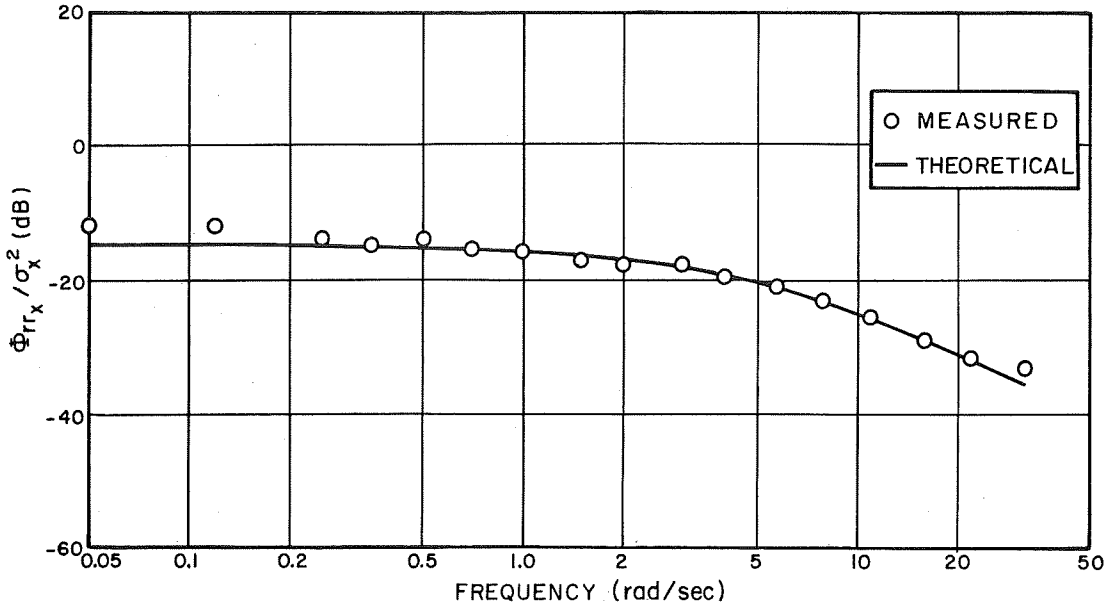

FIG. 10 COMPARISON OF MEASURED AND THEORETICAL NORMALIZED OBSERVATION NOISE SPECTRA

Vehicle Dynamics = K/s

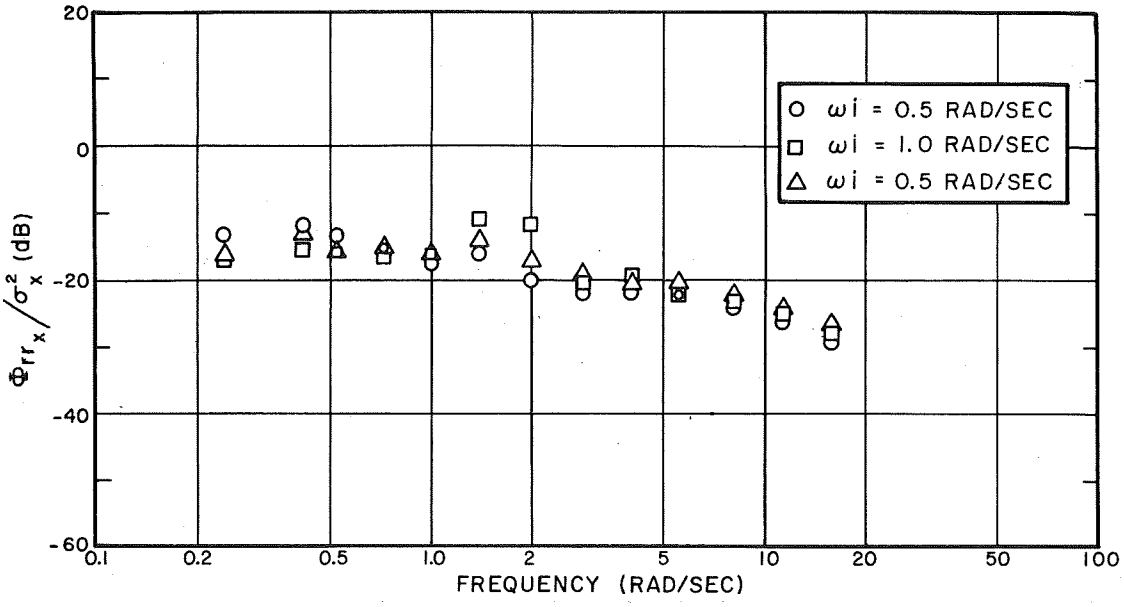

FIG. 11 EFFECT OF INPUT BANDWIDTH ON THE NORMALIZED OBSERVATION NOISE SPECTRUM

Vehicle Dynamics = K/s
Average of 3 Subjects

Effect of input bandwidth.--Equation (27) of Chapter III shows that the level of normalized observation noise spectrum is a function of the ratios $\sigma_{\dot{x}}^2/\sigma_x$ and $\sigma_{\dot{x}}^2/\sigma_x^2$ (which we shall henceforth refer to as the "variance ratios" for economy of notation). The way in which these ratios affect the spectral level depend on the relative contributions of time-delay variations and other noise sources to the generation of controller remnant. Thus, if we are able to analyze a set of experiments in which only these ratios are varied, we might be able to determine whether or not time-delay variations are an important source of remnant.

It was hoped that analysis of a set of experiments in which the input was varied would produce the desired changes in the variance ratios. The command-input control configuration was employed with inputs having cutoff frequencies of 0.5, 1, and 2 rad/sec. Vehicle dynamics were K/s. Normalized observation noise spectra corresponding to these three input bandwidths are compared in Figure 11. The total spread among the curves is generally less than 4 dB, and the differences do not appear to be consistent.

Before we can interpret the invariance of the normalized observation noise with respect to input bandwidth, we must first examine the data to see if the variance ratios have,in fact,been affected by the change in input bandwidth. Unfortunately,we do not have the $\sigma_{\ddot{x}}^2$ data available. We do have the $\sigma_{\dot{x}}^2$ measurements available,however,and these should provide some insight into the importance of time-delay variations. For example, if the $\sigma_{\dot{x}}^2/\sigma_x^2$ ratio varies with input bandwidth and the normalized observation noise spectrum does not, then we can reasonably assume that time-delay variations are not important (unless, of course, $\sigma_{\ddot{x}}^2/\sigma_x^2$ varies in an opposite manner--an unlikely circumstance). On the other hand, if $\sigma_{\dot{x}}^2/\sigma_x^2$ does not change, the results are inconclusive.

The ratios $\sigma_{\dot{x}}^2/\sigma_x^2$ are shown in Table 2 for the three bandwidths investigated. These ratios changed only minimally with changes in bandwidth, ranging from 29 to 40 (a difference of only 1.4 dB). Thus, we cannot conclude on the basis of this experiment whether or not time-delay variations are an important source of remnant. This experiment does serve, nevertheless, to provide additional experimental evidence in support of our model of controller remnant. The model predicts that the normalized observation noise spectrum will remain unchanged so long as the ratio $\sigma_{\dot{x}}^2/\sigma_x^2$ remains unchanged (provided that the vehicle dynamics are not changed), and this is exactly what we observe.

Effect of input injection point.--Our model of controller remnant predicts that the observation noise spectrum will not depend on the spectrum of the displayed error signal, other than as the spectral shape affects the variance ratios. Accordingly, we have compared the observation noise spectra obtained from the command-input and vehicle-disturbance systems in order to test this prediction.

The vehicle dynamics were K/s in both experiments. The rectangular input spectrum used in the input-command system had a cut-off frequency of 2 rad/sec; a simulated first-order noise process having a break frequency of 2 rad/sec was employed in the vehicle-disturbance experiment.

To illustrate that the error spectra were different in the two experiments, error power spectra obtained from the same subject with the two system configurations are compared in Figure 12. The input-correlated portion of the spectrum was approximately a sawtooth function of frequency when the augmented rectangular forcing function was injected as a command signal. The error spectrum was a noticeably smoother function of frequency when a simulated first-order noise process was applied as a disturbance to the vehicle. The

TABLE 2

Effect of Input Bandwidth on the Ratio of Error-Rate Variance to Error Variance

Input Bandwidth (rad/sec)	σ_x^2 deg^2	$\sigma_{\dot{x}}^2$ $(deg/sec)^2$	$\sigma_{\dot{x}}^2/\sigma_x^2$
0.5	.25	10.0	40
1.0	.25	8.6	37
2.0	.13	3.8	29

Average of 3 subjects, 1 run/subject
Command-input configuration

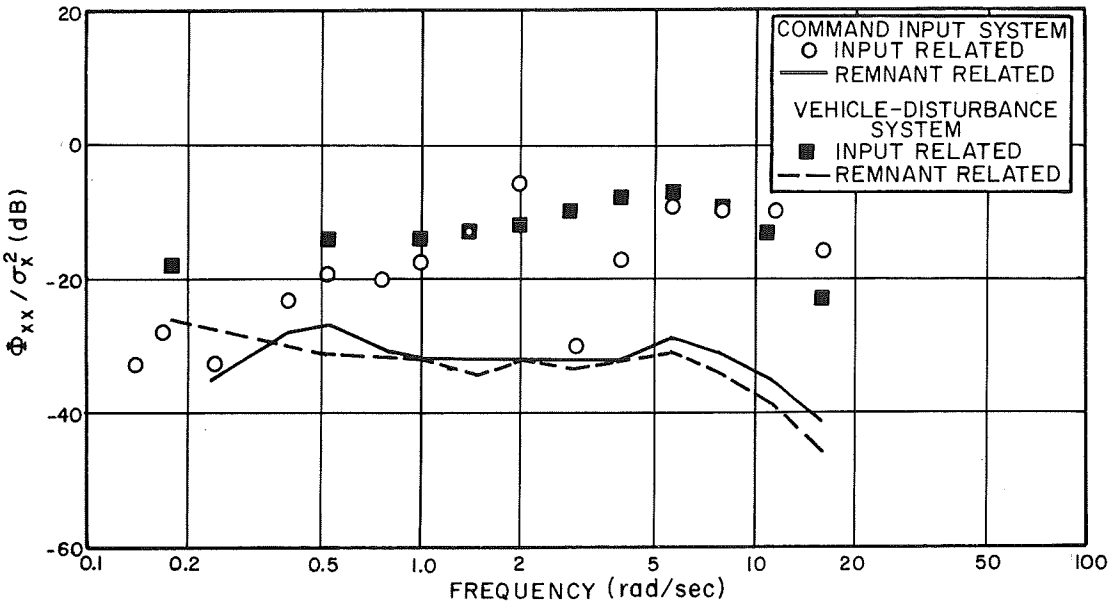

FIG. 12 EFFECT OF INPUT INJECTION POINT ON THE NORMALIZED ERROR SPECTRUM

Vehicle Dynamics = K/s

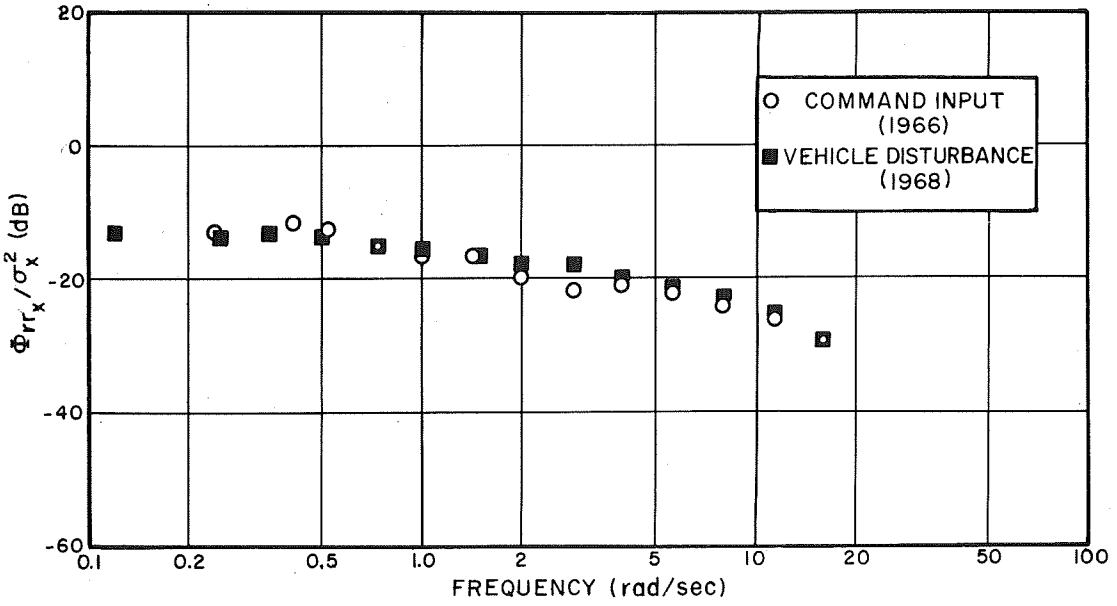

FIG. 13 EFFECT OF INPUT INJECTION POINT ON THE NORMALIZED OBSERVATION NOISE SPECTRUM

Vehicle Dynamics = K/s
Average of 3 Subjects (Command-Input System)
Average of 4 Subjects (Vehicle-Disturbance System)

remnant-related components of the two error spectra were, however, quite similar. We note that the $\sigma^2_{\dot{x}}/\sigma^2_x$ ratios for the command-input and vehicle-disturbance systems were, respectively, 29 and 27. Since we do not have the data available, we must assume that the $\sigma^2_{\ddot{x}}/\sigma^2_x$ ratio was also relatively invariant.

Figure 13 shows that the normalized observation noise spectra are nearly identical, differing by less than 1 dB at most measurement frequencies. We thus have an additional example that controller remnant is relatively invariant with respect to input parameters. Furthermore, the observation noise level is related to system error only in that it scales with the variance of the error and its derivatives.

Summary and Discussion.--We have compared the predictions of the theoretical model for controller remnant developed in Chapter III with the experimental data obtained from a variety of single-display control situations. All the data analyzed thus far confirm our basic hypothesis that controller remnant can be accounted for by linearly independent, white, multiplicative noise components associated with each of the system variables that the controller is required to estimate. Specifically, we have seen (1) that the normalized observation noise is invariant to mean-squared input (which indicates the basic multiplicativity of controller remnant),(2) that it is also invariant with respect to input bandwidth and the point at which the input is injected (which indicates that the underlying processes are functionally independent of input parameters), and (3) that the observation noise measurements vary with respect to system dynamics in the manner predicted (thereby validating the basic structure of our entire model of the human controller).

The observation noise spectra computed from the experiments with K/s dynamics were found to be internally consistent, within the framework of our model, with the noise spectra obtained with

dynamics of K and K/s^2. We identified the latter two measurements with the noise processes associated with the estimation of error and error rate, respectively, and these measures were manipulated according to our model to yield a quantitative prediction of the observation noise spectrum that would be measured when the vehicle dynamics are K/s. This predicted spectrum was seen to coincide with the spectrum computed from the experimental K/s data. This result is extremely important, because it indicates that the noise processes associated with the estimation of the displayed variables are independent of controlled-element dynamics. Although parameters of the input signal and vehicle dynamics may affect the spectrum of the closed-loop remnant (and, thus, the scalar observation noise to which this remnant can be reflected), the sources underlying controller remnant can be modelled as white noise spectra which themselves are independent of control system parameters.

Before we shall be able to specify exactly how the model is to be applied in a general control situation, further experimentation will be necessary to determine the extent to which time-delay variations are important. Since time-delay variations affect the closed-loop remnant differently from other potential remnant sources (scaling with error-rate variance instead of error variance), time-delay effects would appear to be differentiable from other effects via appropriate experimentation. Unfortunately, our experimental data – although entirely consistent with the model – was inadequate to allow us to differentiate among these sources. Note that since the remaining sources of remnant considered in this report (observation noise, motor noise, and gain variations) are seen to be mathematically indistinguishable, our model requires only a single parameter to account for the combined effects of these three sources.

We are intrigued by the discovery that the normalized injected noise spectra measured from the K and K/s^2 data turn out to be white noise spectra having identical power density levels of -20 dB (i.e., 0.01 units of normalized power per rad/sec). Although the -20 dB level does not appear to be of particular significance, the fact that the two spectra are identical implies, at least from one mathematical point of view, that the noise processes associated with the estimation of error and error rate are quantitatively the same. If we extrapolate this result to conclude that a -20 dB multiplicative noise process is associated with each variable that the controller obtains from his display, then we find that we can predict the controller remnant spectrum in a general single-display, multivariable control situation with a model that requires knowledge of only a single parameter. Further experimentation will be necessary to determine the extent to which such an extrapolation is justified. Nevertheless, we have shown that a single-parameter model is adequate to describe remnant in the wide variety of single-display control situations that we have analyzed.

Peripheral Viewing Conditions

We have included results obtained from peripheral tracking experiments because we have found in some of our recent investigations (Ref. 1) that peripheral vision is important in the control of multi-display systems in which the displays are spatially separated. We therefore feel that a study of controller remnant in such situations is important, because it may ultimately lead to design procedures which tend to minimize remnant associated with peripheral viewing and thus improve performance in realistic flight control situations. Furthermore, a comparison of the equivalent observation spectra associated with peripheral and foveal viewing should allow us to investigate directly the nature of true observation noise, unconfounded by the effects of other potential remnant sources.

Frequency dependency of the observation noise spectrum.-- Manual control data were obtained for a peripheral viewing angle of 30^{o} with the input-command system of Figure 6a. Vehicle dynamics were either K or K/s^2. Except for the location of the display, the experimental conditions were identical to the K and K/s^2 experiments that were described previously.

Normalized observation noise spectra for peripheral and foveal viewing are compared in Figure 14. Placement of the display in the periphery increased the level of the normalized observation noise spectra for both K and K/s^2 dynamics. We interpret this result as indicating an increase in the observation noise levels associated with estimation of error and error rate. The peripheral noise spectra may be approximated by a white noise spectrum, although the match is not nearly so good as it was for the spectra corresponding to foveal viewing. The average differences between the peripheral and foveal normalized observation

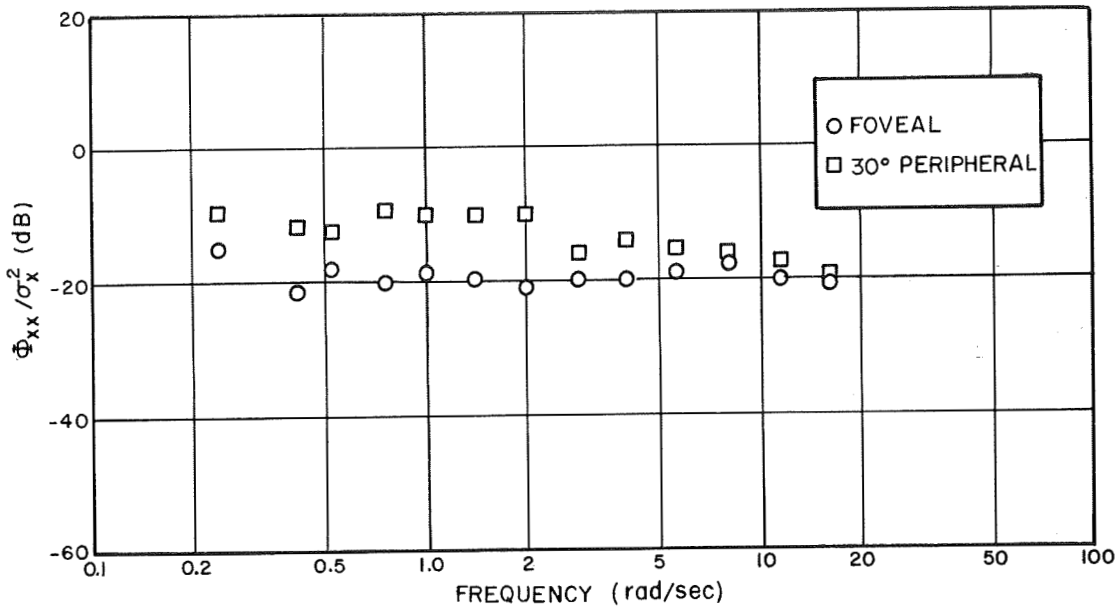

a. Vehicle Dynamics = K

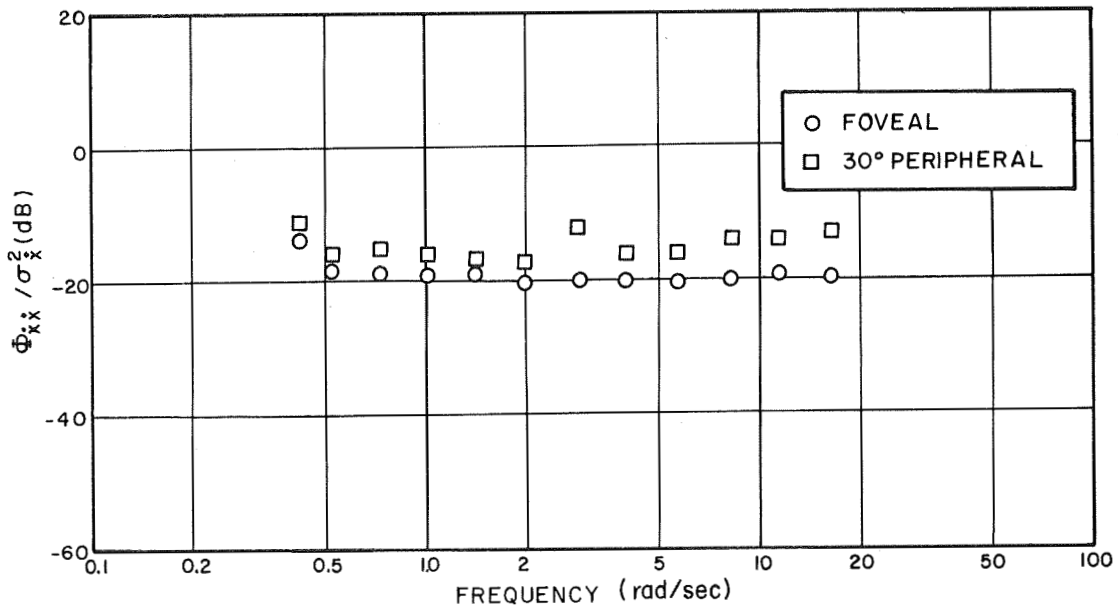

b. Vehicle Dynamics = K/s^2

FIG.14 EFFECT OF DISPLAY LOCATION ON THE NORMALIZED OBSERVATION NOISE SPECTRUM

Average of 2 Subjects

noise spectra were 6.9 dB for K dynamics and 4.5 dB for K/s^2 dynamics, which result suggests that the controller's estimation of error rate is degraded less in the periphery than his estimation of error position.

A set of peripheral tracking experiments was run with K/s vehicle dynamics using the vehicle-disturbance configuration of Figure 6b. Normalized observation noise spectra corresponding to foveal viewing and to three peripheral viewing conditions are shown in Figure 15. The peripheral viewing conditions represented are (1) a 16° viewing angle with reference extrapolation possible, (2) a 16° viewing angle with no reference extrapolation, and (3) a 22° viewing angle without reference extrapolation.

The spectra were all normalized with respect to system error variance. Figure 15 shows that the normalized spectra nearly coincide at frequencies above 2 rad/sec, whereas the spectra differ noticeably at lower frequencies. The trend of the low-frequency behavior of the spectra was consistent with the trend in task difficulty (indicated by the mean-squared error score). The foveal task yielded the lowest MSE score and the lowest level of normalized observation noise, whereas the highest MSE scores and observation noise levels were obtained for the two peripheral viewing conditions that did not permit reference extrapolation. Intermediate performance scores and normalized observation noise levels were obtained for the 16° viewing condition in which reference extrapolation was possible. We conclude, therefore, that the equivalent observation noise levels that we have measured reflect in part the visual characteristics of the display--more precisely, the visual interaction between the display and the observer.

All of the normalized observation noise spectra corresponding to K/s dynamics were approximated by first-order noise processes whose parameters were chosen to minimize the mean-squared differ-

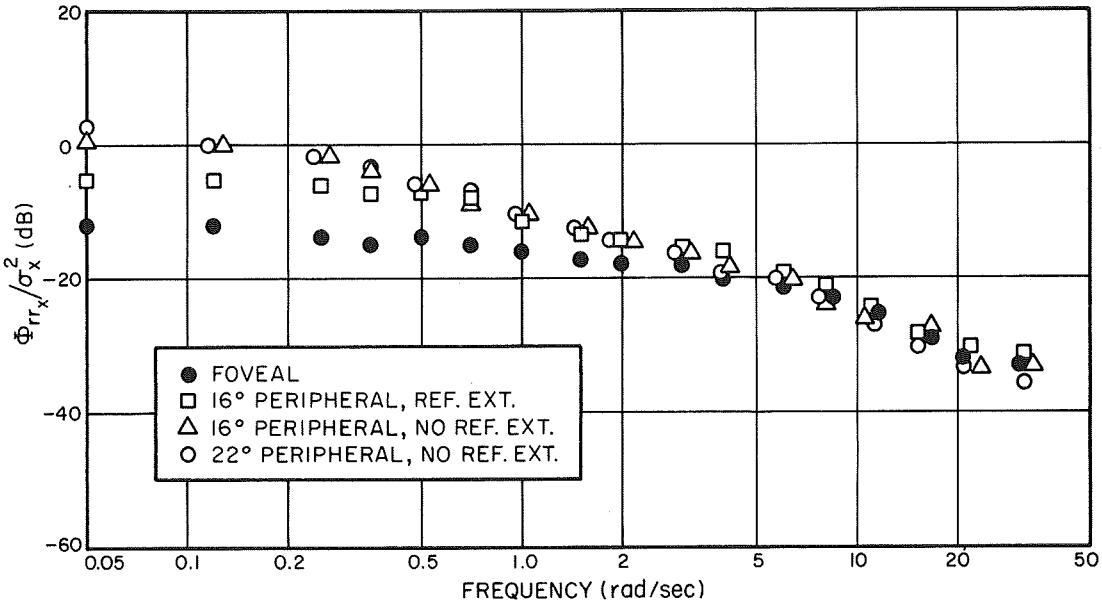

FIG. 15 EFFECT OF VIEWING CONDITIONS ON THE NORMALIZED OBSERVATION NOISE SPECTRUM

Vehicle Dynamics = K/s
Average of 4 Subjects

ence between the experimental and analytical noise processes. Table 3 shows that a progressive degradation of the viewing conditions results in an increase in the asymptotic low-frequency noise level and a decrease in the location of the break frequency.

In summary, we see that the form of the analytic expression that best describes the observation noise spectrum for a given set of vehicle dynamics remains unchanged by placement of the display in the peripheral visual field. The parameter values of these expressions, however, are strongly dependent on the particulars of the viewing conditions.

Multiplicativity.--The data obtained from the peripheral tracking experiments were analyzed to determine whether or not the basic assumption of multiplicativity holds for the remnant sources associated with peripheral viewing. A set of single-variable experiments was performed in which the mean-squared input was varied by a factor of about 4. The control situation was the K/s system-disturbance situation described above, and input power levels of either 0.22 or 0.87 $(deg/sec)^2$ of induced display rate were used.

The observation noise spectra obtained with these two input levels were nearly identical, when normalized with respect to error variance,and are not shown in this report. This identity is a necessary consequence of the model of multiplicativity. It is not sufficient, however, to validate that model. Consider, for example, a situation in which the remnant is caused by a noise injection of a fixed level that is so great that most of the mean-squared system error results from the remnant source rather than from the forcing function. Variations in the forcing function might then have little effect on mean-squared error and, consequently, little effect on the normalized observation noise. An

Table 3

Effect of Viewing Conditions on the Analytic Approximation to the Normalized Observation Noise Spectrum

Viewing Condition	Low-Frequency Level (dB)	Break Frequency (rad/sec)
Foveal	-15.2	3.5
16^{o} peripheral, ref.ext.	- 7.0	1.0
16^{o} peripheral, no ref.ext.	- 4.0	0.8
22^{o} peripheral, no ref.ext.	- 4.0	0.8

Vehicle dynamics = K/s

Average of four subjects, 4 runs/subject

Analytic approximation: $\Phi(\omega) = N \frac{\alpha^2}{\omega^2 + \alpha^2}$

additional consequence of the multiplicative model, then, is that the error variance scale with the input variance.

Table 4 shows that the error variance did not scale with the input variance under all viewing conditions. Although the error variance increased by almost the same factor as the input variance when the display was viewed foveally, the error actually decreased slightly with increasing input variance when the display was viewed peripherally without the benefit of zero reference extrapolation. Table 3 also shows that, except for foveal viewing, the fractional remnant power decreased with increasing input power. Since the fractional remnant power is related to the level of the observation noise, this trend indicates that the absolute level of the observation noise increased by a lesser fraction than the mean-squared input. Thus, for peripheral viewing conditions, our notions of multiplicativity are violated.

Summary and discussion.--We have analyzed the results obtained from a variety of manual control experiments in which the subject was required to view the display peripherally. Normalized observation noise spectra computed from this body of data has been compared with the observation noise spectra obtained from corresponding foveal tracking results. Differences between corresponding pairs of spectra are assumed to reflect differences in the true observation noise process only. Since the manipulator characteristics were held invariant, the motor noise process should have remained invariant also; and since no side tasks were introduced to divert the subject's attention, we would not expect appreciable changes in the time-variational characteristics of the controller's describing function.

Observation noise spectra were computed for control situations in which the vehicle dynamics were K, K/s, K/s^2. As was the case when the display was viewed foveally, the noise spectra obtained

Table 4

Effect of Mean-Squared Input on Error Variance and Fractional Remnant Power

Viewing Conditions	MS Input in $(deg/sec)^2$ 0.22	0.87
a. Error Variance in $deg.^2$		
Foveal	.13	.44
16^o periph. ref.ext.	.38	.71
16^o periph. no ref.ext.	1.0	.88
22^o periph. no ref.ext.	1.3	1.2
b. Fractional Remnant Power*		
Foveal	.19	.25
16^o periph. ref.ext.	.55	.35
16^o periph. no ref.ext.	.66	.53
22^o periph. no ref.ext.	.73	.58

Average of 3 subjects, 1 run/subject

*"Fractional remnant power" is defined as the fraction of signal power that is not linearly correlated with the forcing-function.

under peripheral viewing conditions were approximately white noise processes when the dynamics were K and K/s^2 and were approximately first-order when the dynamics were K/s. The peripheral tracking results thus add further support to our hypothesis that remnant can be considered to arise from an equivalent vector observation noise process of which the components are white noise processes.

Comparison of Foveal and Peripheral Results

The power density levels of the component processes increased as the display was moved from the fovea to the periphery. These changes were interpreted as increases in the noise levels associated with true observation noise; the noise processes corresponding to motor noise, gain variations, and time delay variations were assumed to be invariant with respect to display location and thus to contribute similarly to both the foveal and peripheral remnant data. Since a larger peripheral-foveal difference was found for the normalized observation noise process associated with estimation of error then with estimation of error rate, we conclude that estimation of position is degraded more rapidly than estimation of velocity in the periphery. We note here that the K/s results are consistent with this conclusion. The K/s data revealed that the asymptotic low-frequency behavior of the normalized observation noise spectrum increased, and the break-frequency of the spectrum decreased, as the peripheral viewing conditions were progressively degraded. Our model would account for this behavior by a progressive increase in the gain on error rate and a progressive decrease in the gain on error, and this is exactly how one would expect the controller to behave if his ability to estimate position was degraded relative to his ability to estimate velocity.

The observation noise spectra computed from the peripheral tracking results differ from those computed from the foveal

results in one very important aspect: the peripheral data do not support the notion that controller remnant arises entirely from multiplicative noise processes. This conclusion is based on the failure of the mean-squared system error (particularly the portion related to controller remnant) to scale with mean-squared input. It thus appears that each component of the equivalent vector injected observation noise process should be represented by a model consisting of the sum of three white noise processes: (a) an equivalent multiplicative observation noise process that is scaled by the variance of the corresponding state variable, (b) a multiplicative process to account for time-delay variations which is scaled by the controller's time delay and by the variance of the rate-of-change of the state variable, and (c) an additional process that is related in a manner as yet undetermined to the various factors, both neurophysiological and environmental, that affect the observational characteristics of the particular display.

Because the noise processes subsumed by Item (c) above appear to be the ones that can most easily be manipulated by control system design, a study of these processes may be the most relevant area of investigation in any further studies of controller remnant. We conclude, on the basis of the unexpectedly consistent results obtained from the foveal tracking data, that the truly multiplicative sources of remnant are most likely to represent irreducible noise processes that are inherent to the controller. On the other hand, our experiments on peripheral tracking with and without the facility for zero reference extrapolation show that peripheral observation noise spectra can be significantly affected by the design of the displays. The observation noise spectrum, therefore, should prove to be a useful measure of the true observational characteristics of a display, and means for reducing

this noise process should result in superior displays for multi-display control situations.

VI. CONCLUSIONS

Summary of Results

A white-noise model of equivalent observation noise has been developed for predicting the spectral characteristics of human controller remnant in single-display control situations, and predictions of controller behavior based on this model are verified by the data obtained from a wide variety of manual control experiments. The principal conclusions of this report are as follows.

1. Remnant can be modelled by linearly independent white noise processes injected on each of the variables to be estimated by the controller, where the "estimated" variables are those displayed plus their first derivatives.

2. For control situations in which the display is viewed foveally, the injected noise processes are of the form

$$R_x = P_x \sigma_x^2 + \tau_o^2 P_\tau \sigma_{\dot{x}}^2 \qquad (40)$$

where R_x is the noise process added to the variable "x"; σ_x^2 and $\sigma_{\dot{x}}^2$ are the variances of x and its first derivative, respectively; τ_o is the controller's effective time delay; and P_x and P_τ are white noise processes associated with an equivalent multiplicative observation noise and with time variations in the controller's time delay, respectively. P_x and P_τ are assumed to be entirely independent of system and signal parameters.

3. For all of the foveal tracking data analyzed in this report, we find that the remnant can be modelled by the first term of equation (40) alone; P_x is then given as 0.01 units of normalized power per rad/second, evaluated over positive frequencies only. This parameter is seen to be invariant with respect to mean-squared input, input bandwidth, the point at which the input enters the system, and vehicle dynamics.

4. Equation (40) is not adequate to model the observation noise process when the display is viewed peripherally. An additional white noise process must be included which is related in a complex manner to the characteristics of the displayed variable.

5. It appears that multiplicative processes associated with true observation noise, motor noise, and controller gain variations are indistinguishable in terms of their effects on controller remnant. Time-delay variations should affect remnant somewhat differently; nevertheless, our data base does not allow us to compare the relative contributions of time delay variations and of other potential sources to the production of controller remnant.

Since the data we have are inconclusive as to which of the potential remnant sources are most important, we can only speculate on this matter. The amazing consistency we have found in analyzing the foveal tracking data leads us to suspect that the remnant that we have measured in those situations arises from some sort of irreducible disturbance process operating within the controller's central processor. At this stage in our thinking, we find it most convenient to think of the irreducible component of remnant as arising from time variations in controller gain. (We prefer gain variations to time-delay variations because of the way in which these processes interact with the displayed signals. Our data, however, would support either notion equally well.)

The peripheral tracking results, on the other hand, appear to directly illustrate the effects of true observation noise processes associated with peripheral viewing. Our experimental results with and without the facility for zero reference extrapolation illustrate that this observation noise process, along with system performance as a whole, can be significantly affected by the design of the displays. The observation noise spectrum, therefore, should prove to be a useful measure of the true observational noise characteristics of a display, and a means for reducing this noise process should result in superior displays for multi-display control situations.

Future Work

Although most of the experimental data analyzed in this report confirmed the basic assumptions on which we constructed our model of controller remnant, certain gaps in our knowledge were revealed. We discovered that our data base was not sufficient to allow us to determine the importance of time-delay variations, relative to other potential sources of remnant, and we found that the observation noise associated with peripheral viewing of the displays was related in a nonlinear (and as yet undetermined) way to the characteristics of the observed signals. Consequently, further experimental research will be required before we are able to model adequately the mechanisms responsible for producing controller remnant. Additional theoretical and experimental work will be necessary to develop and test a procedure by which the model of equivalent observation noise can be incorporated into an overall representation of the entire man-vehicle system.

In this chapter we outline additional research along the following paths: (1) investigation of the dependence of observation noise upon system and environmental factors; (2) identification of the processes underlying controller remnant; and (3) application of the observation noise model. The proposed research is summarized in Table 5.

Dependence of observation noise upon system and environment.-- It is clear, both from the neurophysiological structure of the visual system and from studies of perception, that the observation noise process associated with peripheral viewing must be greater than that accompanying foveal viewing. Our measurements of equivalent observation noise (which include the effects of a number of factors besides true observation noise) bear this out in a manual control context. Furthermore, we have seen that the observation noise changes with the display characteristics, as well as with the

Table 5

Outline of Proposed Future Work

A. Dependence of observation noise upon system and environment

1. Relation between observation noise and display parameters:

   a. Distance of display into the periphery

   b. Radial along which display is placed in the periphery.

   c. Type of presentation provided by the display.

2. Dependence on signal characteristics (peripheral viewing):

   a. Signal amplitude

   b. Shape of signal spectrum

3. Dependence on manipulator characteristics

4. Dependence on mode of sensory feedback:

   a. Kinesthetic feedback

   b. Tactile feedback

B. Identification of the sources underlying controller remnant

1. Distinguish between time-delay variations and other effects

2. Distinguish among other effects:

   a. Controller gain variations

   b. True observation noise

   c. Motor noise

C. Application of observation noise model

1. Develop optimal pilot model which incorporates models of equivalent observation noise

2. Apply model to control situations of interest

location of the display within the peripheral field. Clearly, an investigation of peripheral observation noise should examine the effects of display parameters such as: (1) distance of the display into the periphery, (2) direction into the periphery, and (3) type of presentation provided by the display (e.g., moving tape, moving needle, oscilloscopic presentation). In addition, effects of related environmental factors such as illumination of the background and of the visual surround should be investigated.

The relationship between observation noise and the spectral characteristics of the displayed variable – especially for peripheral viewing – should be investigated. We have shown that the observation noise power level fails to vary proportionally with signal power during peripheral viewing, which indicates that the observation noise is a nonlinear function of the signal power. Because of complex phenomena associated with peripheral vision (in particular, the tendency to completely lose sight of signals that are moving relatively slowly), we suspect that observation noise is dependent on the characteristics of the signal in a complex way.

Other investigators (Ref. 32) have shown that tracking performance varies with the force-displacement characteristics of the control device. Since the published data are not detailed enough to allow us to pinpoint the exact nature of this dependency, we can only speculate at this point. One possibility is that performance varies because a change in the manipulator characteristics effectively changes the dynamics of the total plant and thereby makes the system more or less difficult to control. Thus, the effects of manipulator characteristics may be predictable entirely from consideration of the linear aspects of the problem along with the observation noise model of controller remnant as it presently exists. On the other hand, it may be possible that a motor noise process exists which is dependent partly upon the interaction between the neuromuscular system and the characteristics of the control device.

It would be worthwhile, then, to reanalyze those control systems in which the effects of control device characteristics have been demonstrated in order to determine whether or not these effects are related directly to controller remnant. If such is the case, an investigation of the interaction between controller remnant and manipulator characteristics would be profitable.

Only visual inputs to the human controller have been allowed in the experimental situations analyzed in this report. Real flight situations, of course, usually provide kinesthetic as well as visual feedback to the pilot, and laboratory studies have shown that control of certain vehicles is significantly enhanced when motion cues are provided (Refs. 33,34). In addition, studies are being conducted to determine the extent to which the tactile sense may be used to provide useful controller inputs in a manual control context. It would therefore be appropriate to investigate observation noise processes associated with nonvisual presentation of controlled variables.

Processes underlying controller remnant.--The principal focus of this contract has been to develop a model for controller remnant which can be used to predict system behavior in a wide variety of control situations, and we feel we have been largely successful in this aim. Nonetheless, a thorough understanding of controller remnant will not be possible until the underlying noise processes are understood and quantified.

Theoretical analysis of the remnant model indicates that the effects of time variations in the controller's time delay can be differentiated from the effects of other sources of controller remnant by a set of conditions which varies the ratio of error-rate variance to error variance. Surprisingly, the ratio that we compute from our own manual control data is remarkably invariant, even with

respect to changes in input bandwidth. Nevertheless, we suspect that the proper combination of vehicle dynamics and input spectra will serve to vary this ratio over a range sufficient to allow one to determine the relative importance of time-delay variations.

Since the remaining potential sources of remnant considered in this report (true observation noise, motor noise, and gain variations) enter into the system equations in the same manner, it appears that they can be differentiated only by experiments outside the context of manual control. We have given considerable thought to the problem, but we are unable to recommend a specific experimental program. There are two severe stumbling blocks to the design of an appropriate set of experiments. First, there is no guarantee that a psychophysical noise process that is measured outside the manual control context will have the same characteristics as when the subject is engaged in a continuous, compensatory manual control task. Secondly, the limitations of obtaining data at discrete intervals that accompanies such experiments will in general not allow a sufficiently small inter-sample interval to permit the computation of a power spectrum at high enough frequencies to be of interest. An experimental procedure which can resolve these considerations satisfactorily has the potential to advance significantly our understanding of human controller remnant.

Application of the observation noise model.--In order for the observation noise model of controller remnant to be of practical value, it must be incorporated into a larger model of the entire man-vehicle system so that controller behavior and total system performance may be predicted. We have, under other NASA contracts, been developing computer programs which include the intrinsic human limitations of time delay and remnant in an optimal-theoretic framework; preliminary work has been reported in the literature (Ref. 35).

In its present state of development, the model of the control system contains the following elements: (a) a description of the vehicle dynamics, including a list of the variables to be displayed to the controller, (b) a perceptual processor to allow for the injection of observation noise, (c) an optimum control law, (d) a predictor, and (e) a Kalman estimator. The predictor element attempts to compensate for the pilot's time delay. Since we have chosen to reflect controller remnant to noise sources injected at the controller's input (i.e., as an observation noise vector), we have incorporated an estimator to reduce the effects of this noise on system performance. In order to be able to treat control situations with separated displays, the model also includes a procedure for choosing a near-optimal visual scanning pattern by considering the relative effects of the foveal and peripheral observation noise terms. A preliminary test of the model (as yet to be reported)* has yielded very accurate predictions of both the controller's describing function and the equivalent scalar injected noise spectrum.

For control situations in which all variables are displayed foveally, the procedure for incorporating the observation noise model into the optimal framework is straightforward and quite simple. Each variable that is to be estimated by the controller has added to it a white observation noise spectrum whose power density level is 0.01 σ_x^2 units of power per rad/sec, where x is the variable to be estimated and "power" is in units of x^2. (This procedure is based on an extrapolation of the foveal tracking results presented in Chapter V. If additional experimentation reveals that both time-delay variations and other remnant sources are important, the additive noise will consist of two white noise terms – one which scales with σ_x^2 and the other which scales with $\dot{\sigma}_x^2$.)

*The optimal model is currently undergoing exhaustive testing under NASA Contract No. NAS1-2104.

Consideration of systems with separated displays complicates the implementation of the model somewhat because of the dependency of the peripheral observation noise process on the characteristics of the signal. At least two white noise terms will have to be associated with each observed variable:a process which scales with σ_x^2, and an additional term to account for peripheral viewing effects which is presumed to depend upon the spectrum of x in a complex manner.

Our optimal pilot model can, at present, handle only additive noise processes of a fixed level. (In order to simulate the effects of a multiplicative noise process, the optimal model has been operated in an iterative fashion so that the injected noise is ultimately scaled correctly with σ_x^2.) Clearly, a need exists for a technique which can directly implement the proper scaling of the injected noise. Ideally, a model will be developed to handle a large class of functional relationships between the injected noise level and the characteristics of the spectrum of the displayed signal. Because of our current lack of understanding of the peripheral noise process, we cannot at this time specify what these relationships might be.

APPENDIX A

SOME THEORETICAL ASPECTS OF REMNANT

Introduction

In this appendix we investigate the multiplicative noise model for human controller remnant in a simple manual control task. Our main objective is to show for this case that the assumption of linear independence between the input and observation noise processes — made in Chapter IV for measurement purposes — introduces a relatively small error in the computation of observation noise spectra.

The compensatory tracking task which is considered is shown in Figure A-1. $x(t)$ represents the displayed system error between plant output $y(t)$ and input driving noise $z(t)$. The human operator is represented by a linear portion $\mathcal{L}$ plus an additive equivalent observation noise. The differential equation governing the behavior of the closed-loop system is therefore

$$\dot{x}(t) = -k_v \mathcal{L}(x(t)) - k_v \mathcal{L}(r(t)) + \xi(t) \qquad (1)$$

where $\xi(t) \equiv \dot{z}(t)$.

We assume that $\mathcal{L}(\cdot)$ is represented merely by a pure gain k_h in order to simplify the analysis.* Equation (1) then simplifies to

$$\dot{x}(t) = -a\, x(t) - a\, r(t) + \xi(t) \qquad (2)$$

where $a = k_v k_h$.

*Although we conduct the analysis for a simplified case, it is possible to use matrix calculus to examine multi-output systems and/or more complex representations of the human operator. However, it is not felt that a more involved analysis is justified or will add materially to our study of remnant at the present time.

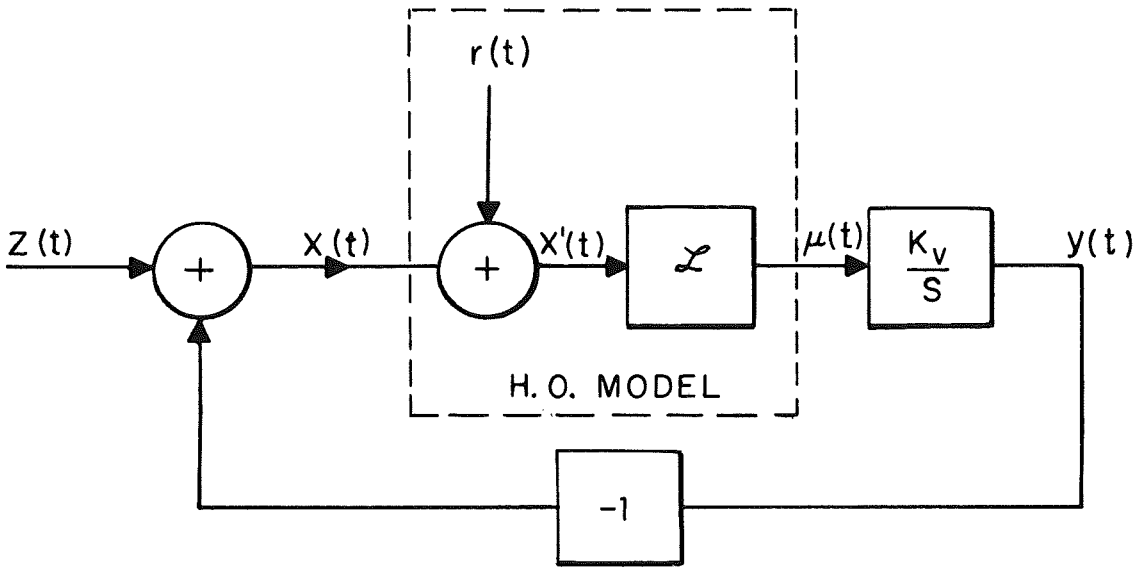

FIG.A-1 MODEL OF COMPENSATORY TRACKING SITUATION

The noise process $\xi(t)$ is stationary with an autocorrelation function

$$\phi_{\xi\xi}(\tau) = E\{\xi(t)\xi(t+\tau)\} = \frac{\alpha\sigma_1^2}{2} e^{-\alpha|\tau|} \tag{3}$$

and spectral density

$$\Phi_{\xi\xi}(\omega) = \frac{\sigma_1^2 \alpha^2}{\omega^2+\alpha^2} \tag{4}$$

It is possible to investigate other forms for $\Phi_{\xi\xi}(\omega)$ by differentiating with respect to α or by taking the sum of a set of $\Phi_{\xi\xi}$ corresponding to different values of α.

Preliminary Considerations

The structural form of the remnant process $r(t)$ is considered to be multiplicative in nature, viz,

$$r(t) = n(t)\cdot x(t) \tag{5}$$

where $n(t)$ is a stationary gaussian white-noise process. Therefore, Eq. (2) becomes

$$\dot{x}(t) = -a(1+n(t))x(t) + \xi(t) \tag{6}$$

with

$$E\{n(t)n(s)\} = \sigma_n^2 \delta(t-s) \tag{7}$$

Thus, the analysis of Eq. (6) is equivalent to the study of a linear system with a random coefficient (i.e., a random linear system). Equations of this type have been examined in the literature (see Refs. 36 - 38,) primarily with regard to their stability properties only.

Our objective is to study the steady-state ($t \to \infty$) behavior of Eq. (6). We thus assume that the x(t) process began at $t_o = -\infty$ with $x(-\infty) = 0$. The "solution" x(t) may then be written formally as

$$x(t) = \int_{-\infty}^{t} \phi(t,\tau)\xi(\tau)d\tau \tag{8}$$

where

$$\phi(t,\tau) = e^{-\int_{\tau}^{t} a[1+n(\sigma)]d\sigma} = e^{-a(t-\tau)} e^{-\int_{\tau}^{t} an(\sigma)d\sigma} \tag{9}$$

Thus, $\phi(t,\tau)$ is a function of the random variable $n(\cdot)$. Since n(t) is white we have in addition:

1. $w(t) = \int_{o}^{t} an(\sigma)d\sigma$ is a Wiener process of zero mean and variance $a^2\sigma_n^2 t$.
2. Since w(t) has independent increments, $\int_{a}^{b} n(\sigma)d\sigma$ and $\int_{c}^{d} n(\sigma)d\sigma$ are independent for $a<b\leq c<d$. Thus,

$$E\{\phi(b,a)\phi(d,c)\} = E\{\phi(b,a)\} \cdot E\{\phi(d,c)\} \tag{10}$$

3. $E\{e^{w}\} = E\{e^{jvw}\}\big|_{v=-j}$ where $E\{e^{jvw}\}$ is the characteristic function of w(t). Hence,

$$E\{e^{w}\} = e^{(jv)^2 a^2 \sigma_n^2 t/2}\Big|_{v=-j} = e^{a^2 \sigma_n^2 t/2}$$

and

$$E\{\phi(t,\tau)\} = e^{-\bar{a}(t-\tau)} \tag{11}$$

where

$$\left.\begin{aligned} \bar{a} &= a-\sigma^2/2 \\ \sigma^2 &= a^2\sigma_n^2 \end{aligned}\right\} \tag{12}$$

Statistical Properties of x(t)

In this section we derive expressions for the variance, autocovariance function and power density spectrum of x(t).

Variance of x(t).--Using Eq. (8) we obtain

$$\sigma_x^2 = E\{x^2(t)\} = E\left\{\int_{-\infty}^{t}\int_{-\infty}^{t} \phi(t,\tau)\phi_{\xi\xi}(\tau-\sigma)\phi(t,\sigma)d\sigma d\tau\right\}$$

Making use of Eqs. (10) and (11) it is possible to show that this expression evaluates to

$$\sigma_x^2 = \frac{\alpha\sigma_1^2}{2(\bar{a}+\alpha)(a-\sigma^2)} \tag{13}$$

Note that we require

$$a-\sigma^2 = a-a^2\sigma_n^2 > 0 \tag{14}$$

This is a sufficient (and necessary) condition for x(t) to remain finite for bounded noise input $\xi(t)$.

Autocovariance function of x(t).--The autocovariance function of x(t) is defined by $R(s,t) = E\{x(s)x(t)\}$. Thus from Eq. (8),

$$R(s,t) = E\left\{\int_{-\infty}^{s}\phi(s,\tau)\xi(\tau)d\tau \int_{-\infty}^{t}\phi(t,\sigma)\xi(\sigma)d\sigma\right\}$$

$$= E\left\{\phi(s,t)\int_{-\infty}^{t}\int_{-\infty}^{t}\phi(t,\tau)\phi_{\xi\xi}(\tau-\sigma)\phi(t,\sigma)d\sigma d\tau\right\}$$

$$+ E\left\{\int_{t}^{s}\phi(s,\tau)d\tau \int_{-\infty}^{t}\phi_{\xi\xi}(\tau-\sigma)\phi(t,\sigma)d\sigma\right\}$$

Taking expectations yields, since s> t and since in the second integral $\tau>\sigma$ (hence $s>\tau>t>\sigma$),

$$R(s,t) = E\{\phi(s,t)\}\cdot\sigma_x^2 + \frac{\alpha\sigma_1^2}{2}\int_{\infty}^{t}E\{\phi(t,\sigma)\}d\sigma\int_{t}^{s}e^{-\alpha(\tau-\sigma)}E\{\phi(s,\tau)\}d\tau$$

Substituting for $E\{\phi(\cdot,\cdot)\}$ and integrating we obtain

$$R(s,t) = e^{-\bar{a}(s-t)}\sigma_x^2 + \frac{\alpha\sigma_1^2}{2(\bar{a}^2 - \alpha^2)}[e^{-\alpha(s-t)} - e^{-\bar{a}(s-t)}] \tag{15}$$

Thus $R(s,t) = R(s-t)$ (i.e., the error process is stationary) and we can write the autocorrelation function of $x(t)$ as

$$\phi_{xx}(\tau) = E\{x(t)x(t+\tau)\}$$

$$= \sigma_x^2 e^{-\bar{a}|\tau|} + \frac{\alpha\sigma_1^2}{2(\bar{a}^2 - \alpha^2)}(e^{-\alpha|\tau|} - e^{-\bar{a}|\tau|}) \tag{16}$$

Spectral density of x(t).--The power density spectrum $\Phi_{xx}(\omega)$ of $x(t)$ is computed by taking the Fourier transform of $\phi_{xx}(\tau)$. Thus,

$$\Phi_{xx}(\omega) = \frac{2\bar{a}\,\sigma_x^2}{\omega^2+\bar{a}^2} + \frac{\alpha\sigma_1^2}{\bar{a}^2-\alpha^2}\left[\frac{\alpha}{\omega^2+\alpha^2} - \frac{\bar{a}}{\omega^2+\bar{a}^2}\right]$$

Substituting Eq. (13) for σ_x^2 and noting Eq. (4) for $\phi_{\xi\xi}(\omega)$ this expression may be written most conveniently as

$$\Phi_{xx}(\omega) = \frac{\sigma_x^2}{\omega^2+\bar{a}^2} \cdot \sigma^2 + \frac{1}{\omega^2+\bar{a}^2} \cdot \Phi_{\xi\xi}(\omega) \tag{17}$$

which clearly shows how the spectrum of $x(t)$ consists of input and remnant-related portions.

Computation of Observation Noise Spectrum

In order to obtain the covariance of r(t) it will be necessary to first find $aE\{\xi(s)r(t) + r(s)\xi(t)\} = Q(s,t)$. This quantity can be obtained by multiplying Eq. (6) by $\xi(s)$ and taking expectations. Thus,

$$aE\{r(t)\xi(s)\} = -E\{\dot{x}(t)\xi(s)\} - aE\{x(t)\xi(s)\} + E\{\xi(t)\xi(s)\}$$

But

$$E\{x(t)\xi(s)\} = \int_{-\infty}^{t} E\{\phi(t,\tau)\}\phi_{\xi\xi}(s-\tau)d\tau \qquad (18)$$

Therefore, differentiating Eq. (18) with respect to t yields

$$E\{\dot{x}(t)\xi(s)\} = -\bar{a}\, E\{x(t)\xi(s)\} + \phi_{\xi\xi}(s-t) \qquad (19)$$

Hence,

$$aE\{r(t)\xi(s)\} \doteq -\frac{\sigma^2}{2} E\{x(t)\xi(s)\}$$

Similarly (for s>t) we can show

$$aE\{r(s)\xi(t)\} = -\frac{\sigma^2}{2} E\{x(s)\xi(t)\} \qquad (20)$$

Thus

$$Q(s,t) = -\frac{\sigma^2}{2} [E\{x(s)\xi(t)\} + E\{x(t)\xi(s)\}]$$

Now, from Eq. (18),

$$E\{x(t)\xi(s)\} = \frac{\alpha\sigma_1^2}{2} \cdot \frac{1}{\bar{a}+\alpha} e^{-\alpha(s-t)}$$

Similarly

$$E\{x(s)\xi(t)\} = \int_{-\infty}^{s} e^{-\bar{a}(s-\tau)} \phi_{\xi\xi}(\tau-t)d\tau$$

$$= \frac{\alpha\sigma_1^2}{2} \cdot \frac{1}{\bar{a}+\alpha} e^{-\bar{a}(s-t)} + \frac{\alpha\sigma_1^2}{2} \cdot \frac{1}{\bar{a}-\alpha} \left[e^{-\alpha(s-t)} - e^{-\bar{a}(s-t)} \right]$$

Thus,

$$Q(s,t) = \frac{\alpha\sigma_1^2\sigma^2}{2(\bar{a}^2-\alpha^2)} \left[\alpha e^{-\bar{a}(s-t)} - \bar{a}\ e^{-\alpha(s-t)} \right] \qquad (21)$$

Furthermore, we can obtain the cross-correlation function

$$a\phi_{\xi r}(\tau) + a\phi_{r\xi}(\tau) = aE\{\xi(t)r(t+\tau) + r(t)\xi(t+\tau)\}$$

$$= \frac{\alpha\sigma^2\sigma_1^2}{2(\bar{a}^2-\alpha^2)} \left[\alpha\ e^{-\bar{a}|\tau|} - \bar{a}\ e^{-\alpha|\tau|} \right] \qquad (22)$$

and in addition the associated power density spectrum

$$a\Phi_{\xi r}(\omega) + a\Phi_{r\xi}(\omega) = -\frac{\bar{a}\alpha^2\,\sigma^2\sigma_1^2}{(\omega^2+\bar{a}^2)(\omega^2+\alpha^2)}$$

$$= -\frac{\bar{a}\alpha^2}{\omega^2+\bar{a}^2}\,\Phi_{\xi\xi}(\omega) \qquad (23)$$

We now compute the power density spectrum of the injected observation noise process. Since

$$\dot{x}(t) + a\,x(t) = a\,r(t) + \xi(t) \qquad (24)$$

we obtain

$$(\omega^2+a^2)\Phi_{xx}(\omega) = a^2\Phi_{rr}(\omega) - a\,\Phi_{\xi r}(\omega) - a\,\Phi_{r\xi}(\omega) + \Phi_{\xi\xi}(\omega) \qquad (25)$$

Substituting Eqs. (12), (17) and (23) into the above we find

$$\Phi_{rr}(\omega) = \sigma_n^2\sigma_x^2 \cdot \frac{\omega^2+a^2}{\omega^2+\bar{a}^2} + \frac{\sigma_n^2}{4} \cdot \frac{a^2}{\omega^2+\bar{a}^2}\,\Phi_{\xi\xi}(\omega) \qquad (26)$$

Equation (26) is valid for any noise spectrum $\Phi_{\xi\xi}(\omega)$ which can be obtained from the spectrum of Eq. (4) using linear operations. In particular, note that r(t) contains a component which is directly related to the input noise $\xi(t)$. This is a consequence of r(t) being related to x(t) which in turn is dependent on $\xi(t)$. Note, however, if $a\sigma_n^2 \ll 1$ then

$$\Phi_{rr}(\omega) \approx \sigma_n^2\sigma_x^2 \qquad (27)$$

Analysis of Experimental Technique

In the experimental study of remnant the input driving function z(t) (and hence $\xi(t) = \dot{z}(t)$) was composed of M independent sinusoids. Thus,

$$\phi_{\xi\xi}(\tau) = \sum_{i=1}^{M} A_i \cos \omega_i \tau \tag{28}$$

$$\Phi_{\xi\xi}(\omega) = \sum_{i=1}^{M} \frac{A_i}{2} [\delta(\omega-\omega_i) + \delta(\omega+\omega_i)] \tag{29}$$

Since $2 \cos \omega_i \tau = e^{j\omega_i \tau} + e^{-j\omega_i \tau}$, the autocorrelation function $\phi_{\xi\xi}(\tau)$ can be constructed by linear operations on the expression in Eq. (3). Therefore the results derived above for $\Phi_{xx}(\omega)$, $\Phi_{rr}(\omega)$, etc. remain valid for the sinusoidal case.

The experimental technique used to determine the observation noise spectrum $\Phi_{rr}(\omega)$ is described in Chapter IV. The method was to obtain the input- and remnant-correlated portions of the control signal (given by $\Phi_{uu_z}(\omega)$ and $\Phi_{uu_r}(\omega)$ respectively) and then show

$$\Phi'_{rr}(\omega) = \frac{\Phi_{uu_r}(\omega)}{\Phi_{uu_z}(\omega)} \cdot \Phi_{zz}(\omega) \tag{30}$$

It was assumed that z(t) and r(t) are uncorrelated in deriving Eq. (30). Below, we compute $\Phi_{uu}(\omega)$ and obtain $\Phi'_{rr}(\omega)$ by Eq. (30). The result is compared with the actual observation noise spectrum, Eq. (26).

From the equation $k_v u(t) = \dot{x}(t) - \xi(t)$ we obtain

$$k_v^2 E\{u(s)u(t)\} = E\{\dot{x}(s)x(t)\} + E\{\xi(t)\xi(s)\} - E\{\dot{x}(s)\xi(t) + \dot{x}(t)\xi(s)\} \tag{31}$$

Using Eqs. (19)-(23) it is then possible to derive

$$k_v^2 \Phi_{uu}(\omega) = \sigma^2\sigma_x^2 \frac{\omega^2}{\omega^2+\bar{a}^2} + \frac{\bar{a}^2}{\bar{a}^2+\omega^2} \Phi_{\xi\xi}(\omega) \tag{32}$$

Since $\Phi_{\xi\xi}(\omega) = \omega^2 \Phi_{zz}(\omega)$ and $\sigma^2 = \sigma_n^2 a^2$, Eq. (32) becomes

$$\Phi_{uu}(\omega) = k_n^2 \sigma_n^2 \sigma_x^2 \frac{\omega^2}{\omega^2+\bar{a}^2} + k_n^2 \frac{\bar{a}^2}{a^2} \frac{\omega^2}{\omega^2+\bar{a}^2} \Phi_{zz}(\omega) \tag{33}$$

The spectrum obtained from Eq. (30) is therefore

$$\Phi'_{rr}(\omega) = \frac{a^2}{\bar{a}^2} \cdot \sigma_x^2 \cdot \sigma_n^2 \tag{34}$$

which is constant independent of frequency (i.e., white noise). The largest fractional difference between the actual and measured normalized observation noise spectra is thus

$$\left(\frac{a}{\bar{a}}\right)^2 = \frac{1}{\left[1-\frac{a\sigma_n^2}{2}\right]^2} \tag{35}$$

We can estimate the magnitude of this ratio from the data that has been analyzed under this contract. For foveal tracking, typical experimental values of the variable "a" (which is equivalent to the gain-crossover frequency) were on the order of 5 rad/sec, and white normalized observation noise spectra on the order of 0.01 units of normalized power per rad/sec (positive frequencies only) were found when the variable to be estimated was either display position or display rate. The corresponding noise covariance is thus $\sigma_n^2 = (.01)\pi$. Substitution of these numerical values into equation (35) yields

$$\left(\frac{a}{\bar{a}}\right)^2 = 1.17 = 0.7 \text{ dB} \qquad (36)$$

Thus, the observation noise spectra computed for foveal tracking are on the order of 0.7 dB above the actual noise levels.

APPENDIX B

DETAILED ANALYSIS OF CLOSED-LOOP REMNANT SPECTRA

In this appendix we reanalyze a set closed-loop remnant spectra that has been published in an earlier report (Ref.29). Three control stick spectra are shown in Figure B-1, corresponding to 1-axis foveal, 1-axis peripheral, and 2-axis tracking conditions. Each spectrum is composed of two parts: a line spectrum, which represents the input-correlated portion of the subject's response, and a stepwise-continuous approximation to the remnant portion of the response. Each spectrum represents the results of a single experimental trial of a single subject. Since this subject's control behavior was found to be representative in other respects to that of all the subjects who participated in our experimental programs, we feel that the spectra shown here are therefore also typical of pilot behavior. These results were obtained using the command-input configuration of Figure 6a. Vehicle dynamics were K/s, the input bandwidth was 2 rad/sec, and the displays were separated by 30° visual arc.

We present these spectra here because the remnant portions have been analyzed in great detail. We attempted to analyze the spectra in such a way as to reveal whether or not controller remnant was caused by low-bandwidth time variations of the controller's describing function, as suggested by McRuer, et al (Ref. 4). We divided the frequency domain into successive bandwidths of 1/4 octave, half of which were centered about the input frequencies, the remainder of which fell midway between input frequencies. (Input frequencies above 0.5 rad/sec were spaced a half octave apart.) Fast-Fourier transform techniques allowed us to compute samples of the stick spectrum each of which represented a bandwidth of about 0.035 rad/sec. All samples within a given quarter-octave band were averaged, and

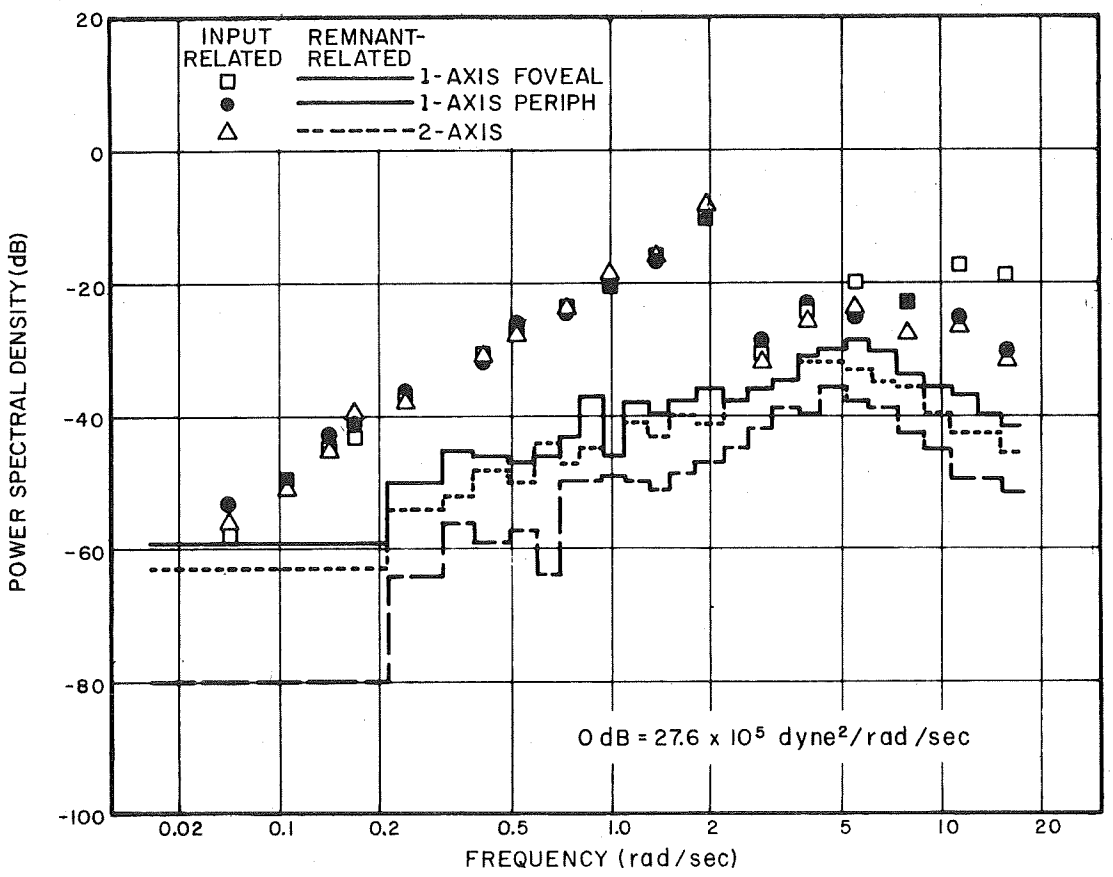

FIG.B-1 COMPARISON OF 1-AXIS FOVEAL, 1-AXIS PERPHERAL, AND 2-AXIS CONTROL STICK POWER SPECTRA

Vehicle Dynamics = K/s
Input Bandwidth = 2 Rad/Sec
Display Separation = 30 Degrees
Subject: PM

(From Fig.9 of Ref.29)

the power density level within the band was plotted as a constant equal to this average; hence, the stepwise-continuous remnant curves of Figure B-1.

Let us consider the results we would expect if the time variations were caused by a low-bandwidth noise process. If we look at the equivalent injected observation noise (which is simply a linear transformation of the closed-loop controller remnant), we see that

$$\underline{r}_x(t) = \hat{\underline{N}}(t) \cdot \underline{x}(t-\tau_o) \tag{1}$$

where $\hat{N}(t)$ is interpreted here as a gain-variational noise term, and $\underline{x}(t-\tau_o)$ is the (vector) displayed signal. If the components of $\underline{N}$ and $\underline{x}$ are linearly independent and Gaussian, the spectrum of each component of the injected noise vector is equal to the convolution of the spectra of the corresponding components of the noise matrix and state vector. Thus,

$$\Phi_{rr_i} = \Phi_{nn_i} \circledast \Phi_{xx_i} \tag{2}$$

In control situations for which the remnant-related portion of x_i comprises a small fraction of the total signal power, the spectrum Φ_{xx_i} will be primarily a line spectrum with components at input frequencies, plus a low-level smooth function to account for remnant. If the spectrum is narrowband, relative to the spacing between input frequencies, then the spectrum Φ_{rr_i} should show peaks in the immediate vicinity of input frequencies and valleys midway in between. Since the controller's describing function is presumed to be a smooth function of frequency (it can be measured only at input frequencies, of course), transformation of the observation

noise spectrum to the closed-loop remnant spectrum Φ_{uu_r} should preserve this spectral characteristic.

Figure B-1 fails to show any appreciable peaking effect correlated with the locations of the input frequencies. From this result we must conclude, therefore, that remnant is not caused by any type of narrowband multiplicative noise process — time variations included. The data do not rule out the possibility of a wideband noise process, however, and in the main body of this report we conclude that remnant can be attributed to one or more white multiplicative noise processes.

APPENDIX C. EXPERIMENTAL AND ANALYTICAL TECHNIQUES

This appendix contains a partial description of the experimental techniques and analytical procedures employed in a recent experimental program conducted under Contract No. NAS2-3080. The material contained in this appendix pertains to the vehicle-disturbance configuration of Figure 6b which provided some of the experimental data analyzed in the main body of this report. (The earlier command-input experiments are described in Ref. 29. The experimental and analytical procedures used during the earlier experimental program were essentially the same as those described in this appendix.)

Principal Experimental Hardware

Figure C-1 provides a diagram of the physical layout of our experimental apparatus and indicates the paths of information flow. Forcing functions were generated by a digital computer, converted to analog waveforms, and fed to an analog computing system. A separate control signal was generated simultaneously by the digital system to control the analog operations. The forcing functions and human controller outputs were processed by the analog system to produce the appropriate vehicle outputs. These outputs were used to drive the displays, which, along with the human controller and the manipulator, were housed in an isolated subject booth. All pertinent analog variables were converted to digital format for later off-line analysis of the data. All data analysis was performed on the digitized samples of the tracking data.

Computing machinery.--An Applied Dynamics AD/4 Analog Computer was used to simulate vehicle dynamics, drive the displays, and compute mean-squared system errors. An SDS-940 time-shared digital facility was used to generate forcing functions, convert analog data to digital format for storage on magnetic tape, and aid in data analysis.

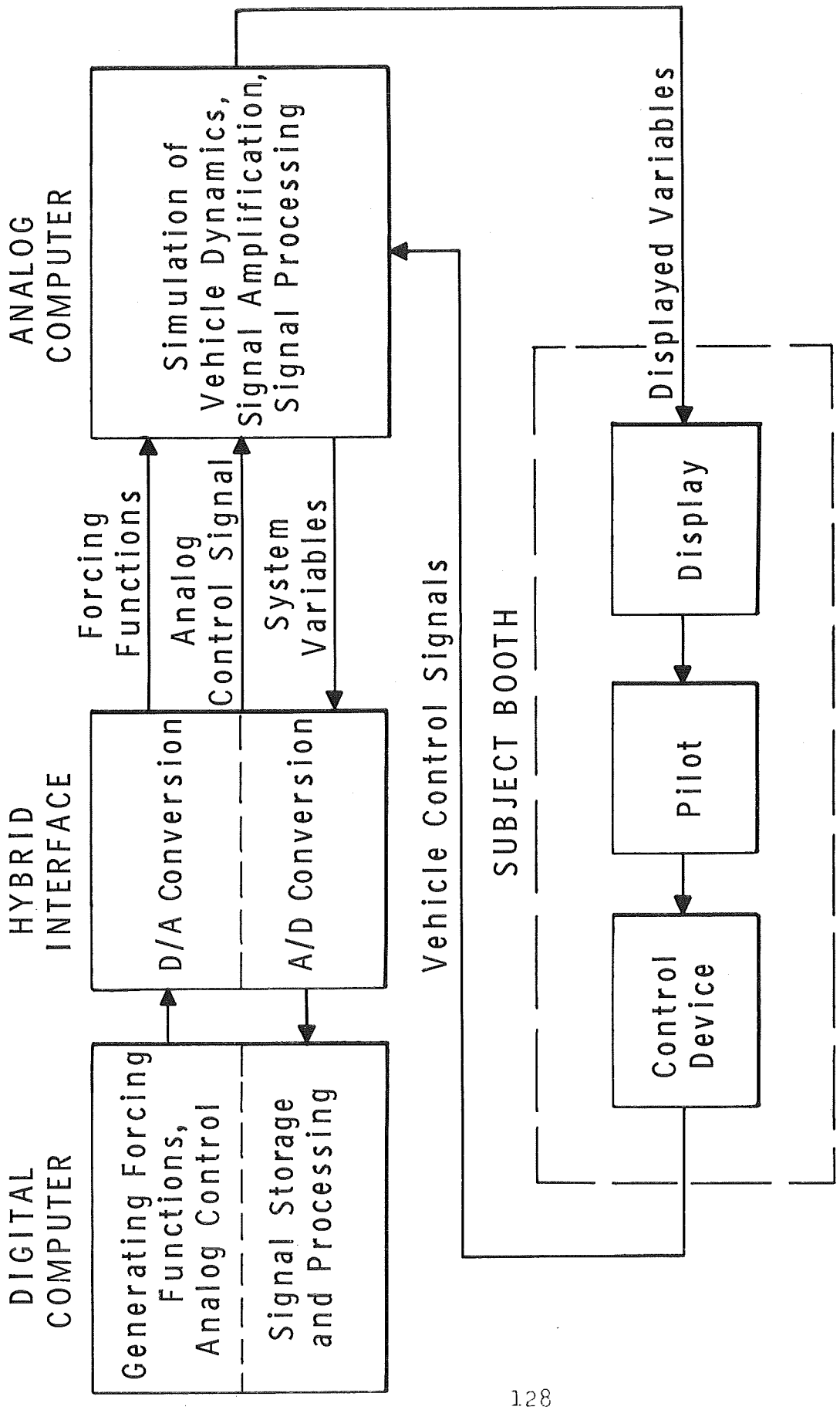

FIG.C-1 EXPERIMENTAL SETUP FOR MANUAL CONTROL

Subject booth.--The displays and controls were located in a subject booth that was isolated both acoustically and visually. A chin rest was provided to control the subject's point of regard and to minimize rotational head motions.

Displays.--The subject was provided with four oscilloscopic displays arranged on a plane surface located 72 cm in front of the subject's point of regard. Each scope face was masked with black paper to produce a rectangular background of 5 by 10 cm. The 'scope phosphor was type P-11, which gave a bluish cast to the reference and error indicators. An overlaid reticle provided a rectangular array of grid lines separated by about 1/2 cm. Intensity levels for the display and background were adjusted to be the same for all 'scopes and were kept the same throughout the experimental program. A constant low level of room lighting was maintained. A typical display presentation (minus the grid lines) is shown in Figure C-2; the dimensions shown indicate degrees of visual arc with reference to the subject's point of regard.

The four displays were located at the corners of an imaginary square, as shown in the scaled drawing of Figure C-3. The centers of the displays were separated by about 16 degrees of visual arc along the sides of the square and about 22 degrees along the diagonal. The displays were arranged so that the error indicators of the upper left (UL) and lower right (LR) displays moved horizontally, whereas the indicators on the upper right (UR) and lower left (LL) displays moved vertically. This particular arrangement was chosen because it provided similar visual interactions among displays. No matter which display was fixated, there was a display located 16° along the horizontal into the periphery, another located 16° vertically into the periphery, and another located 22° along the diagonal.

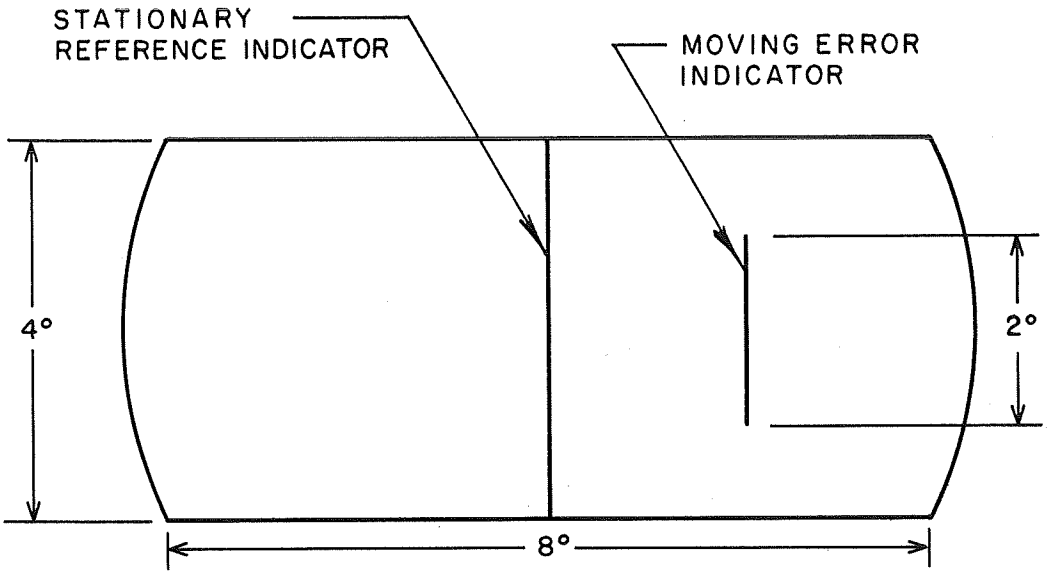

FIG.C-2 TYPICAL DISPLAY PRESENTATION

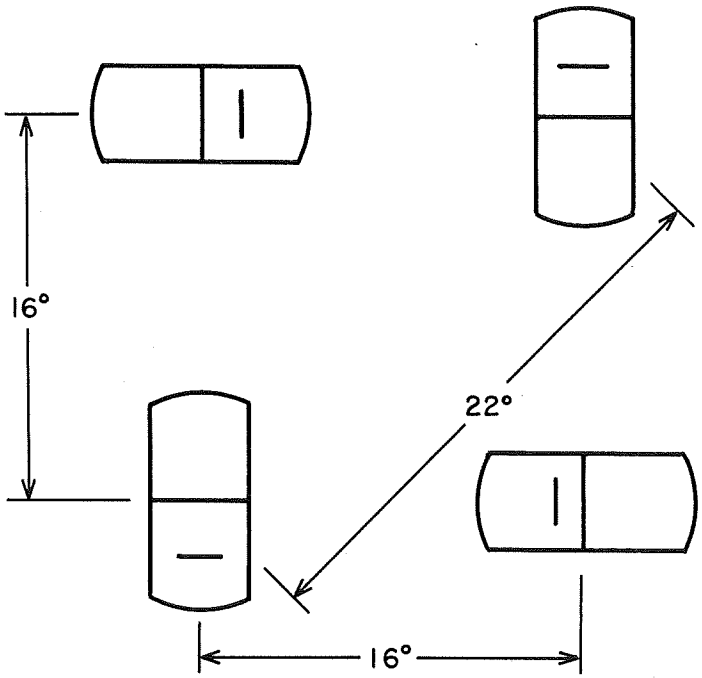

FIG.C-3 DISPLAY CONFIGURATION USED IN THE MULTI-DISPLAY TRACKING EXPERIMENTS

The most important visual interaction was the ability to extend a zero reference from the center of one display to the display in the nearest clockwise position. This ability was an important aid to peripheral tracking, since a peripherally-located baseline tended to disappear after a few seconds. Consider, for example, a fixation point at the center of the LL display. It was possible to extend mentally a zero reference to the UL display, since the baseline shown on that display was itself a stationary vertical line located above the center of the LL display. The rectangular grid lines displayed on the fixated (i.e., LL) display presumably aided in the reference extension. Note that the subject could not similarly extend a reference from the LL fixation point to the LR display, since the true reference for the latter display was orthogonal to the line connecting the centers of the displays. There was, of course, no reference extension to the diagonally-located peripheral display.

Controls.--The subject manipulated two aluminum sticks, each of which was attached to a force-sensitive hand control (Measurement Systems Hand Control, Model 435). The stick-control combination provided an omnidirectional spring restraint with a restoring force of about 8×10^6 dynes per centimeter deflection of the tip of the stick. The subject used wrist and finger motions to manipulate the sticks and was provided with arm rests to support his forearms.

The transducer of each hand control provided two independent electrical outputs, one proportional to the horizontal and the other proportional to the vertical component of deflection. The sticks were allowed to move freely in both axes in all experiments. The error indicators in the inactive axes were clamped electronically at zero displacement.

In order to provide a high degree of control-display compatibility, each control was oriented so that the stick was horizontal and could be moved in a plane parallel to the plane of the displays. Each display was controlled by a component of stick movement along the same axis as the motion of the error indicator. Thus, the UL display was controlled by x-axis (i.e., horizontally-directed) deflections of the left control stick, the LL display by y-axis motions of the left stick, the UR display by y-axis motions of the right stick, and the LR display by x-axis motions of the right stick. The response of an error indicator was in the same direction as the corresponding component of control deflection.

Control System Parameters

Controlled-element dynamics.--The controlled-element dynamics were K/s in all axes for all experiments. In all but one experiment, the control gains were the same on all axes. For most of the experiments, the control gain was such that 1 Newton of force produced an error rate of 2 degrees visual arc per second.

Forcing functions.--Forcing functions were provided via a multichannel FM magnetic tape system during training and were generated by the 940 digital system during data-taking sessions. Up to 13 sinusoids were summed to provide signals that were random-appearing and whose spectra approximated white noise processed by a first-order filter with a pole at -2 rad/sec. In order to assure orthogonality among the component sinusoids, an integral number of cycles of each component was contained in the measurement interval (about 200 seconds). Thus, each component was a harmonic of the fundamental frequency

$$\omega_o = 2\pi/200 = .031 \text{ rad/sec}$$

The mean-squared input was the same on all axes for all but one experimental condition and was usually about 2.2 $(deg/sec)^2$ referred to system output.

Table C-1 lists the radian frequency, the number of wavelengths in the measurement interval, and the relative amplitude of each of the 13 sinusoidal components which constitute a typical forcing function. The initial phase shifts associated with each component of a forcing function were generated by a random process having a uniform distribution between 0 and 2π.

TABLE C-1

Parameters of a Typical Forcing Function

Number of wavelengths in measurement interval	Frequency (rad/sec)	Relative Amplitude
6	.18	1346
17	.52	1492
32	.98	1542
48	1.5	1423
66	2.0	1399
94	2.9	1382
130	4.0	1273
186	5.7	1142
262	8.0	974
366	11.2	842
522	16.0	713
733	22.5	606
1052	32.3	485

Training and Experimental Procedures

Subjects.--Four subjects, all of them instrument-rated Air Force pilots, participated in the experimental program. Three subjects were currently active in the Air National Guard and the remaining subject was active as a commercial pilot.

Instructions.--The subjects were instructed to minimize mean-squared tracking error. When tracking more than one axis simultaneously, they were instructed to minimize a total score given as the sum of the mean-squared error scores obtained from each axis. (The scores were weighted equally in this computation.) The subjects were informed of their scores after each session, and histories of the performance of all subjects were posted and shown to each subject in an attempt to foster a spirit of competition.

Run Length.--All training and experimental trials lasted four minutes and were generally presented in sessions of three or four trials each with a minimum rest period of 10 minutes between sessions. Minimum rest periods of 1 minute were provided between successive trials within a session. All mean-squared error scores and other measurements were obtained from samples of data 3 minutes and 20 seconds long, beginning 20 seconds after the onset of the forcing function.

Inputs.--A number of forcing functions were used during training under a given condition to minimize learning of the input. These forcing functions were of the type shown in Table C-1, except that the highest frequency component was absent, and were presented in a balanced order. In order to minimize the effects of input differences on the experimental results, however, a single set of forcing functions was used in a given experiment.

Training.--The subjects were trained under each condition until an apparently stable performance level was achieved. In general, the subjects were trained in an equal mixture of the conditions to be investigated in each experiment.

Typical Experimental Waveforms.--Typical time tracings of input, system error, and pilot control signals are presented in Figure C-4. Since these tracings have been obtained from a display of the digitized data, they appear as sets of discrete points. The analog waveforms from which these samples were obtained were, of course, signals that were continuous in time.

Data Recording

All experimental data were recorded onto digital magnetic tape via the SDS-940 system and its associated peripheral hardware. Control of the experiment was effected through the STOREDATA system, a program written in a 940-compatible version of FORTRAN II which (1) generated the forcing functions, (2) provided a signal for controlling the analog computer, (3) performed on-line computations of the incoming data, and (4) converted the data to digital format for storage. Data were sampled at the rate of 20 samples/second. All experimental trials were 4800 samples (4 minutes) in length. Nearly all of the analyses described in the following section were performed on 4096* samples (about 3 minutes, 20 seconds) beginning about 20 seconds after the onset of the trial.

Descriptive Measures

Mean-Squared errors.--Mean-squared error (MSE) scores were computed for each axis in a given experimental trial, and a total performance measure was computed as the sum of these scores. Analyses of variance were performed on selected sets of MSE scores to test the significance of differences in scores that accompanied changes in experimental conditions.

*The fast-Fourier transform technique used in obtaining power spectra and describing function required 2^N data points.

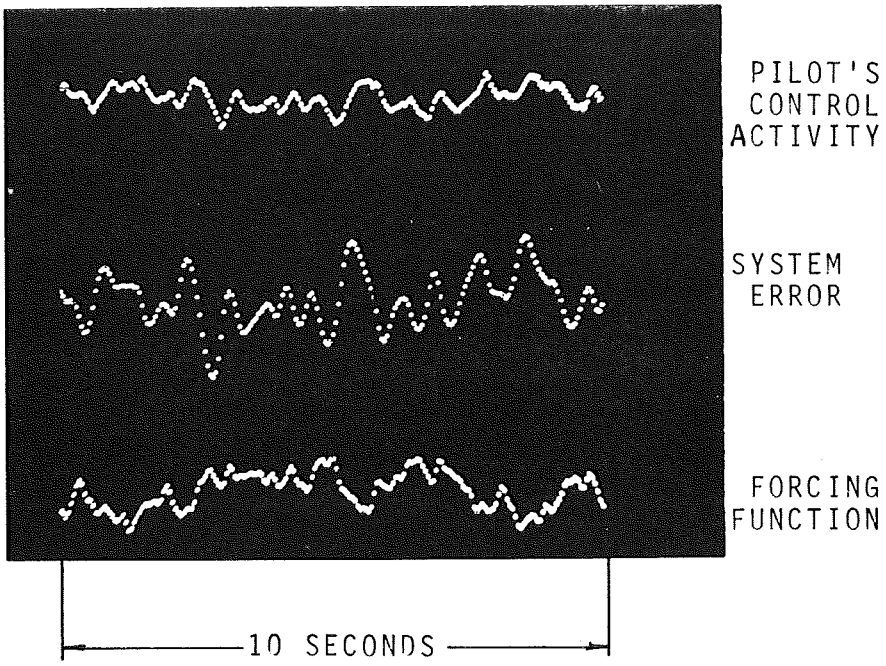

FIG.C-4 TYPICAL TIME TRACINGS
Vehicle Dynamics = K/s

Power Spectra.--Power spectra were obtained using Fourier analysis techniques based on the Cooley-Tukey method of computing transforms (Ref. 39). Samples of the time histories of each signal were converted to frequency-domain representations by the algorithm

$$F_m = \frac{1}{N} \sum_{n=0}^{N-1} f_n \, e^{-j \frac{2\pi nm}{N}}$$

where f_n is the sampled value of the signal at the n^{th} discrete time interval, N is the total number of sample points in the measurement interval, and F_m is the Fourier coefficient at the m^{th} harmonic of the fundamental frequency. The fundamental frequency is given as

$$\omega_o = \frac{2}{N\Delta T}$$

where ΔT is the interval between successive time samples. N was 4096 and ΔT was 0.05 sec for the vehicle-disturbance experiments reported here. In order to enhance the interpretability of the results, the fundamental frequency ω_o of the Fourier analysis was the same as the base frequency about which the forcing functions were constructed. Each spectrum, therefore, consisted of a set of lines spaced by approximately 0.031 rad/sec and extending from 0.031 to about 64 rad/sec.* Measurements beyond 37 rad/sec were disregarded.

*Since the measurement length is finite, each spectral "line" represents the power contained in a measurement window of the form $\{[\sin \pi\omega/\omega_o]/[\pi\omega/\omega_o]\}^2$ centered about the nominal measurement frequency.

It was convenient for analytical purposes to consider each power spectrum as the sum of two component spectra: (a) the "input-correlated" spectrum, consisting only of those measurements coincident with the forcing-function frequencies, and (b) the remnant spectrum, consisting of the remainder of the power spectrum. The input-correlated portion of the spectrum was interpreted as the linear response to the forcing function; conversely, the remnant portion was considered to account for all of the signal power that was not linearly related to the forcing function. These interpretations were based on the underlying assumptions that (a) only a negligible amount of power measured at an input frequency was due to random or nonlinear controller behavior, and (b) only a negligible fraction of the remnant occurred at input frequencies.

Computation of the power spectrum allowed the partitioning of the signal variance onto the portion of signal power correlated with the input and the portion due to remnant. These component scores were obtained by summing the spectral measurements obtained at input frequencies and at all frequencies excepting input frequencies, respectively. (The power measurement at 0 frequency, representing the square of the mean, was not included in the latter summation.)

Estimates of the remnant component of the spectrum at input frequencies were needed for the computation of observation noise (discussed below) and also for a test of the above assumptions. This measurement could not be obtained directly, since there was no way to subdivide a single measurement into input-related and remnant-related components. Instead, estimates were provided by averages of the power spectral measurements obtained on either side of (but not including) an input frequency. The assumption was made that the remnant spectrum was a continuous function of frequency in the vicinity of the input frequencies. This has been

shown to be a reasonably good assumption (see Appendix B). The averaging windows extended roughly 1/8 octave on either side of each input frequency. Since the spectral measurements yielded by the Fourier analysis were spaced linearly with frequency, the number of measurements included in the average increased with increasing frequency.

Describing functions.--Human controller describing functions were obtained using the Fourier analysis techniques described above. Samples of the controller describing function — at input frequencies only — were obtained by dividing the transform of the control signal by the transform of the error signal. This technique is similar to those employed by Tustin (Ref. 6), McRuer, et al (Ref. 4), and Taylor (Ref. 31). Estimates of the validity of the error and control signal transforms at a given frequency were obtained from a comparison of the power measured at that frequency and the remnant estimated at that frequency. If the error and control remnant estimates were not jointly more than 4 dB below the corresponding "input-correlated" measures, the estimate of the describing function at that frequency was considered to be invalid. This acceptance criterion allowed for a maximum error in the amplitude ratio of about 1.5 dB.

Observation noise.--(Procedures for computing observation noise are described in Chapter IV of the main body of this report and are not repeated here.)

REFERENCES

1. Levison, W. H. and J. I. Elkind, "Two-Dimensional Manual Control Systems with Separated Displays," IEEE Trans. on HFE, Vol. HFE-8, No. 3, September 1967, pp. 202-209.

2. Elkind, J. I., "Characteristics of Simple Manual Control Systems," MIT Lincoln Laboratory, TR-111, 6 April 1956.

3. McRuer, D. T. and E. S. Krendel, "Dynamic Response of Human Operators," WADC-TR-56-524, WPAFB, Ohio, October 1957.

4. McRuer, D. T., D. Graham, E. S. Krendel, and W. Reisener, Jr., "Human Pilot Dynamics in Compensatory Systems Theory, Models and Experiments with Controlled-element and Forcing Function Variations," AFFDL-TR-65-15, WPAFB, Ohio, July 1965.

5. Russell, Lindsay, "Characteristics of the Human as a Linear Servo-Element, MIT, MS Thesis, 18 May 1951.

6. Tustin, A., "The Nature of the Operator's Response in Manual Control and Its Implication for Controller Design," J. IEEE, Vol. 94, Part IIA, 1947.

7. (Goodyear Aircraft) "Investigation of Control "Feel" Effects on the Dynamics of a Piloted Aircraft System," Goodyear Aircraft Corporation Report, GER 6726, 25 April, 1955.

8. McRuer, D. T. and H. Jex, "A Review of Quasi-Linear Pilot Models," IEEE Trans. on HFE, Vol. HFE-8, No. 3, September 1967, pp. 231-249.

9. Bekey, G. A. and J. M. Biddle, "The Effect of a Random-Sampling Interval on a Sampled-Data Model of the Human Operator," 3rd Annual NASA-Univ. Conf. on Manual Control, University of Southern California, Los Angeles, Calif., NASA SP-144, March 1-3, 1967.

10. Pew, R. W., J. C. Duffendack and L. K. Frensch, "Sine-Wave Tracking Revisited," IEEE Trans. on HFE, HFE-8, June 1967, pp. 130-134.

11. Ferrell, W. R., "Remote Manipulation with Transmission Delay," IEEE Trans. HFE, Vol. HFE-6, September 1965, pp. 24-32.

12. Stevens, S. S., "Problems and Methods of Psychophysics," Psychol. Bull. 55: July 1958, pp. 177-196.

13. Stevens, S. S. and E. H. Galanter, "Ratio Scales and Category Scales for a Dozen Perceptual Continua," J. Exp. Psychol. 55: 1957, pp. 377-411.

14. Rachlin, Howard C., "Scaling Subjective Velocity, Distance and Duration," Perception and Psychophysics, Vol. 1, No. 2, February 1966.

15. Brown, J. S., E. B. Knauft and G. Rosenbaum, "The Accuracy of Positioning Responses as a Function of Their Direction and Extent," Amer. J. Psych., Vol. 61, April 1948, pp. 167-182.

16. Weiss, B., "Movement Error, Pressure Variations and the Range Effect," J. Exper. Psychol., Vol. 50, September 1965, pp. 191-196.

17. Burg, A., "Visual Acuity as Measured by Dynamics and Static Tests: A Comparative Evaluation," J. Appl. Psych. Vol. 50, 1966, pp. 460-66.

18. Hoogerheide, J., "Preliminary Report Concerning Peripheral Dynamic Vision," Aeromed. Acta, Vol. 9, (1963-1964), pp. 139-145.

19. Westheimer, Gerald, "Visual Acuity," Ann. Rev. Psych., Vol. 16, 1965.

20. Weymouth, Frank W., "Visual Sensory Units and the Minimal Angle of Resolution," Amer. J. Ophthal., Vol. 46, No. 1, Part II, 1958, pp. 102-113.

21. Gordon, D. A., "The Relation Between the Thresholds of Form, Motion and Displacement in Parafoveal and Peripheral Vision at a Scotopic Level of Illumination," Amer. J. Psych., Vol. 60, April 1947, pp. 202-225.

22. Graham, C. H. (ed.), Vision and Visual Perception. Wiley & Sons, New York City, New York, 1965.

23. Brown, J. F., "The Thresholds for Visual Movement." in: Spigel, E. M.: Readings in the Study of Visually Perceived Movement. Harper & Row, New York City, New York, 1965.

24. Dwyer-Joyce, P., "Studies in Perception III," Trans. Ophth. Soc. (U.K.) 85, 1964, pp. 701-712.

25. Rashbass, C., "The Relationship Between Saccadic and Smooth Tracking Eye Movements," J. Physiol., Vol. 159, 1961, pp. 326-388.

26. Young, L. R., "A Sampled Data Model for Eye-Tracking Movements," MIT, Sc.D. Thesis, June 1962.

27. Birmingham, H. P. and F. V. Taylor, "A Human Engineering Approach to the Design of Man-Operated Continuous Control Systems," NRL Report 4333, Naval Research Lab., Washington, D. C., April 1954.

28. Bard, P. (ed.), Medical Physiology (11th ed.), C. V. Mosby, St. Louis, Mo., 1961.

29. Levison, W.H., and Elkind, J.I., "Studies of Multivariable Manual Control Systems," NASA Contractor Report No. CR-875, October 1967.

30. Levison, W. H. and J. I. Elkind, "Studies of Multi-Variable Manual Control Systems: Four-Axis Compensatory Systems with Separated Displays and Controls. (In preparation)

31. Taylor, L. W., Jr., "A Comparison of Human Response Modelling in the Time and Frequency Domains," 3rd Ann. NASA, Univ. Conf. on Manual Control, NASA SP-144, March 1-3, 1967, pp. 137-156.

32. Magdaleno, R.E., and McRuer, D.T., "Effects of Manipulator Restraints on Human Operator Performance," Tech. Report No. AFFDL-TR-66-72, Air Force Flight Dynamics Laboratory, Wright-Patterson AFB, Dec. 1966.

33. Shirley, R.S., "Motion Cues in Man-Vehicle Control," MVT-68-1, Man-Vehicle Laboratory, Center for Space Research, MIT, Cambridge, Mass., Sc.D. Thesis, Jan. 1968.

34. Young, Laurence R., "Some Effects of Motion Cues on Manual Tracking," Vol. 4, No. 10, Journal of Spacecraft and Rockets, October 1967, pp. 1300-1303.

35 Baron, S., and Kleinman, D.L., "The Human as an Optimal Controller and Information Processor," NASA Contractor Report No. CR-1151, Sept. 1968.

36. Caughey, T.K., and Gray, A.H., "On the Almost Sure Stability of Linear Dynamic Systems with Stochastic Coefficients," ASME J. Appl. Mech., Vol. 87, pp. 365-372, 1965.

37. Bertram, J.E., and Sarachik, P.E., "On the Stability of Systems with Random Parameters," IRE Trans. Circuit Theory, Vol. 5, pp. 260-270, 1959.

38. Nevelson, M.B. and Khasminskii, R.Z., "Stability of a Linear System with Random Disturbances of its Parameters," PMM J. Applied Math. and Mech., Vol.30, pp. 487-494, 1967.

39. Cooley, J.W. and Tukey, J.W., "An Algorithm for the Machine Calculation of Complex Fourier Series," Mathematics of Computation, Vol. 19, No. 90, pp. 297-301, April 1965.